

1991

Reactions of an excited state of carbon- and sulfur-centered radicals with transition metal complexes

Patrick L. Huston
Iowa State University

Follow this and additional works at: <https://lib.dr.iastate.edu/rtd>

 Part of the [Inorganic Chemistry Commons](#), and the [Radiochemistry Commons](#)

Recommended Citation

Huston, Patrick L., "Reactions of an excited state of carbon- and sulfur-centered radicals with transition metal complexes " (1991). *Retrospective Theses and Dissertations*. 9648.
<https://lib.dr.iastate.edu/rtd/9648>

This Dissertation is brought to you for free and open access by the Iowa State University Capstones, Theses and Dissertations at Iowa State University Digital Repository. It has been accepted for inclusion in Retrospective Theses and Dissertations by an authorized administrator of Iowa State University Digital Repository. For more information, please contact digirep@iastate.edu.

92

12150

U·M·I

MICROFILMED 1992

INFORMATION TO USERS

This manuscript has been reproduced from the microfilm master. UMI films the text directly from the original or copy submitted. Thus, some thesis and dissertation copies are in typewriter face, while others may be from any type of computer printer.

The quality of this reproduction is dependent upon the quality of the copy submitted. Broken or indistinct print, colored or poor quality illustrations and photographs, print bleedthrough, substandard margins, and improper alignment can adversely affect reproduction.

In the unlikely event that the author did not send UMI a complete manuscript and there are missing pages, these will be noted. Also, if unauthorized copyright material had to be removed, a note will indicate the deletion.

Oversize materials (e.g., maps, drawings, charts) are reproduced by sectioning the original, beginning at the upper left-hand corner and continuing from left to right in equal sections with small overlaps. Each original is also photographed in one exposure and is included in reduced form at the back of the book.

Photographs included in the original manuscript have been reproduced xerographically in this copy. Higher quality 6" x 9" black and white photographic prints are available for any photographs or illustrations appearing in this copy for an additional charge. Contact UMI directly to order.

U·M·I

University Microfilms International
A Bell & Howell Information Company
300 North Zeeb Road, Ann Arbor, MI 48106-1346 USA
313/761-4700 800/521-0600



Order Number 9212150

Reactions of an excited state and of carbon- and sulfur-centered radicals with transition metal complexes

Huston, Patrick L., Ph.D.

Iowa State University, 1991

U·M·I
300 N. Zeeb Rd.
Ann Arbor, MI 48106



**Reactions of an excited state and of carbon- and sulfur-centered
radicals with transition metal complexes**

by

Patrick L. Huston

**A Dissertation Submitted to the
Graduate Faculty in Partial Fulfillment of the
Requirements for the Degree of
DOCTOR OF PHILOSOPHY**

**Department: Chemistry
Major: Inorganic Chemistry**

Approved:

Signature was redacted for privacy.

In Charge of Major Work

Signature was redacted for privacy.

For the Major Department

Signature was redacted for privacy.

For the Graduate College

**Iowa State University
Ames, Iowa**

1991

TABLE OF CONTENTS

	Page
GENERAL INTRODUCTION	1
Explanation of dissertation format	2
PART I QUENCHING OF ${}^*CrL_3^{3+}$ WITH TITANIUM(III)	3
INTRODUCTION	4
EXPERIMENTAL	7
Solvents and reagents	7
Kinetics	8
Laser actinometry	9
RESULTS	11
Acid dependence	12
Quantum yields	17
DISCUSSION	21
REFERENCES	30
APPENDIX	33
PART II ALKYL RADICAL COLLIGATION AND RELEASE BY A CHROMIUM MACROCYCLE	44
INTRODUCTION	45
EXPERIMENTAL	48
Materials	48
Analyses	50
Kinetics	51
RESULTS	54
Reaction of $R\cdot$ with MV^{*+}	56

Reaction of R• with Cr([15]aneN ₄) ²⁺	58
DISCUSSION	61
Homolysis reactions	61
Colligation reactions	65
Equilibrium	66
REFERENCES	69
APPENDIX	72
PART III REACTIONS OF THIYL RADICALS WITH TRANSITION METAL COMPLEXES	100
INTRODUCTION	101
EXPERIMENTAL	106
Materials	106
Analyses	108
Laser experiments	109
RESULTS	111
Generation of radicals	111
Kinetics	112
Product studies	122
DISCUSSION	124
REFERENCES	131
APPENDIX	135
GENERAL SUMMARY	147
ACKNOWLEDGEMENTS	148

LIST OF ABBREVIATIONS

bpy	2,2'-bipyridine
phen	1,10-phenanthroline
ABTS ²⁻	2,2'-azino-bis(ethylbenz-thiazoline-6-sulfonate) ion
MV ^{•+}	methyl viologen radical cation
TMPD	N,N,N',N'-tetramethyl-1,4-phenylenediamine
dmgH ⁻	3,4-dimethylglyoximate
[14]aneN ₄	1,4,8,11-tetraazacyclotetradecane
[15]aneN ₄	1,4,8,12-tetraazacyclopentadecane
Me ₆ [14]aneN ₄	5,7,7,12,14,14-hexamethyl-1,4,8,11-tetraazacyclotetradecane
Me ₆ [14]dieneN ₄	<i>meso</i> -(1,8)-5,7,7,12,14,14-hexamethyl-1,4,8,11-tetraazacyclotetradeca-4,11-diene
RSH	thiol
RSSR	disulfide
CysSH	cysteine
GSH	glutathione
GC	gas chromatography
ICP/MS	inductively coupled plasma mass spectrometry

GENERAL INTRODUCTION

In Part I the quenching of the 2E excited state of chromium polypyridine complexes by Ti(III) is discussed. Experiments were done to evaluate emission lifetimes as a function of the important concentration variables, [Ti(III)] and [H⁺]. Also, the second order rate constants of the quenching by both $Ti(H_2O)_6^{3+}$ and $Ti(H_2O)_5OH^{2+}$ were examined in terms of the Marcus cross relation. Studies were carried out in the transient absorption mode to detect $Cr(NN)_3^{2+}$ and to determine if back electron transfer occurs to yield ground state $Cr(NN)_3^{3+}$ and Ti(III). The quantum yields of this reductive quenching by Ti(III) were determined as a function of [Ti(III)].

Part II involves the colligation of a series of carbon-centered radicals with a chromium(II) macrocyclic complex. Colligation reactions of alkyl radicals and metal complexes studied to date divide cleanly into two groups. The first group includes $Cr(H_2O)_6^{2+}$ and $Co(N_4mac)^{2+}$, where the rates decrease relatively little as the substituents on the α carbon atom increase in bulk. In contrast, the second group, which includes both isomers of $Ni([14]aneN_4)^{2+}$, shows rates that decrease markedly with the size of the substituents. The system studied here involved the complex $Cr([15]aneN_4)^{2+}$, chosen to learn whether incorporation of the chromium into a macrocycle causes its reactivity pattern to shift to that of the nickel macrocycles. The equilibrium constants for radical binding are discussed in terms of Cr-C and Cr-OH₂ bond making and bond breaking.

The study of sulfur-centered thiyl radicals makes up Part III. In general studies involving thiyl radicals have been carried out using pulse radiolysis. However, a much simpler method for generating thiyl radicals and studying their

reactions is available using laser flash photolysis. This method involves well-established reactions to generate thiyl radicals and allows the study of a wide variety of their reactions in aqueous solution. The repair reaction is examined for the methyl and ethyl radicals with several thiols. Also, studies of reactions of ethane thiyl radicals with a number of metal complexes are described.

Explanation of dissertation format

The dissertation is organized into three sections following the "Alternate Thesis Format." Each section corresponds to a manuscript submitted for publication in *Inorganic Chemistry*. Each section is self-contained with its own tables, figures, schemes and references in standard format for *Inorganic Chemistry*. All the work described here was performed by P.L. Huston.

PART I QUENCHING OF $^*CrL_3^{3+}$ WITH TITANIUM(III)

INTRODUCTION

Electron transfer reactions of Ti(III) have been widely studied in recent years. Many studies have been carried out with complexes of Ru(III)¹ and of Co(III)² as oxidants. Other oxidants used include iodine³, 1-hydroxy-1-methylethyl radicals⁴, V(IV)⁵, V(V)⁶, and complexes of Ni(III)⁷ and Os(III).⁸ Often an inverse dependence on [H⁺] is found, indicating TiOH²⁺ rather than Ti³⁺ is the active reductant. Both Ti³⁺ and TiOH²⁺ are effective reductants of Ru(III) complexes only if an electron delocalizing ligand is present on the oxidant. In the reduction of Co(III) complexes the presence of a sufficiently hard bridging ligand on the oxidant is necessary if both species are to be effective, otherwise, only TiOH²⁺ is effective. Thus, both Ti³⁺ and TiOH²⁺ are effective in reducing Ru₂(OAc)₄⁺, but only TiOH²⁺ can reduce tris(pentane-2,4-dionato)ruthenium (III).^{1,9} Other cases where both are effective include Co(NH₃)₄C₂O₄⁺,¹⁰ complexes of Os(III),⁸ and derivatives of salicylatocobalt(III).¹¹ When both Ti(III) species react, TiOH²⁺ is generally at least an order of magnitude faster than Ti³⁺. Since the Ti(IV) species formed is TiO²⁺, then it might be expected that a transient intermediate with a shorter Ti-O bond as in TiOH²⁺ would be more favorable.

Inner sphere mechanisms have been found to operate in cases where there is an efficient bridging ligand such as oxalate,^{10,12} thiocyanate,¹³ salicylate¹⁴ or acetate.¹⁵ However, ligands such as Cl⁻ or SO₄²⁻ that are generally considered to be good bridges in inner sphere processes are not always efficient for Ti(III) electron transfer reactions. In these inner sphere reactions it is sometimes the case that substitution on Ti(III) is the rate limiting step.¹⁶

Outer sphere electron transfer processes involving Ti(III) have often shown agreement with Marcus theory.¹⁷ Studies with oxidants such as Ru(III) complexes lacking an efficient bridging ligand have linear free energy relationships. In a study involving poly(pyridine)osmium (III) complexes self-exchange rates were estimated to be $> 3 \times 10^{-4} \text{ L mol}^{-1}\text{s}^{-1}$ for $\text{Ti}^{4+/3+}$ and $\geq 10^{-2} \text{ M}^{-1}\text{s}^{-1}$ for $\text{TiOH}^{3+/2+}$.⁸ In the case of Ni(III) complexes the reactions were found to fit a Marcus correlation despite the large driving forces.⁷

The Ti(IV) species formed in solution by these reactions has been uncertain for many years due to conflicting indirect evidence. Based on ionic strength variation studies, the Ti(IV) species has a charge of 2+ (TiO^{2+} or $\text{Ti}(\text{OH})_2^{2+}$).⁵ Ion exchange elution techniques indicated that a hydroxo species, $\text{Ti}(\text{OH})_2^{2+}$ is present in HClO_4 up to 1.5 M.¹⁸ A potentiometric investigation of Ti(IV) hydrolysis indicated that TiO^{2+} is the only species present.^{8,19} The adsorption of Ti(IV) from HCl and H_2SO_4 solutions by ion exchange resins indicated that TiO^{2+} is the predominant species.²⁰ Kinetic studies of electron transfer and complexation reactions have given conflicting results, but generally support the TiO^{2+} species. In a study of Cr^{2+} reduction of Ti(IV) there was no evidence for Cl^- complexation, seemingly ruling out $\text{Ti}(\text{OH})_2^{2+}$.²¹ As recently as 1985 $\text{Ti}(\text{OH})_2^{2+}$ has been suggested to be the predominant species, based on determinations of $[\text{Ti}(\text{IV})]/[\text{Ti}(\text{III})]$ ratios in solutions of Ti(IV) chloride equilibrated with $\text{H}_2(\text{g})$.²² But, also in 1985, the first direct evidence for TiO^{2+} was reported²³ when the TiO Raman stretch was observed. Since that time it has been reported that TiO^{2+} is in equilibrium with low concentrations of hydroxo and oligomeric species such as $\text{Ti}_3\text{O}_4^{4+}$, $\text{Ti}_3\text{O}_3\text{O}_2\text{H}_3^{5+}$ and $\text{Ti}_4\text{O}_4\text{O}_2\text{H}_4^{8+}$ in more concentrated Ti(IV) solutions ($>0.1 \text{ M}$).²⁴

A number of factors must be considered in studying Ti(III). Oxygen does not react with Ti^{3+} , but it oxidizes $TiOH^{2+}$ in an outer sphere process ($k = (4.25 \pm 0.13) M^{-1}s^{-1}$ at $25\text{ }^{\circ}C$ in 1 M LiCl).²⁵ Ti(III) reduces perchlorate in a slow reaction that is retarded by Cl^{-} and accelerated by H^{+} .²⁶ To avoid this complication a LiCl/HCl medium is generally used. The complexation of Ti(III) with Cl^{-} has a measured stability constant $K_1 = 0.07 - 0.2\text{ M}^{-1}$.²⁷ Earley has suggested that the stability of such a Cl^{-} complex must be small as no Cl^{-} effect is observed.²⁸ Finally, stainless- steel needles must be avoided because of dissolution in HCl giving Fe(II) in Ti(III) solutions.^{6a}

Ti(III) was previously reported⁶ to quench the excited state emission of (polypyridine)ruthenium(II) complexes. This is believed to occur via an energy transfer mechanism based on the lack of electron transfer products observed and on the rate, which is much faster than that expected for reductive quenching in this system. Also, there is considerable overlap between Ru(II) emission (570-660 nm) and Ti(III) absorption (502 nm with a shoulder at 575 nm).

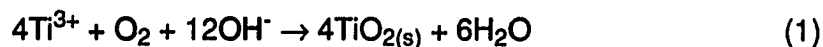
In this study Ti(III) was used to quench the excited state emission of (polypyridine)chromium(III) complexes.

EXPERIMENTAL

Solvents and reagents

Tris-(2,2'-bipyridine)chromium(III) perchlorate was prepared²⁹ by electrochemically reducing $\text{Cr}(\text{ClO}_4)_3$ at constant voltage (1.77 V) under argon. Free bpy (G.F. Smith) was added to form $\text{Cr}(\text{bpy})_3^{2+}$ which was then oxidized to $\text{Cr}(\text{bpy})_3^{3+}$ by adding Br_2 in HClO_4 . Excess free ligand was removed by repeatedly extracting with chloroform until no bpy was seen in the organic layer. A saturated solution of NaClO_4 was added and $\text{Cr}(\text{bpy})_3(\text{ClO}_4)_3$ precipitated out on cooling in an ice-salt bath. The yellow solid was filtered and washed with small amounts of ice-cold water and ether. The $\text{Cr}(\text{bpy})_3^{3+}$ was characterized by comparison with the published UV-vis spectrum³⁰ and by the lifetime of the lowest energy excited state.^{6a} Other polypyridyl complexes were available from earlier studies.³¹

Solutions of Ti(III) were prepared^{13b} as follows, using Teflon needles to avoid contact with metal. Titanium sponge (Alfa) was dissolved in 3.3 M HCl by stirring at 30-40 °C under argon for 36-48 hours. The resulting purple solution was filtered through a Metricel membrane filter (5 μm) and stored under argon at 0 °C. The Ti(III) concentration was determined spectrophotometrically at 502 nm ($\epsilon = 3.97 \text{ M}^{-1}\text{cm}^{-1}$) and the Ti(IV) at 310 nm ($\epsilon_{\text{III}} = 0.3 \text{ M}^{-1}\text{cm}^{-1}$ and $\epsilon_{\text{IV}} = 15.2 \text{ M}^{-1}\text{cm}^{-1}$).^{6a} The acid content was determined by direct titration with NaOH to a phenolphthalein endpoint. The titrations were carried out slowly with constant stirring to prevent formation of a blue-gray polymer.^{9c} A white precipitate, TiO_2 , formed according to equation 1. The acid concentration was calculated from



the relation $[\text{OH}^-] = [\text{H}^+] + 3[\text{Ti}^{3+}]$, by assuming the TiO_2 formed quantitatively.

All water used in this study was in-house distilled, deionized water passed through a Millipore-Q purification system. LiCl (Baker) was recrystallized three times from water and standardized by passing through a Dowex H^+ exchange column followed by titration with NaOH. The hydrochloric acid (Mallinckrodt), perchloric acid (Fischer) and LiClO_4 (Aldrich) were used as purchased. The argon (99.99% pure, Air Products Corp.) used for purging was passed through chromous towers to remove any trace oxygen. $[\text{Co}(\text{NH}_3)_5\text{Br}]\text{Br}_2$ and $[\text{Co}(\text{NH}_3)_5(\text{H}_2\text{O})](\text{ClO}_4)_3$ were available in our laboratory stores. The $[\text{Co}(\text{NH}_3)_5\text{Br}]\text{Br}_2$ was converted to the more soluble perchlorate salt by recrystallizing three times from dilute HClO_4 in the presence of a large excess of LiClO_4 .

Kinetics

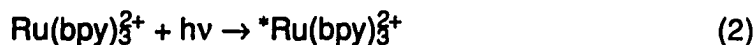
The laser flash photolysis system used for this study was a flash-lamp pumped dye laser (Phase-R model DL-1100). The pulse width is $\sim 0.6 \mu\text{s}$ and the excitation dyes used were Coumarin-460 ($1.5 \times 10^{-4} \text{ M}$ in MeOH) and LD-423 ($2 \times 10^{-4} \text{ M}$ in MeOH). The arrangement is similar to one described in the literature.³² The single-shot laser pulse impinges on a square 1-cm fluorescence cell. The emission of the excited states was monitored at 727 nm with a Hamamatsu R928 photomultiplier tube positioned at 90° to the exciting pulse. Transient absorbance measurements of $\text{Cr}(\text{NN})_3^{2+}$ species and the excited states were monitored at appropriate wavelengths^{30,33} using a 50-W quartz-halogen analyzing lamp. The voltage vs. time data was collected, digitalized and displayed on a Nicolet model 2090-3A digitalizing oscilloscope. The data was transferred to an interfaced Apple II+ microcomputer for storage

and processing using a least-squares, first-order kinetics fitting program. The error in reported rate constants is estimated to be $\leq 10\%$ based on scatter in replicate laser shots.

Cells containing LiCl and HCl were prepared using Teflon needles in all experiments involving Ti(III), and the Ti(III) was added only after cells were degassed. All cells were degassed at least 15 minutes prior to flashing. The Cr(III) was injected just before flashing using a fresh metal needle tip. Cells were generally flashed just once, but those that were flashed twice were moved so that a different portion of the cell was exposed to the laser pulse.

Laser actinometry

The excited state extinction coefficient at 445 nm was measured by laser actinometry with $\text{Ru}(\text{bpy})_3^{2+}$. LD-423 dye was chosen to maximize $\text{Cr}(\text{bpy})_3^{3+}$ absorbance and to minimize "bleaching" of $\text{Ru}(\text{bpy})_3^{2+}$ solutions. A solution of $1.89 \times 10^{-5} \text{ M}$ $\text{Ru}(\text{bpy})_3^{2+}$ ($\epsilon_{423} = 10,600 \text{ M}^{-1}\text{cm}^{-1}$)³⁴ has an absorbance of 0.20. The natural decay rate of the $^*\text{Ru}(\text{bpy})_3^{2+}$ excited state



in D_2O is $1.0 \times 10^6 \text{ s}^{-1}$.⁴³ $\text{Co}(\text{NH}_3)_5\text{Br}^{2+}$ is known to quench the excited state in a reaction that is nearly diffusion controlled ($k = 2.5 \times 10^9 \text{ L mol}^{-1}\text{s}^{-1}$).³⁵



Based on these rates, $5.0 \times 10^{-3} \text{ M}$ $\text{Co}(\text{NH}_3)_5\text{Br}^{2+}$ should quench $\sim 93\%$ of the $\text{Ru}(\text{bpy})_3^{2+}$ excited state. This concentration of $\text{Co}(\text{NH}_3)_5\text{Br}^{2+}$ ($\epsilon_{423} = 12.3 \text{ M}^{-1}\text{cm}^{-1}$) has an absorbance of 0.0615. The labile Co(II) complex formed in the oxidative quenching reaction rapidly dissociates preventing return electron transfer.

A 1-cm cell containing these concentrations of $\text{Ru}(\text{bpy})_3^{2+}$ and $\text{Co}(\text{NH}_3)_5\text{Br}^{2+}$ in 0.10 M HClO_4 in D_2O was flashed. A permanent (longer than 200 μs) loss of absorbance was observed at 445 nm due to the loss of $\text{Ru}(\text{bpy})_3^{2+}$ ($\epsilon_{445} = 12,700 \text{ M}^{-1}\text{cm}^{-1}$) and formation of $\text{Ru}(\text{bpy})_3^{3+}$ ($\epsilon_{445} = 1500 \text{ M}^{-1}\text{cm}^{-1}$).³⁴

In the second part of this experiment the above conditions were matched as closely as possible. A $2.78 \times 10^{-4} \text{ M}$ solution of $\text{Cr}(\text{bpy})_3^{3+}$ ($\epsilon_{423} = 720 \text{ M}^{-1}\text{cm}^{-1}$)³⁰ has an absorbance of 0.20. Because $\text{Co}(\text{NH}_3)_5\text{Br}^{2+}$ quenches the ${}^2\text{E}$ excited state³⁶ of $\text{Cr}(\text{bpy})_3^{3+}$ so rapidly, $\text{Co}(\text{NH}_3)_5\text{H}_2\text{O}^{3+}$ was substituted. It quenches the excited state with a rate constant of $1 \times 10^6 \text{ L mol}^{-1}\text{s}^{-1}$ ³⁷ and has an ϵ_{423} of $21.6 \text{ M}^{-1}\text{cm}^{-1}$. Thus, a concentration of $2.85 \times 10^{-3} \text{ M}$ is required to match the absorbance of $\text{Co}(\text{NH}_3)_5\text{Br}^{2+}$ in the $\text{Ru}(\text{bpy})_3^{2+}$ experiment.

A 1-cm cell containing these concentrations of $\text{Cr}(\text{bpy})_3^{3+}$ and $\text{Co}(\text{NH}_3)_5\text{H}_2\text{O}^{3+}$ in 0.10 M HClO_4 was flashed. The absorbance of the $\text{Cr}(\text{bpy})_3^{3+}$ excited state was monitored at 445 nm. The maximum absorbance change was taken as due to the loss of the ground state $\text{Cr}(\text{III})$ complex and formation of the excited state. The concentration of the excited state formed in the flash was assumed to be equal to the ${}^* \text{Ru}(\text{bpy})_3^{2+}$ formed in the previous experiment. Thus, the $\Delta\epsilon$ could be calculated.

RESULTS

The lifetimes of the 2E excited states were measured in 1 M HCl by monitoring the emission at 727 nm. For each complex the Cr(III) ground state concentration was varied so that τ° , the lifetime at infinite Cr(III) dilution, could be obtained by extrapolation. The concentrations and observed rate constants are listed in the Appendix in Tables A1 through A7. The τ° values are given in Table 1 and agree with previously reported values.^{29,38,39}

Table 1. Emission lifetimes of $\text{Cr}(\text{NN})_3^{3+}$ excited states^a

NN	$\tau^\circ / \mu\text{s}$	$\tau^\circ / \mu\text{s}^b$	$\tau^\circ / \mu\text{s}^c$	$\tau^\circ / \mu\text{s}^d$
bpy	69	63	66	—
4,4'-(CH ₃) ₂ bpy	197	230	180	200
phen	271	270	270	330
5-Clphen	136	130	156	180
5-(CH ₃)phen	320	-	310	420
5,6-(CH ₃) ₂ phen	314	-	-	420 ^e
4,7-(CH ₃) ₂ phen	451	340	580	570 ^e

^a In 1 M HCl; τ° values obtained by extrapolation to infinite $\text{Cr}(\text{NN})_3^{3+}$ dilution. ^b Ref. 8. ^c Ref. 29. ^d Ref. 39. ^e Solutions contained 4 % CH₃CN.

Upon addition of Ti(III) the emission lifetime was shortened significantly. Also, the formation of the corresponding Cr(II) complex could be observed by monitoring its absorbance increase. The absorbance change was permanent,

indicating the Cr(II) complex was stable for at least 200 μs . For example, in the case of $\text{Cr}(\text{5-Clphen})_3^{3+}$, formation of $\text{Cr}(\text{5-Clphen})_3^{2+}$ was monitored at 410 nm. A typical trace is shown in Figure 1. To further support the $\text{Cr}(\text{NN})_3^{2+}$ formation the absorption spectrum of the product in the case of $\text{Cr}(\text{bpy})_3^{3+}$ was taken point by point and is shown in Figure 2. This spectrum agrees with that reported for $\text{Cr}(\text{bpy})_3^{2+}$.³³

Quenching rate constants were measured in 1 M HCl by monitoring the emission at 727 nm and varying the Ti(III) concentration. The specific observed rate constants and concentrations used are listed in the Appendix in Tables A8 through A14. Plots of k_{obs} vs. $[\text{Ti(III)}]_{\text{T}}$ for the different chromium complexes are shown in Figure 3. For each case the resulting second order rate constant, k_{q} , is listed in Table 2 along with the intercept, k°_{obs} . The intercepts are higher than the k° values that would be predicted from the lifetime measurements. This difference may be accounted for by Cr(II) quenching and is discussed later.

Acid dependence

For each Cr(III) complex the H^+ concentration was varied from 0.1 to 1.0 M with HCl, using LiCl to maintain ionic strength at 1 M. The specific concentrations and observed rate constants are given in the Appendix in Tables A15 through A21. The observed rate constant is due to the terms shown in equation 4.

$$k_{\text{obs}} = k_{\text{obs}}^{\circ} + k_1[\text{TiOH}^{2+}][*Cr^{3+}] + k_2[\text{Ti}^{3+}][*Cr^{3+}] \quad (4)$$

Rearranging and applying the K_{a} expression for $\text{Ti}(\text{H}_2\text{O})_6^{3+}$ yields equation 5.

$$k' = \frac{k_{\text{obs}} - k_{\text{obs}}^{\circ}}{[\text{Ti(III)}]_{\text{T}}} = \frac{k_1 K_{\text{a}} + k_2 [\text{H}^+]}{K_{\text{a}} + [\text{H}^+]} \quad (5)$$

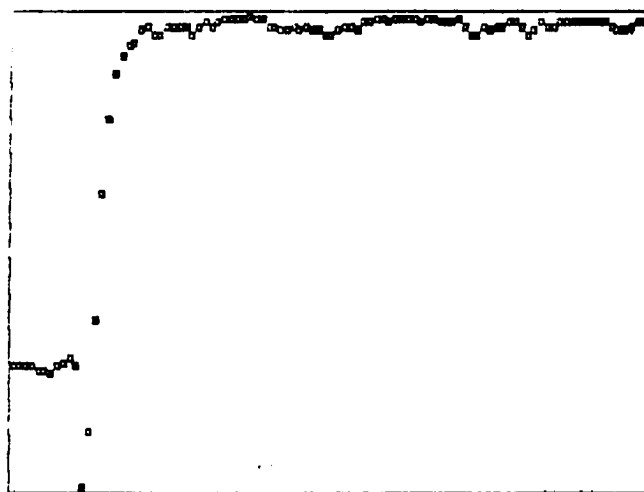


Figure 1. Formation of $\text{Cr}(\text{5-Clphen})_3$ monitored at 410 nm on a time scale of 1 μs per point

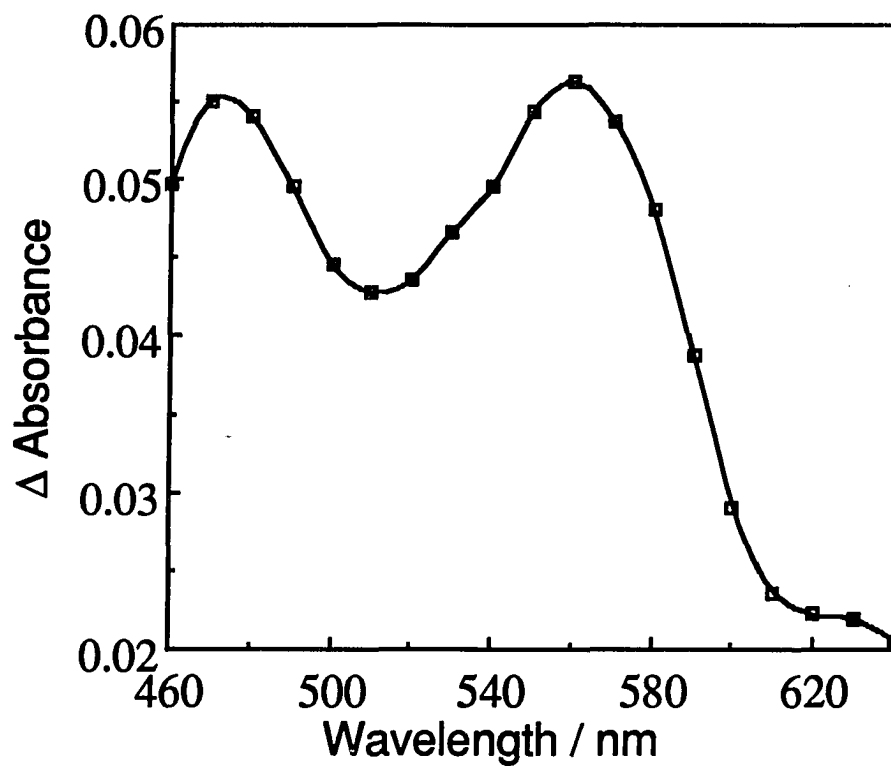


Figure 2. Spectrum of $\text{Cr}(\text{bpy})_3^{2+}$ formed in the quenching of $^*\text{Cr}(\text{bpy})_3^{3+}$ by $\text{Ti}(\text{III})$

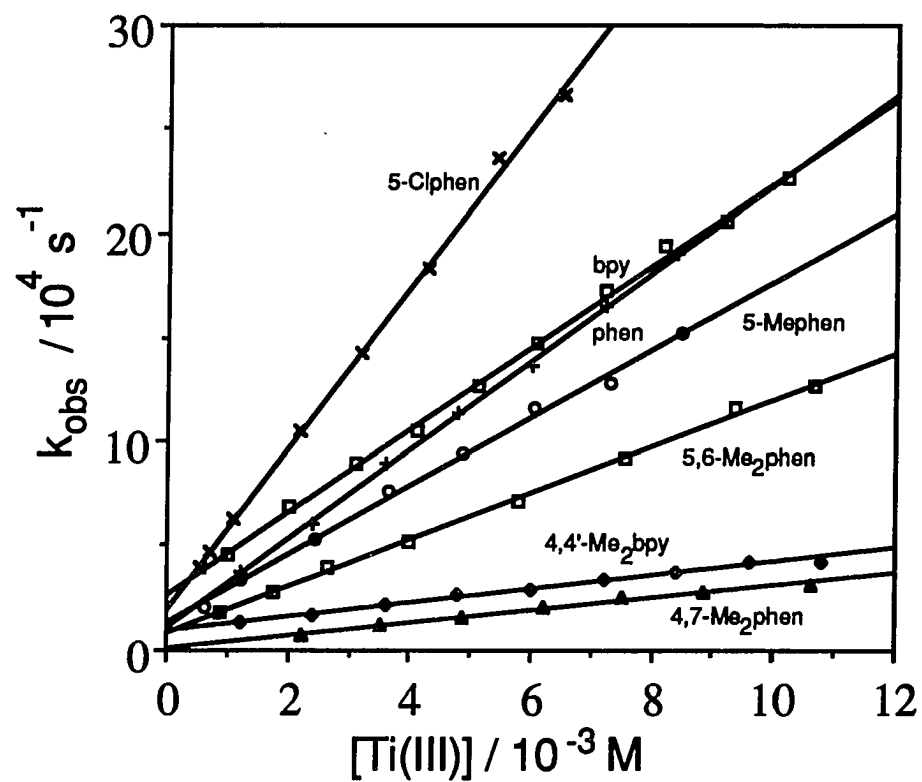


Figure 3. Plots of the linear variation of k_{obs} with $[\text{Ti(III)}]_T$ in the quenching of $^*\text{Cr(NN)}_3^{3+}$ by Ti(III) in 1 M HCl

Table 2. Quenching rate constants in 1 M HCl

NN	$k_q / 10^7$ L mol ⁻¹ s ⁻¹	$k^{\circ}_{\text{obs}}{}^a / 10^4$ s ⁻¹	$k^{\text{ob}} / 10^4$ s ⁻¹
bpy	1.99	2.6	1.5
4,4'-(CH ₃) ₂ bpy	0.334	0.90	0.56
phen	2.12	1.1	0.50
5-Clphen	3.87	1.9	0.90
5-(CH ₃)phen	1.69	1.1	0.63
5,6-(CH ₃) ₂ phen	1.12	0.83	0.53
4,7-(CH ₃) ₂ phen	0.311	0.49	0.46

^a Values obtained from extrapolation to infinite Ti(III) dilution. ^b Values in absence of Ti(III).

$$[\text{Ti(III)}]_{\text{T}} = [\text{Ti(H}_2\text{O)}_5\text{OH}^{2+}] + [\text{Ti(H}_2\text{O)}_6^{3+}] \quad (6)$$

A value for K_a of 4.6×10^{-3} M has been reported⁴⁰ in 1 M ionic strength with LiCl. The data were fit to equation 5 using a non-linear least squares program. Values for k_1 and k_2 are given in Table 3. Fitted plots of k' vs. $[\text{H}^+]^{-1}$ are shown in Figures 4 and 5.

The effect of $[\text{Cl}^-]$ on the rate of quenching was investigated using ClO_4^- to maintain 1 M ionic strength. This was done at relatively low acid concentration (0.1 M) to slow the rate of reduction of ClO_4^- by Ti(III). The Cr(bpy)_3^{3+} ground state concentration was 4.93×10^{-4} M and the total Ti(III) concentration was 5.58×10^{-3} M. The average k_{obs} in 1M Cl^- was 2.32×10^5 s⁻¹. The average k_{obs} in 0.9 M ClO_4^- and 0.1 M Cl^- was 9.81×10^4 s⁻¹.

Table 3. Quenching rate constants for TiOH^{2+} (k_1) and Ti^{3+} (k_2)^a

NN	$k_1 / 10^8$	$k_2 / 10^7$
	$\text{L mol}^{-1}\text{s}^{-1}$	$\text{L mol}^{-1}\text{s}^{-1}$
bpy	6.0	1.9
4,4'-(CH_3) ₂ bpy	1.0	0.26
phen	4.6	1.6
5-Clphen	9.7	3.7
5-(CH_3)phen	4.7	1.5
5,6-(CH_3) ₂ phen	3.0	1.2
4,7-(CH_3) ₂ phen	0.81	0.28

^a In HCl / LiCl with $\mu = 1.0$ M.

Quantum yields

The $\text{Cr}(\text{bpy})_3^{3+}$ excited state extinction coefficient at 445 nm was measured by laser actinometry to be ca. $3000 \text{ M}^{-1}\text{cm}^{-1}$. Small signals limited the accuracy of this experiment. This value was used to determine the concentration of $^*\text{Cr}(\text{bpy})_3^{3+}$ formed in the flash. The total amount of $\text{Cr}(\text{bpy})_3^{2+}$ formed was measured at 560 nm ($\epsilon = 4800 \text{ M}^{-1}\text{cm}^{-1}$). Thus, the quantum yield for $\text{Cr}(\text{bpy})_3^{2+}$ formation was calculated from equation 7. Values for ϕ_{Cr} at different $\text{Ti}(\text{III})$ concentrations are listed in Table 4.

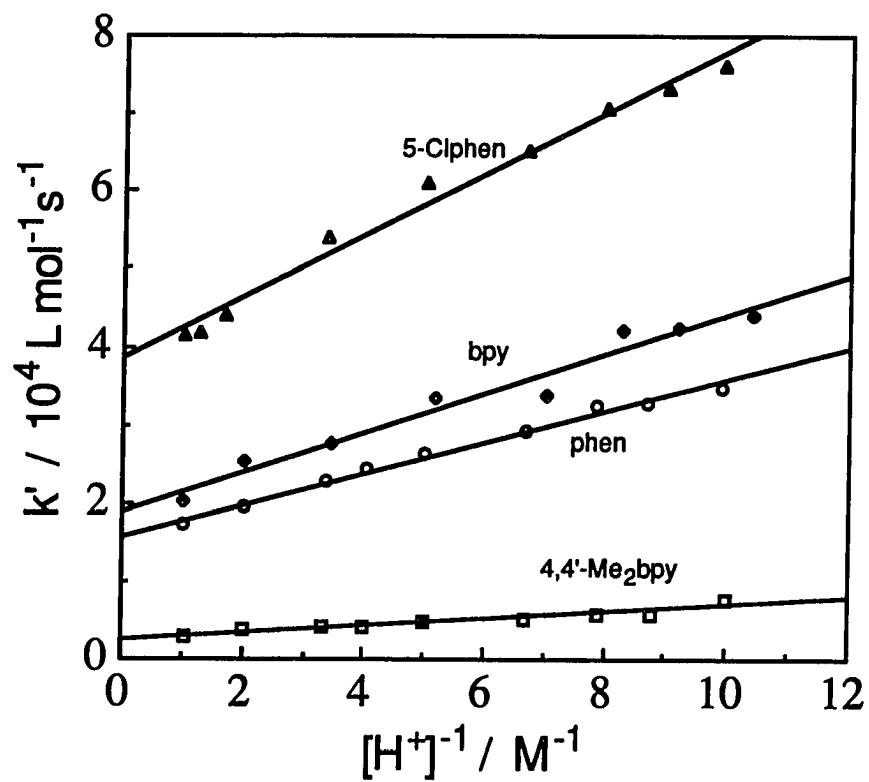


Figure 4. Effect of $[\text{H}^+]$ on the quenching of ${}^*\text{Cr}(\text{NN})_3^{3+}$ by $\text{Ti}(\text{III})$

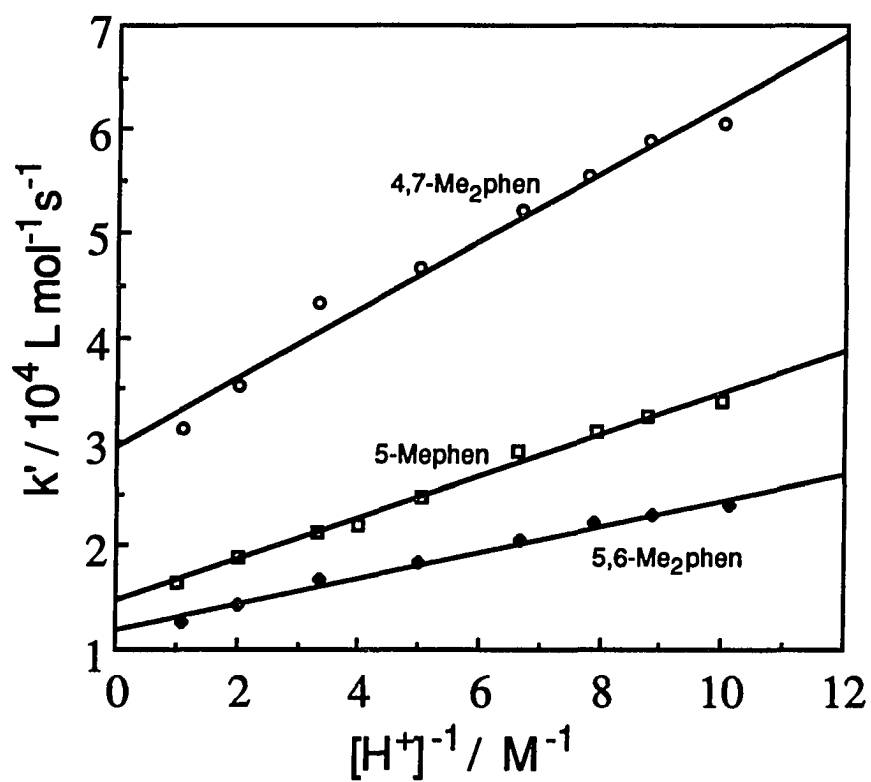


Figure 5. Effect of $[\text{H}^+]$ on the quenching of ${}^*\text{Cr}(\text{NN})_3^{3+}$ by $\text{Ti}(\text{III})$

Table 4. Quantum yields for formation of $\text{Cr}(\text{bpy})_3^{2+}$ ^a

$[\text{Ti(III)}] /$ 10^{-3} M	$[\text{*Cr}^{3+}]^{\text{b}} /$ 10^{-5} M	$1/2 [\text{Cr(II)}]_{\infty}^{\text{c}} /$ 10^{-5} M	ϕ_{obs}	$\phi_{\text{calc}}^{\text{d}}$
1.69	1.08	0.53	0.49	0.46
1.85	2.89	1.14	0.39	0.40
6.78	1.08	7.70	0.71	0.75
7.43	2.89	2.05	0.71	0.66
8.09	1.21	1.17	0.97	0.74
8.45	1.55	1.36	0.88	0.73
11.3	1.31	1.20	0.92	0.80

^a In 1 M HCl. ^b Measured at 445 nm. ^c Estimated by KINSIM program (see discussion). ^d Calculated according to equation 18

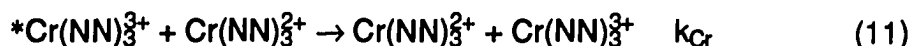
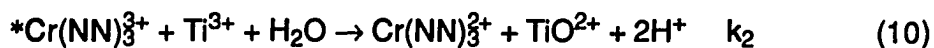
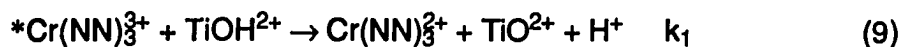
DISCUSSION

The acid dependence indicates that both an acid-independent path and an acid-dependent path are functioning. Such behavior is common in Ti(III) redox reactions and is attributed to reduction by both Ti^{3+} and TiOH^{2+} . As seen in Table 3, the rate of quenching by TiOH^{2+} is always much faster than that of Ti^{3+} . This is also generally true in Ti(III) redox chemistry and is explained in terms of the product. The Ti(IV) species formed is believed to be TiO^{2+} and so a shorter TiO bond such as in TiOH^{2+} has a lower barrier to reaction.

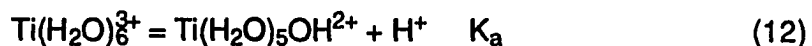
As the Cr(II) product formed is stable for time scales used here, there is no return electron transfer occurring, despite a favorable driving force. This means there must be some barrier to reaction, perhaps due to the stability of TiO^{2+} . The immediate product of outer sphere electron transfer would be TiO^+ , which must be too unstable.

The quenching of the doublet excited state of $\text{Cr}(\text{NN})_3^{3+}$ is shown in Scheme I.

Scheme I:



The $\text{Ti}(\text{H}_2\text{O})_6^{3+}$ is in acid equilibrium as in equation 12.



This leads to a rate law as in equation 13 and a k_{obs} as in equation 14.

$$\frac{-d[*Cr(NN)_3^{3+}]}{dt} = (k^{\circ} + k_{Cr}[Cr(NN)_3^{2+}] + k_1[TiOH^{2+}] + k_2[Ti^{3+}] [*Cr(NN)_3^{3+}] \quad (13)$$

$$k_{obs} = k^{\circ} + k_{Cr}[Cr(NN)_3^{2+}] + k_1[TiOH^{2+}] + k_2[Ti^{3+}] \quad (14)$$

When the k_{obs} values are plotted against $[Ti(III)]_T$ at constant acid concentration, the extrapolated intercepts, k°_{obs} , are always significantly higher than measurements in the absence of Ti(III) (see Table 2). This may be accounted for by $Cr(NN)_3^{2+}$ quenching (equation 11). The rate constant for this quenching, k_{Cr} , in the case of $Cr(bpy)_3^{2+}$ has been measured to be $(5 \pm 3) \times 10^9 M^{-1}s^{-1}$.⁴¹ The concentration of $Cr(bpy)_3^{2+}$ depends on equations 9 and 10 and increases as the reaction proceeds. Also, the concentrations of $*Cr^{3+}$ and Cr^{2+} both depend on $[Ti(III)]_T$ as well as the relative amounts of Ti^{3+} and $TiOH^{2+}$ present (i.e. they are acid dependent).

The fraction of quenching by Ti(III) species at constant H^+ is given by equation 15 where $k_q = k_1K_a/[H^+] + k_2$.

$$\frac{k_q[Ti(III)]_T}{k^{\circ} + k_{Cr}[Cr(NN)_3^{2+}] + k_q[Ti(III)]_T} = \frac{[Cr(NN)_3^{2+}]_{\infty}}{[*Cr(NN)_3^{3+}]_0} \quad (15)$$

The remaining fraction that goes via reactions 8 and 11 is given by equation 16.

$$\frac{k^{\circ} + k_{Cr}[Cr(NN)_3^{2+}]}{k^{\circ} + k_{Cr}[Cr(NN)_3^{2+}] + k_q[Ti(III)]_T} = \frac{[*Cr(NN)_3^{3+}]_0 - [Cr(NN)_3^{2+}]_{\infty}}{[*Cr(NN)_3^{3+}]_0} \quad (16)$$

By taking the ratio of these two fractions and rearranging, an expression for $k_{Cr}[Cr(NN)_3^{2+}]$ is obtained as in equation 17.

$$k_{Cr}[Cr(NN)_3^{2+}] = \frac{([*Cr(NN)_3^{2+}]_0 - [Cr(NN)_3^{2+}]_{\infty})(k_q[Ti(III)])}{[Cr(NN)_3^{2+}]_{\infty}} - k^{\circ} \quad (17)$$

However, the concentration of $Cr(NN)_3^{2+}$ is not constant as the reaction progresses. The $[Cr(NN)_3^{2+}]$ in these equations (15-17) is the amount that, if it were constant throughout the reaction, would account for the lowering of the quantum yield of $Cr(NN)_3^{2+}$ due to reaction 11.

For the case involving $Cr(bpy)_3^{3+}$ calculations were carried out to correct the k°_{obs} value for quenching by $Cr(II)$. The program KINSIM⁴² was used to estimate the infinity value for $[Cr(bpy)_3^{2+}]$ at each $Ti(III)$ concentration and the excited state initial concentration was assumed to be 10% of the ground state concentration of $Cr(bpy)_3^{3+}$. Thus, using equation 17, a value of $[Cr(bpy)_3^{2+}]$ was calculated for each $Ti(III)$ concentration at constant $[H^+]$.

The term $k_{Cr}[Cr(NN)_3^{2+}]$ can be subtracted from k_{obs} , giving a corrected value, k_{obs}' , so that a plot of k_{obs}' vs. $[Ti(III)]_T$ is linear with an intercept of k° . The values calculated for $[Cr(bpy)_3^{3+}]_{\infty}$, $k_{Cr}[Cr(bpy)_3^{3+}]$ and k_{obs}' are given in Table 5 and a plot of k_{obs}' vs. $[Ti(III)]_T$ is shown in Figure 6. The corrected intercept of $2.17 \times 10^4 \text{ s}^{-1}$ is closer to but still somewhat higher than the expected value of $1.5 \times 10^4 \text{ s}^{-1}$ at this $Cr(NN)_3^{3+}$ ground state concentration. If the initial excited state concentration is greater than 10% of the ground state concentration, as has been observed at concentrations such as these, then the contribution of $Cr(bpy)_3^{2+}$ quenching would be larger (according to equation

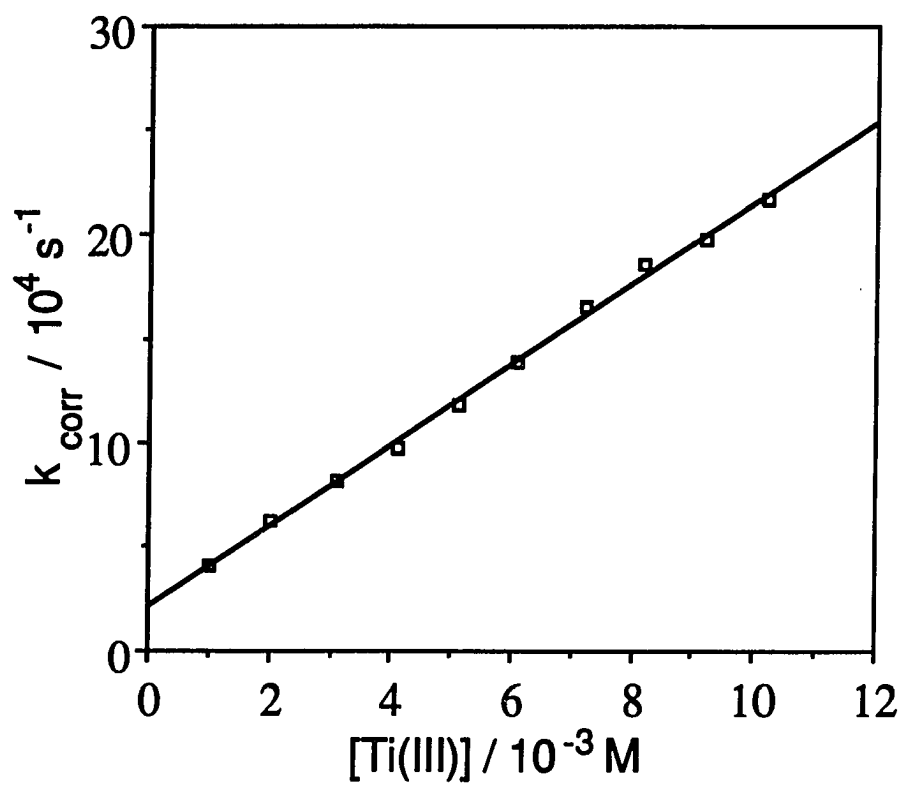


Figure 6. Quenching of ${}^*\text{Cr}(\text{bpy})_3^{3+}$ by Ti(III) corrected for quenching by $\text{Cr}(\text{bpy})_3^{2+}$

Table 5. Values calculated from KINSIM^a in correction for Cr(bpy)₃²⁺ quenching^b

$[\text{Ti(III)}]_{\text{T}} /$ 10^{-3} M	$[\text{Cr}^{2+}]_{\infty} /$ 10^{-6} M	$k_{\text{Cr}}[\text{Cr}^{2+}] /$ 10^{-3} s^{-1}	$k_{\text{obs}}' /$ 10^{-4} s^{-1}
1.0	1.93	4.6	4.1
2.0	2.49	6.2	6.2
3.1	2.81	7.0	8.2
4.1	3.00	7.0	9.8
5.1	3.11	7.8	12
6.1	3.20	8.1	14
7.2	3.29	7.5	17
8.2	3.34	7.8	19
9.2	3.37	8.7	20
10.2	3.41	8.6	22

^a Kinetic simulation program. ^b [^{*}Cr(bpy)₃³⁺] assumed to be $3.8 \times 10^{-6} \text{ M}$ (see text); $[\text{H}^+] = 1 \text{ M}$.

17). Thus, the larger intercept can be reasonably attributed to Cr(bpy)₃²⁺ quenching competing with Ti(III) quenching.

Using this value of $k_{\text{Cr}}[\text{Cr(II)}]$ in equation 18, an estimated value for the quantum yield of Cr(II) may be calculated at different Ti(III) concentrations.

$$\phi_{\text{calc}} = \frac{k_q[\text{Ti(III)}]_T}{k^\circ + k_q[\text{Ti(III)}]_T + k_{\text{Cr}}[\text{Cr(NN)}_3^{2+}]} \quad (18)$$

The quantum yields obtained from this calculation are listed in Table 4 and agree well with the observed quantum yield. This indicates the Cr(II) quenching is significant and suggests the excited state extinction coefficient is accurate.

The value of $3000 \pm 200 \text{ M}^{-1}\text{cm}^{-1}$ for the excited state extinction coefficient at 445 nm agrees with previous reports.⁴³ A value of $4800 \text{ M}^{-1}\text{cm}^{-1}$ was previously reported by this lab.⁴¹ However, that experiment required an extrapolation back to time zero on the kinetic trace to estimate the concentration of $^*\text{Ru}(\text{bpy})_3^{2+}$. In this work $\text{Co}(\text{NH}_3)_5\text{Br}^{2+}$ was added as a quencher so that $\text{Ru}(\text{bpy})_3^{3+}$ was formed with a quantum yield (estimated from k_q and the k° in D_2O) of 0.92. Since this $\text{Ru}(\text{bpy})_3^{3+}$ is relatively stable under the conditions used here, its absorbance at 445 nm could be monitored directly, giving a more reliable value for the initial excited state concentration.

Problems with this experiment included bleaching of the ground state $\text{Ru}(\text{bpy})_3^{2+}$ and/or small signals in the $\text{Cr}(\text{bpy})_3^{3+}$ experiment. A more intense, lower wavelength dye would improve the accuracy of this experiment. At lower wavelengths, $\text{Ru}(\text{bpy})_3^{2+}$ absorbs less and $\text{Cr}(\text{bpy})_3^{3+}$ absorbs more. Thus, higher concentrations of $\text{Ru}(\text{bpy})_3^{2+}$ could be used allowing a higher laser power to be applied without bleaching the ground state concentration. This higher laser power would allow larger, more reliable signals in the $\text{Cr}(\text{bpy})_3^{3+}$ experiment.

The reduction potential for Ti(IV/III) has been measured in 1 M HCl as -16 mV and equation 19 applies.⁸

$$E = -0.016 - 0.059 \log\left(\frac{[\text{Ti(III)}]}{[\text{Ti(IV)}][\text{H}^+]^2}\right) \quad (19)$$

Table 6. Data for linear free energy relationship

NN	*E ^o _a / V	ΔE ₁ ^b / V	ΔE ₂ ^c / V	log k ₁	log k ₂
bpy	1.44	1.54	1.37	8.78	7.27
4,4'-(CH ₃) ₂ bpy	1.25	1.35	1.18	8.00	6.41
phen	1.42	1.52	1.35	8.66	7.20
5-Clphen	1.53	1.63	1.46	8.99	7.57
5-(CH ₃)phen	1.39	1.49	1.32	8.67	7.16
5,6-(CH ₃) ₂ phen	1.40 ^d	1.50	1.33	8.47	7.08
4,7-(CH ₃) ₂ phen	1.23	1.33	1.16	7.91	6.45

^a Ref. 29. ^b E^o_{TiOH} = -0.10 V. ^c E^o_{Ti} = 0.07 V. ^d Ref. 40.

Utilizing expressions for hydrolysis constants of Ti(IV) ($K_{H1}K_{H2} \sim 25 \text{ M}^2$), the potential for the reduction of Ti⁴⁺ (equation 20) is estimated to be ~-0.07 V.



Similarly, the potential for the reduction of TiOH³⁺ (equation 21) is estimated to be ~-0.10 V. Table 6 gives values for the driving force of the quenching of each of the *Cr(NN)₃³⁺ complexes by TiOH²⁺ and Ti³⁺. Figure 7 shows that there is a linear dependence on driving force for both. The slopes of these lines are 4.0 for Ti³⁺ and 3.7 for TiOH²⁺. The large driving forces of these reactions do not

allow application of the Marcus cross relation to estimate the self-exchange rate constants for $\text{Ti}^{4+}/\text{Ti}^{3+}$ and $\text{TiOH}^{3+}/\text{TiOH}^{2+}$.

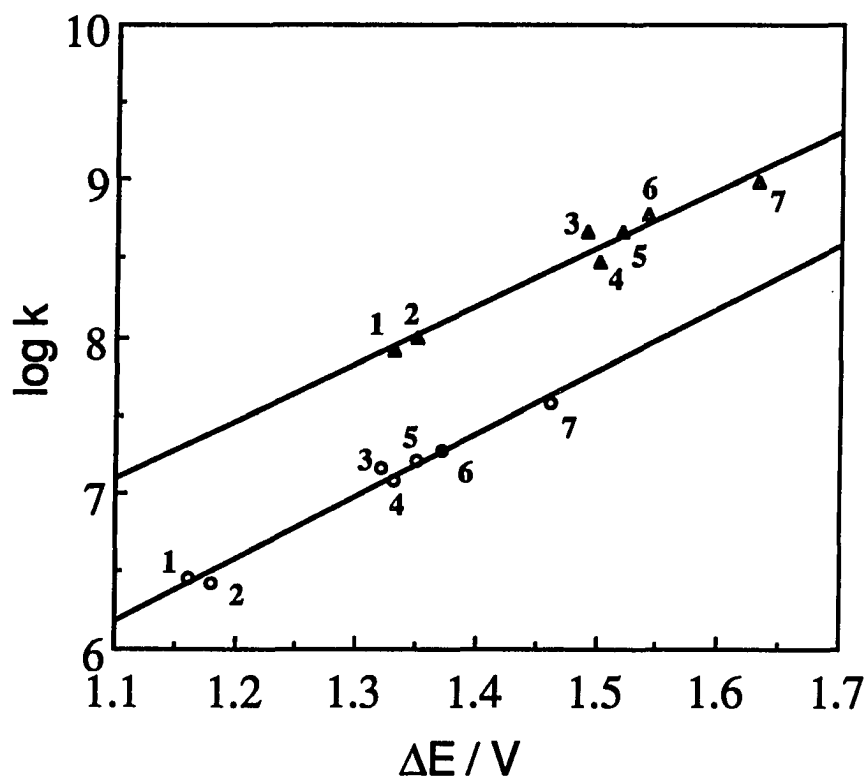


Figure 7. Variation with driving force of second-order rate constants for quenching of ${}^3\text{Cr}(\text{NN})_3^{3+}$ by TiOH_2^+ (triangles) and Ti^{3+} (circles)

REFERENCES

1. Barone, P.; Earley, J.E. *Inorg. Chem.* **1988**, *27*, 1378.
2. Thompson, G.A.K.; Sykes, A.G. *Inorg. Chem.* **1976**, *15*, 638.
3. Adegite, A.; Iyun, J.F. *Inorg. Chem.* **1979**, *18*, 3602.
4. Bakac, A.; Espenson, J.H.; Lovric, J.; Orhanovic, M. *Inorg. Chem.* **1987**, *26*, 4096.
5. Ellis, J.D.; Sykes, A.G. *J. Chem. Soc. Dalton Trans.* **1973**, 537.
6. (a) Ellis, J.D.; Sykes, A.G. *J. Chem. Soc. Dalton Trans.* **1973**, 2553; (b) Birk, J.P.; Logan, T.P. *Inorg. Chem.* **1973**, *12*, 580.
7. McAuley, A.; Olubuyide, O.; Spencer, L.; West, P.R. *Inorg. Chem.* **1984**, *23*, 2594.
8. Brunschwig, B.S.; Sutin, N. *Inorg. Chem.* **1979**, *18*, 1731.
9. (a) Iadevia, R.; Earley, J.E. *Inorg. Chim. Acta.* **1981**, *53*, L143; (b) Davies, K.M.; Earley, J.E. *Inorg. Chem.* **1978**, *17*, 3350; (c) Earley, J.E.; Bose, R.N.; Berrie, B.H. *Inorg. Chem.* **1983**, *22*, 1836.
10. Olubuyide, O.; Earley, J.E. *Inorg. Chem.* **1981**, *20*, 3569.
11. Martin, A.H.; Gould, E.S. *Inorg. Chem.* **1976**, *15*, 1934.
12. Olubuyide, O.; Lu, K.; Oyetunji, O.; Earley, J.E. *Inorg. Chem.* **1986**, *25*, 4798.
13. (a) Lee, R.A.; Earley, J.E. *Inorg. Chem.* **1981**, *20*, 1739; (b) Bakac, A.; Orhanovic, M. *Inorg. Chim. Acta* **1977**, *21*, 173.
14. Bose, R.N.; Earley, J.E. *Inorg. Chem.* **1981**, *20*, 2739.
15. Marcec, R.; Orhanovic, M. *Inorg. Chim. Acta* **1979**, *37*, 67.
16. Bose, R.N.; Cornelius, R.D.; Mullen, A.C. *Inorg. Chem.* **1987**, *26*, 1414.
17. Marcus, R.A. *J. Chem. Phys.* **1965**, *43*, 679, 2654.
18. Beukenkamp, J.; Herrington, K.D. *J. Am. Chem. Soc.* **1960**, *82*, 3025.

19. Caglioti, V.; Ciavatta, L.; Liberti, A. *J. Inorg. Nucl. Chem.* **1960**, *15*, 115.
20. Nabivanets, B.I. *Russ. J. Inorg. Chem.* **1962**, *7*, 212.
21. Ellis, J.D.; Thompson, G.A.K.; Sykes, A.G. *Inorg. Chem.* **1976**, *15*, 3172.
22. Ciavatta, L.; Ferri, D.; Riccio, G. *Polyhedron* **1985**, *4*, 15.
23. Gratzel, M.; Rotzinger, F.P. *Inorg. Chem.* **1985**, *24*, 2320.
24. Comba, P.; Merbach A. *Inorg. Chem.* **1987**, *26*, 1315.
25. Rotzinger, F.P.; Gratzel, M. *Inorg. Chem.* **1987**, *26*, 3704.
26. Duke, F.R.; Quinney, P.R. *J. Am. Chem. Soc.* **1954**, *76*, 3800.
27. Gardner, H.J. *Aust. J. Chem.* **1967**, *20*, 2357.
28. Chalilpoyil, P.; Davies, K.M.; Earley, J.E. *Inorg. Chem.* **1977**, *16*, 3344.
29. Brunschwig, B.; Sutin, N. *J. Am. Chem. Soc.* **1978**, *100*, 7568.
30. Konig, E.; Herzog, S. *J. Inorg. Nucl. Chem.* **1970**, *32*, 585.
31. Simmons, C.A.; Espenson, J.H.; Bakac, A. *Inorg. Chem.* **1989**, *28*, 581.
32. Hoselton, M.A.; Lin, C.-T.; Schwarz, H.A.; Sutin, N. *J. Am. Chem. Soc.* **1978**, *100*, 2383.
33. Serpone, N.; Jamieson, M.A.; Emmi, S.S.; Fucchi, P.G.; Mulazzani, Q.G.; Hoffman, M.Z. *J. Am. Chem. Soc.* **1981**, *103*, 1091.
34. Kalyanasundaram, K. *Coord. Chem. Rev.* **1982**, *46*, 159.
35. Navon, G.; Sutin, N. *Inorg. Chem.* **1974**, *13*, 2159.
36. For simplicity, the excited state is designated as a 2E state, whereas there are really two emission bands (at 695 and 727 nm), that have been shown to have the same lifetimes; the emitting states are believed to be in thermal equilibrium. The emission bands have been assigned to $^4A \rightarrow ^2E$ and $^4A \rightarrow ^2T_1$ transitions.
37. Gandolfi, M.T.; Maestri, M.; Sandrini, D.; Balzani, V. *Inorg. Chem.* **1983**, *22*, 3435.

38. Serpone, N.; Jamieson, M.A.; Henry, M.S.; Hoffman, M.Z.; Bolletta, F.; Maestri, M. *J. Am. Chem. Soc.* **1979**, *101*, 2907.
39. Serpone, N.; Jamieson, M.A.; Sriram, R.; Hoffman, M.Z. *Inorg. Chem.* **1981**, *20*, 3983.
40. Orhanovic, M.; Earley, J.E. *Inorg. Chem.* **1975**, *14*, 1478.
41. Bakac, A.; Zahir, K.; Espenson, J.H. *Inorg. Chem.* **1988**, *27*, 315.
42. Barshop, B.A.; Wrenn, C.F.; Frieden, C. *Anal. Biochem.* **1983**, *130*, 134. We are grateful to Professor Frieden for a copy of this program.
43. Maestri, M.; Bolletta, F.; Moggi, L.; Balzani, V.; Henry, M.S.; Hoffman, M.Z. *J. Am. Chem. Soc.* **1978**, *100*, 2694.

APPENDIX

Table A1. Ground state quenching of $^*Cr(bpy)_3^{3+a}$

$[Cr(bpy)_3^{3+}] / 10^{-5} M$	$k_{obs} / 10^3 s^{-1}$
2.08	15.22
4.15	14.79
6.23	15.36
8.31	15.49
10.38	16.02
12.46	16.56

^a In 1 M HCl.

Table A2. Ground state quenching of $^*Cr(4,4-(CH_3)_2bpy)_3^{3+a}$

$[Cr(4,4-(CH_3)_2bpy)_3^{3+}] / 10^{-5} M$	$k_{obs} / 10^3 s^{-1}$
1.70	5.32
3.40	5.54
5.10	5.92
6.80	6.09
8.50	6.27
10.20	6.60

^a In 1 M HCl.

Table A3. Ground state quenching of $^*Cr(phen)_3^{3+a}$

$[Cr(phen)_3^{3+}] / 10^{-5} M$	$k_{obs} / 10^3 s^{-1}$
1.50	4.10
2.90	4.50
4.40	4.25
5.90	4.95
7.30	5.60
8.80	5.25
10.30	5.80

^a In 1 M HCl.**Table A4.** Ground state quenching of $^*Cr(5-Clphen)_3^{3+a}$

$[Cr(5-Clphen)_3^{3+}] / 10^{-5} M$	$k_{obs} / 10^3 s^{-1}$
1.4	8.0
2.9	8.9
4.3	10.6
5.7	12.0
7.2	12.0
8.6	12.6
10.0	13.1

^a In 1 M HCl.

Table A5. Ground state quenching of $^*Cr(5-(CH_3)phen)_3^{3+a}$

$[Cr(5-(CH_3)phen)_3^{3+}] / 10^{-5} M$	$k_{obs} / 10^3 s^{-1}$
1.7	4.84
3.3	6.27
5.0	7.36
6.6	8.84
8.3	8.84
9.9	13.2

^a In 1 M HCl.**Table A6.** Ground state quenching of $^*Cr(5,6-(CH_3)_2phen)_3^{3+a}$

$[Cr(5,6-(CH_3)_2phen)_3^{3+}] / 10^{-5} M$	$k_{obs} / 10^3 s^{-1}$
1.45	4.04
2.90	5.32
4.35	6.20
5.80	7.04
7.26	8.24
8.70	8.68

^a In 1 M HCl.

Table A7. Ground state quenching of ${}^*Cr(4,7-CH_3)_2phen)_3^{3+a}$

$[Cr(4,7-(CH_3)_2phen)_3^{3+}] / 10^{-5} M$	$k_{obs} / 10^3 s^{-1}$
1.59	2.99
3.18	4.61
4.77	4.78
6.36	6.38
7.95	6.38
9.54	7.82

^a In 1 M HCl.

Table A8. Quenching of ${}^*Cr(bpy)_3^{3+}$ In 1 M HCl^a

$[Ti(III)] / 10^{-3} M$	$k_{obs} / 10^4 s^{-1}$
1.0	4.52
2.0	6.86
3.1	8.91
4.1	10.48
5.1	12.64
6.1	14.66
7.2	17.26
8.2	19.35
9.2	20.65
10.2	22.69

^a $[Cr(bpy)_3^{3+}] = 3.83 \times 10^{-5} M$.

Table A9. Quenching of ${}^*Cr(4,4'-(CH_3)bpy)_3^{3+}$ in 1 M HCl^a

$[Ti(III)] / 10^{-3} M$	$k_{obs} / 10^4 s^{-1}$
1.2	1.27
2.4	1.70
3.6	2.16
4.8	2.61
6.0	2.94
7.2	3.37
8.4	3.70
9.6	4.16
10.8	4.24

^a $[Cr(4,4'-(CH_3)_2bpy)_3^{3+}] = 3.39 \times 10^{-5} M$.

Table A10. Quenching of ${}^*Cr(phen)_3^{3+}$ in 1 M HCl^a

$[Ti(III)] / 10^{-3} M$	$k_{obs} / 10^4 s^{-1}$
1.2	3.69
2.4	6.02
3.6	8.91
4.8	11.28
6.0	13.64
7.2	16.48
8.4	18.99

^a $[Cr(phen)_3^{3+}] = 3.0 \times 10^{-5} M$.

Table A11. Quenching of $^*Cr(5-Clphen)_3^{3+}$ in 1 M HCl^a

$[Ti(III)] / 10^{-3} M$	$k_{obs} / 10^4 s^{-1}$
0.54	4.00
0.72	4.72
1.1	6.24
2.2	10.5
3.2	14.2
4.3	18.3
5.4	23.6
6.5	26.6

^a $[Cr(5-Clphen)_3^{3+}] = 2.87 \times 10^{-5} M$.

Table A12. Quenching of $^*Cr(5-(CH_3)phen)_3^{3+}$ in 1 M HCl^a

$[Ti(III)] / 10^{-3} M$	$k_{obs} / 10^4 s^{-1}$
0.61	2.04
1.21	3.38
2.42	5.32
3.64	7.62
4.85	9.34
6.06	11.61
7.28	12.77
8.49	15.14

^a $[Cr(5-(CH_3)phen)_3^{3+}] = 3.31 \times 10^{-5} M$.

Table A13. Quenching of $^*Cr(5,6-(CH_3)_2phen)_3^{3+}$ in 1 M HCl^a

$[Ti(III)] / 10^{-3} M$	$k_{obs} / 10^4 s^{-1}$
0.88	1.80
1.77	2.80
2.66	3.93
4.00	5.23
5.78	7.13
7.56	9.13
9.34	11.57
10.66	12.65

^a $[Cr(5,6-(CH_3)_2phen)_3^{3+}] = 2.90 \times 10^{-5} M$.

Table A14. Quenching of $^*Cr(4,7-(CH_3)_2phen)_3^{3+}$ in 1 M HCl^a

$[Ti(III)] / 10^{-3} M$	$k_{obs} / 10^4 s^{-1}$
0.88	0.746
2.21	1.23
3.54	1.57
4.87	2.01
6.19	2.47
7.53	2.74
8.85	3.19
10.62	3.83

^a $[Cr(4,7-(CH_3)_2phen)_3^{3+}] = 3.18 \times 10^{-5} M$.

Table A15. Acid dependence of quenching of $^*Cr(bpy)_3^{3+a}$

$[H^+]^{-1} / M^{-1}$	$\frac{k_{obs} - k_{obs}^{\circ}}{[Ti(III)]_T} / 10^7 L mol^{-1}s^{-1}$
1.02	2.03
2.03	2.54
3.44	2.76
5.15	3.33
6.99	3.38
8.26	4.20
9.17	4.25
10.4	4.39

^a Ionic strength 1 M with LiCl; $[Ti(III)]_T = 2.05 \times 10^{-3} M$; $[Cr(bpy)_3^{3+}] = 3.83 \times 10^{-5} M$.

Table A16. Acid dependence of quenching of $^*Cr(4,4'-(CH_3)_2bpy)_3^{3+a}$

$[H^+]^{-1} / M^{-1}$	$\frac{k_{obs} - k_{obs}^{\circ}}{[Ti(III)]_T} / 10^7 L mol^{-1}s^{-1}$
1.04	2.85
2.00	3.71
3.33	4.29
4.00	4.31
5.00	4.76
6.67	5.26
7.87	5.94
8.77	5.82
10.0	7.67

^a Ionic strength 1 M with LiCl; $[Ti(III)]_T = 3.61 \times 10^{-3} M$; $[Cr(bpy)_3^{3+}] = 3.39 \times 10^{-5} M$.

Table A17. Acid dependence of quenching of $^*Cr(phen)_3^{3+a}$

$[H^+]^{-1} / M^{-1}$	$\frac{k_{obs} - k_{obs}^{\circ}}{[Ti(III)]_T} / 10^7 \text{ L mol}^{-1} \text{ s}^{-1}$
1.01	1.72
2.00	1.95
3.34	2.27
4.02	2.43
5.00	2.65
6.68	2.92
7.85	3.26
8.68	3.28
9.89	3.46

^a Ionic strength 1 M with LiCl; $[Ti(III)]_T = 2.54 \times 10^{-3} \text{ M}$; $[Cr(phen)_3^{3+}] = 3.14 \times 10^{-5} \text{ M}$.

Table A18. Acid Dependence of quenching of $^*Cr(5-Clphen)_3^{3+a}$

$[H^+]^{-1} / M^{-1}$	$\frac{k_{obs} - k_{obs}^{\circ}}{[Ti(III)]_T} / 10^7 \text{ L mol}^{-1} \text{ s}^{-1}$
1.01	4.14
1.25	4.18
1.67	4.41
3.34	5.41
4.99	6.10
6.69	6.52
7.98	7.07
9.00	7.33
9.91	7.63

^a Ionic strength 1 M with LiCl; $[Ti(III)] = 2.01 \times 10^{-3} \text{ M}$; $[Cr(5-Clphen)_3^{3+}] = 3.73 \times 10^{-5}$.

Table A19. Acid dependence of quenching of $^*Cr(5-(CH_3)phen)_3^{3+a}$

$[H^+]^{-1} / M^{-1}$	$\frac{k_{obs} - k_{obs}^{\circ}}{[Ti(III)]_T} / 10^7 \text{ L mol}^{-1} \text{ s}^{-1}$
1.02	1.66
2.02	1.89
3.32	2.13
4.00	2.20
5.03	2.48
6.62	2.90
7.94	3.09
8.77	3.23
10.0	3.39

^a Ionic strength 1 M with LiCl; $[Ti(III)] = 2.90 \times 10^{-3} \text{ M}$; $[Cr(5-(CH_3)phen)_3^{3+}] = 3.49 \times 10^{-5} \text{ M}$.

Table A20. Acid dependence of quenching of $Cr(5,6-(CH_3)_2phen)_3^{3+a}$

$[H^+]^{-1} / M^{-1}$	$\frac{k_{obs} - k_{obs}^{\circ}}{[Ti(III)]_T} / 10^7 \text{ L mol}^{-1} \text{ s}^{-1}$
1.09	1.27
2.00	1.44
3.36	1.68
5.00	1.85
6.67	2.05
7.87	2.22
8.85	2.31
10.1	2.40

^a Ionic strength 1 M with LiCl; $[Ti(III)] = 8.09 \times 10^{-3} \text{ M}$; $[Cr(5,6-(CH_3)_2phen)_3^{3+}] = 2.9 \times 10^{-5} \text{ M}$.

Table A21. Acid dependence of quenching of $\text{Cr}(4,7\text{-(CH}_3)_2\text{phen)}_3^{3+a}$

$[\text{H}^+]^{-1} / \text{M}^{-1}$	$\frac{k_{\text{obs}} - k_{\text{obs}}^{\circ}}{[\text{Ti(III)}]_{\text{T}}} / 10^7 \text{ L mol}^{-1} \text{ s}^{-1}$
1.09	3.12
2.02	3.52
3.33	4.32
5.00	4.67
6.67	5.21
7.78	5.55
8.77	5.89
10.0	6.05

^a Ionic strength 1 M with LiCl; $[\text{Ti(III)}] = 8.09 \times 10^{-3} \text{ M}$; $[\text{Cr}(4,7\text{-(CH}_3)_2\text{phen)}_3^{3+}] = 3.18 \times 10^{-5} \text{ M}$.

**PART II ALKYL RADICAL COLLIGATION AND RELEASE
BY A CHROMIUM MACROCYCLE**

INTRODUCTION

Efforts to learn more about the metal-carbon bonds in transition-metal complexes have included studies of the homolysis of organometallic complexes in aqueous solution (equation 1).



In the case of complexes of Cr(III) the rates of homolysis have been measured by shutting off the reverse colligation reaction. This was done by adding a scavenger to remove either or both of the products of the homolysis, thereby pulling the reaction to completion. Homolysis studies have been carried out for the series of complexes $(H_2O)_5CrR^{2+}$ 1-3 and $([15]aneN_4)CrR^{2+}$.⁴ From the temperature dependence studies of these homolysis reactions, the activation parameters were determined and the activation enthalpies were taken as an approximate measure of the chromium-carbon bond dissociation enthalpy. The rates of homolysis are strongly dependent on steric factors and the estimates of the bond strengths decline regularly with degree of substitution. The highly endothermic homolysis occurs by chromium-carbon bond scission unassisted to any appreciable extent by compensating bond-making reactions.

The reverse reaction (colligation) was studied pulse radiolytically for a series of aliphatic radicals with $Cr(H_2O)_6^{2+}$.⁵ A simpler laser-flash-photolysis method was later developed that generated radicals by photohomolysis of $RCo([14]aneN_4)^{2+}$ complexes.⁶ This method was applied to the study of colligation reactions of carbon-centered radicals with Co(II) macrocyclic complexes⁷ and $Ni([14]aneN_4)^{2+}$ 8 in addition to the $Cr(H_2O)_6^{2+}$ studies.

Organochromium complexes containing the macrocyclic ligand 1,4,8,12-tetraazacyclopentadecane ([15]aneN₄) were first prepared⁹ by reaction of Cr([15]aneN₄)²⁺ with RX. The rate of colligation of 5-hexenyl radical and this complex was derived by the method of Kochi and Powers¹⁰ to be $(0.9 \pm 0.2) \times 10^7 \text{ L mol}^{-1}\text{s}^{-1}$.⁹ Colligation rates for ([15]aneN₄)CrCH₂OH²⁺ of $(1.2 \pm 0.2) \times 10^8 \text{ L mol}^{-1}\text{s}^{-1}$ and for ([15]aneN₄)CrC(CH₃)₂OH²⁺ of $(4.9 \pm 0.5) \times 10^7 \text{ L mol}^{-1}\text{s}^{-1}$ were measured by pulse radiolysis.¹¹

This study fills some of the gaps of knowledge in the homolysis and colligation reactions of ([15]aneN₄)CrR²⁺ complexes. The simple carbon-centered radicals, many of which are not readily available in pulse radiolysis studies are generated here by photohomolysis of RCo(dmgh)₂ complexes (equation 2).



In the absence of any other reagents the radicals react according to equation 3 in combination and/or in disproportionation reactions at diffusion controlled rates.¹² With Cr([15]aneN₄)²⁺ present the radical is captured by the metal ion forming an organochromium complex (equation 4). This may be considered formally as an electron transfer process with the organic radical oxidizing the chromium(II). Because of the low molar absorptivities of the organo-

chromium complexes in the visible region, a kinetic probe, methyl viologen radical cation (equation 5), was used to monitor the rate of colligation. In this manner a large number of colligation rates of carbon-centered radicals with $\text{Cr}([\text{15}] \text{aneN}_4)^{2+}$ have been determined.

Also, several of those complexes of $\text{Cr}([\text{15}] \text{aneN}_4)^{2+}$ that had previously been observed only by pulse radiolysis have been prepared by the modified Fenton's reagent method.^{1,13-15} This method has proven to be useful in the preparation of $(\text{H}_2\text{O})_5\text{CrR}^{2+}$ complexes.¹ In this case $\text{Cr}([\text{15}] \text{aneN}_4)^{2+}$ reduces H_2O_2 in (equation 6) in a manner analogous to that of $\text{Fe}(\text{II})$,¹⁶ $\text{Ti}(\text{III})$,¹⁷ Cr^{2+} ,¹⁸ and VO^{2+} .¹⁷ The hydroxyl radical formed extracts a hydrogen atom from an alcohol or ether, yielding a carbon-centered radical (equation 7) which may be captured by $\text{Cr}([\text{15}] \text{aneN}_4)^{2+}$.



From these two approaches and with data available in the literature equilibrium constants and values for ΔG°_{298} may be calculated for reaction 1.

EXPERIMENTAL

Materials

All water used in this study was in-house distilled, deionized water passed through a Millipore-Q purification system. All chemicals were used as received unless noted below. The argon (99.99% pure, Air Products Corp.) used for purging was passed through chromous towers to remove any trace oxygen. $[\text{Co}(\text{NH}_3)_5\text{Br}]\text{Br}_2$ ¹⁹ and $[\text{Co}(\text{NH}_3)_5\text{Cl}](\text{ClO}_4)_2$ ²⁰ were prepared by literature procedures. The $[\text{Co}(\text{NH}_3)_5\text{Br}]\text{Br}_2$ was converted to the more soluble perchlorate salt by recrystallizing three times from dilute HClO_4 in the presence of a large excess of LiClO_4 . Methyl viologen dichloride hydrate (Aldrich) was recrystallized twice from methanol and stock solutions were protected from light and O_2 . Solutions of MV^{+} were prepared by reduction over Zn/Hg amalgam ~20 seconds and were stored (<2 hours) in a gas-tight syringe.

Many of the organocobaloximes having pyridine in the trans position were available from previous studies.^{21,22} These were recrystallized from $\text{CH}_3\text{OH}/\text{H}_2\text{O}$ and dissolved in 0.01 M HClO_4 . The more soluble aqua complexes of benzyl- and neopentylcobaloximes were prepared by hydroxide-promoted disproportionation.²³ In the case of neopentylcobaloxime 80 ml of methanol was degassed in a 250-ml round-bottomed flask. To this was added 6.38 g (0.055 mol) dmgH_2 (dimethylglyoxime) and 6.53 g (0.027 mol) $\text{CoCl}_2 \cdot 6\text{H}_2\text{O}$. The flask was cooled in an ice-salt bath and 5 ml (0.04 mol) neopentyl bromide was added. Immediately following this, 3.3 g NaOH dissolved in 11 ml H_2O was very slowly added. The reaction mixture was allowed to stir ca. 1.5 hr. warming

slowly to room temperature. Approximately 20 ml H₂O was added and the product solution was filtered to remove a black tar-like precipitate. Methanol was removed by rotary evaporation and product was collected by filtration. The reddish-brown product was recrystallized twice from CH₃OH/H₂O to give red crystals.

The complexes CH₃Co([14]aneN₄)²⁺, C₂H₅Co([14]aneN₄)²⁺, BrCH₂Co([14]aneN₄)²⁺ and CH₃OCH₂Co([14]aneN₄)²⁺ were available from previous studies.²³

Aqueous solutions of Cr(II) were prepared as follows.²⁵ Several pellets (ca. 2 g) of chromium metal (99.99+%, Alfa) were placed in a 24/40 S.T. 6" test tube. The tube was degassed with chromous-scrubbed argon and 25 ml of degassed 6 M HCl was added. The reaction started quickly and was accelerated by gentle heating. After ca. 2 hours most of the chromium was dissolved. The volume was reduced to ~5 ml by heating with a Bunsen burner. At this point a green precipitate formed that turned dark blue on cooling. The solid was washed with acetone until the wash was colorless. Any white solid present was dissolved by adding 2-3 ml of water to one of the last acetone washes. The blue solid was dissolved in degassed water, transferred to storage vials and stored at -5 °C under argon.

To prepare (H₂O)₂Cr([15]aneN₄)²⁺ a solution of 1,4,8,12-tetraazacyclopentadecane (Strem) was thoroughly degassed and a slight deficiency (~95%) of Cr(II) was added.⁹ The resulting brown solution turned purple over several minutes with stirring. The solution was stirred for 10-15 minutes longer to dissolve any precipitate that was formed. In more concentrated solutions the precipitate did not dissolve completely. To avoid

this, high quality chromous (not more than 3 weeks old) and dilute $(\text{H}_2\text{O})_2\text{Cr}([\text{15]aneN}_4)^{2+}$ solutions were used. In the presence of acid no purple color appears and if acid is added to a solution of the Cr(II) complex, the purple color rapidly fades.

In a typical organochromium preparation a solution ~ 0.05 M $(\text{H}_2\text{O})_2\text{Cr}([\text{15]aneN}_4)^{2+}$ was prepared. To this was added 0.5 M degassed CH_3OH or $\text{C}_2\text{H}_5\text{OH}$ (or the solution was saturated with CH_3OCH_3), followed by slightly less than a stoichiometric amount of H_2O_2 . The resulting brown solution was acidified to pH 1 and placed on a degassed and ice-water cooled Sephadex C-25 20 cm column that had been washed with 0.15 M HClO_4 . $\text{RCr}([\text{15]aneN}_4)^{2+}$ was eluted with 0.15 M HClO_4 .

Analyses

Chromium analyses were carried out on the organochromium complexes to determine extinction coefficients. However, the results were initially irreproducible. To improve reproducibility, the macrocyclic ligand was decomposed by heating very strongly in concentrated HClO_4 before analyzing for chromate at 372 nm ($4830 \text{ L mol}^{-1}\text{cm}^{-1}$) in basic peroxide.²⁶

Cobalt(II) yields were determined at 623 nm ($1842 \text{ L mol}^{-1}\text{cm}^{-1}$) by addition of NH_4SCN in 50% acetone.²⁷

Acetaldehyde was determined using a Hewlett Packard 5790Å gas chromatograph with an OV101 column (Alltech) at 30 °C. Calibration curves were constructed using standard solutions cooled in ice to prevent loss of volatile CH_3CHO . A blank experiment was carried out to show that no acetaldehyde is formed in the preparation of $([\text{15]aneN}_4)\text{CrCH}(\text{CH}_3)\text{OH}^{2+}$. A freshly prepared solution of organochromium was injected and acetaldehyde

was observed to be present, presumably produced at the injection port by the decomposition of organochromium complex. However, more importantly, no acetaldehyde was found in the gas phase above the organochromium solution.

Kinetics

Rates of Decomposition of $([15]aneN_4)Cr(H_2O)CH(OH)CH_3^{2+}$ were measured using a Cary 219 spectrophotometer equipped with a Forma Scientific 2800 temperature controlled bath. Loss of the complex was monitored at 383 and 320 nm. The reaction temperature, $[H^+]$ and ionic strength were precisely controlled.

Colligation rates were measured using a laser flash photolysis system like that described in part 1 of this dissertation. The excitation dyes (Exciton) used were Coumarin-460 (1.5×10^{-4} M in CH_3OH) and LD 490 (1×10^{-4} M in CH_3OH containing 1% Ammonyx LO). Temperature control was maintained using an RC6 Lauda temperature control bath with circulation through the walls of the cell holder. The loss in absorbance due to $MV^{+\bullet}$ was monitored at 600 nm ($13,700 \text{ L mol}^{-1}\text{cm}^{-1}$).²⁸ The data was transferred to an interfaced Apple II+ microcomputer for storage and processing using a least-squares, first-order kinetics fitting program. The first-order treatment of data is really an approximation as there is a second-order contribution to the observed rate. The validity of this approximation is explained below.

A radical is formed in the laser flash by reaction 2. In the absence of $Cr(II)$ $R\bullet$ may react with another $R\bullet$ (equation 3) or with $MV^{+\bullet}$ (equation 5). The observed rate constant is given by equation 8a when $MV^{+\bullet}$ is in pseudo-first-order excess. The literature value for k_d for $\bullet CH_3$ is $1.24 \times 10^9 \text{ L}$

$\text{mol}^{-1}\text{s}^{-1}$ ¹² and the value for k_{MV} for methyl radical measured under these conditions is $1.5 \times 10^9 \text{ L mol}^{-1}\text{s}^{-1}$.

$$k_{\text{obs}} = k_{\text{d}}[\text{R}\cdot]^2 + k_{\text{MV}}[\text{MV}^{+\bullet}] \quad (8a)$$

$$k_{\text{obs}} = 2k_{\text{d}}[\text{R}\cdot]_{\text{ave}} + k_{\text{MV}}[\text{MV}^{+\bullet}] \quad (8b)$$

The approximation lies in assuming that $[\text{R}\cdot]$ is a constant or average value, resulting in equation 8b. This is a good approximation because the contribution of the first term is very small. However, it is necessary to make some correction for radical self-reaction, as the first term in equations 8a and 8b is not completely negligible. For example, typical conditions are $3 \mu\text{M}$ $\cdot\text{CH}_3$ produced in the flash and $40 \mu\text{M}$ $\text{MV}^{+\bullet}$. This means that the first term contributes $< 5\%$ to the observed rate constant. The value of $[\text{R}\cdot]_{\text{ave}}$ was taken as the average of the initial and final values. It was calculated from absorbance changes due to loss of $\text{MV}^{+\bullet}$ according to equation 9. This equation is based on the fact that the total radical produced is equal to the radical that reacts with $\text{MV}^{+\bullet}$ ($\Delta[\text{MV}^{+\bullet}]$) divided by the fraction that reacts with $\text{MV}^{+\bullet}$ (f_{MV}) given by equation 10. In the case where Cr(II) is also present and organochromium is formed (equation 4), a third term is included (equation 11) and the radical self-reaction becomes even less significant.

$$[\text{R}\cdot]_{\text{ave}} = \frac{1}{2} \times \frac{\Delta[\text{MV}^{+\bullet}] k_{\text{obs}}}{k_{\text{MV}}[\text{MV}^{+\bullet}]} \quad (9)$$

$$f_{\text{MV}} = \frac{k_{\text{MV}}[\text{MV}^{+\bullet}]}{2k_{\text{d}}[\text{R}\cdot]_{\text{ave}} + k_{\text{MV}}[\text{MV}^{+\bullet}]} = \frac{k_{\text{MV}}[\text{MV}^{+\bullet}]}{k_{\text{obs}}} \quad (10)$$

$$k_{\text{obs}} = 2k_d[\text{R}\cdot]_{\text{ave}} + k_{\text{MV}}[\text{MV}^{+\cdot}] + k_{\text{col}}[\text{Cr}([\text{15}] \text{aneN}_4)^{2+}] \quad (11)$$

The validity of this approximation was also demonstrated by KINSIM.²⁹ The concentration of $\text{MV}^{+\cdot}$ was calculated by the program as a function of time, using the rate constants for methyl radical and the mechanisms corresponding to equations 8a and 8b. First order analysis of the simulated data using equation 8a agreed with the approximate method represented by equation 8b.

RESULTS

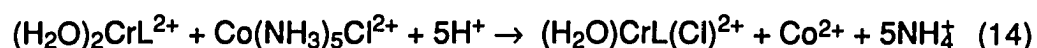
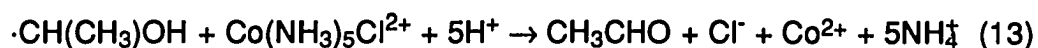
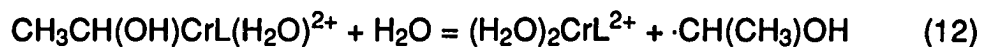
The modified Fenton's reagent method was used to prepare three organochromium complexes: $([15]aneN_4)Cr(H_2O)R^{2+}$ with $R = CH(OH)CH_3$, CH_2OH and CH_2OCH_3 . Attempts to prepare $([15]aneN_4)CrC(CH_3)_2OH^{2+}$ were unsuccessful. The extinction coefficients for these complexes were determined and are given in Table 1.

Table 1. UV-Visible spectra of $RCr([15]aneN_4)(H_2O)^{2+}$ complexes

R	$\lambda / nm (\epsilon / L mol^{-1}cm^{-1})$		
	$\lambda_1 (\epsilon_1)$	$\lambda_2 (\epsilon_2)$	$\lambda_3 (\epsilon_3)$
CH_2OH	270(1030±100)	377(200±10)	450(55±3)
$CH(OH)CH_3$	320(sh)(650±60)	383(203±15)	458(50±8)
CH_2OCH_3	—	377(220±25)	450(68±15)

Decomposition reactions were examined for $RCrL(H_2O)^{2+}$, for $R = CH_2OH$, CH_2OCH_3 and $CH(CH_3)OH$. The first two of these are quite stable, showing negligible changes in their spectra over more than six hours in acidic solution under argon. The complex with $R = CH(CH_3)OH$ undergoes a first-order decomposition reaction in the presence of a scavenger such as $Co(NH_3)_5Cl^{2+}$. This cobalt complex was chosen to establish whether the decomposition occurs by homolysis, equation 12, because $Co(NH_3)_5Cl^{2+}$ is known to react with $\cdot CH(CH_3)OH$ (equation 13, $k = 3.0 \times 10^6 L mol^{-1} s^{-1}$).³⁰ Also, the chromium(II) macrocyclic complex is expected to rapidly reduce

$\text{Co}(\text{NH}_3)_5\text{Cl}^{2+}$ (equation 14), given that $\text{Cr}(\text{H}_2\text{O})_6^{2+}$ does so ($k = 2.6 \times 10^6 \text{ L mol}^{-1}\text{s}^{-1}$).³¹



The kinetics were studied in 0.10 M perchloric acid, ionic strength being maintained at 1.0 M with sodium perchlorate. The reactant concentration was typically 2-3 mM, and $[\text{Co}(\text{NH}_3)_5\text{Cl}^{2+}]$ was varied in the range 6-16 mM. The rate constant, $k = (1.60 \pm 0.15) \times 10^{-4} \text{ s}^{-1}$ at 25.0 °C, was independent of cobalt concentration as expected from the sequence in equations 12-14, and independent of $[\text{H}^+]$, 0.10-1.0 M. If the cobalt scavenger is absent, an absorbance decrease occurs at about the same rate, but the data do not fit as cleanly to first-order kinetics.

The rate constants were evaluated as a function of temperature with values of $k/10^{-4} \text{ s}^{-1} (T / ^\circ\text{C})$ as follows: 0.61(20.2), 1.55(24.8), 2.25(29.7), 5.79(34.5), 9.80(39.5). These values were not analyzed according to the equation from activated complex theory, because the rate constant is, as presented in the Discussion, a composite of two and likely three parallel reactions.

The yields of acetaldehyde and Co^{2+} were determined on solutions in which the reaction was allowed to go to completion. The value of $[\text{CH}_3\text{CHO}]_\infty$

$/ [\text{RCrL}(\text{H}_2\text{O})^{2+}]_0$ was 0.52 ± 0.08 in the absence of cobalt, and 0.82 ± 0.09 when 8.8 mM $\text{Co}(\text{NH}_3)_5\text{Cl}^{2+}$ was present in a solution of 3.5 mM organochromium complex at 0.16 M perchloric acid. The same solutions gave $[\text{Co}^{2+}]_\infty / [\text{RCrL}(\text{H}_2\text{O})^{2+}]_0 = 0.56 \pm 0.04$. This ratio, unlike the kinetic data, depends also on cobalt and acid concentrations. Yields of Co^{2+} increase at higher $\text{Co}(\text{NH}_3)_5\text{Cl}^{2+}$ concentrations and lower acid concentrations. In 0.058 M HClO_4 with 10.1 mM $\text{Co}(\text{NH}_3)_5\text{Cl}^{2+}$ present the $[\text{Co}^{2+}]_\infty / [\text{RCrL}(\text{H}_2\text{O})^{2+}]_0 = 1.76$. Also, in the absence of cobalt, H_2 is detected as a product by the test with palladium chloride.³³ However, with excess cobalt present no H_2 is detected.

Reaction of R· with MV⁺

The rates of reaction of the carbon-centered radicals listed in Table II-2 with MV^{+} were studied at 25 °C. Methyl viologen radical cation $(0.1-1) \times 10^{-4}$ M is stable with respect to thermal reaction in the presence of freshly purified $\text{RCo}(\text{dmgH})_2$ ($< 2 \times 10^{-4}$). Under typical reaction conditions $\sim 3 \mu\text{M}$ radical was produced in the 490 nm laser flash depending on the energy of the flash. At 600 nm the loss of MV^{+} was monitored due to reaction 3, varying the concentration of MV^{+} . A plot of k_{corr} (equation 15) vs. $[\text{MV}^{+}]$ for two radicals is given in Figure 1. The intercept should be zero because the small k_d term was subtracted out at each $[\text{MV}^{+}]$. The observed and corrected first order rate constants are listed in Tables A2-A14; they agree with previous determinations, where available.⁶

$$k_{\text{corr}} = k_{\text{obs}} - 2k_d[\text{R}\cdot]_{\text{ave}} = k_{\text{MV}}[\text{MV}^{+}] \quad (15)$$

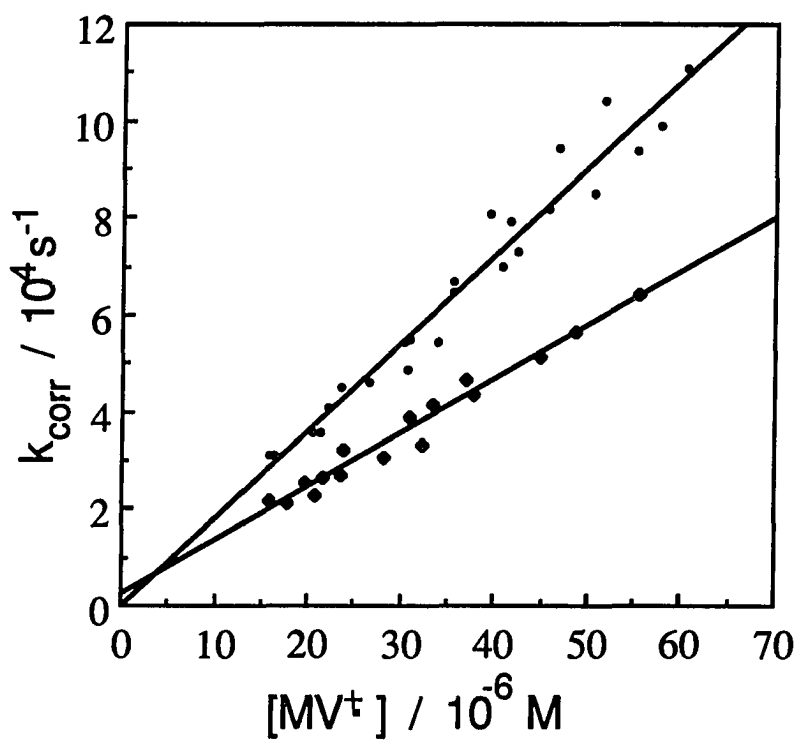


Figure 1. The observed pseudo-first-order rate constants, corrected for radical self-reactions, vary linearly with $\text{MV}^{+\bullet}$ for the reactions of CH_2Br (squares) and $\text{CH}_2\text{CH}(\text{CH}_3)_2$ radicals

Reaction of R· with Cr([15]aneN₄)²⁺

In this work it was imperative that the organocobaloxime was freshly purified. Any trace amount of inorganic cobalt resulted in the formation of H₂, identified by the PdCl₂ test.³² This was presumably formed in a reaction analogous to the evolution of H₂ in acidic solutions of Cr(H₂O)₆²⁺ catalyzed by cobalt(II).³³

In the presence of Cr([15]aneN₄)²⁺ the loss in absorbance at 600 nm is faster and not as large for a given radical concentration due to the formation of organochromium complex (reaction 4). A value of k_{corr} was calculated for each [Cr([15]aneN₄)²⁺] using equation 16.

$$k_{\text{corr}} = k_{\text{obs}} - 2k_{\text{d}}[\text{R}\cdot]_{\text{ave}} - k_{\text{MV}}[\text{MV}^+] = k_{\text{col}}[\text{Cr}([15]\text{aneN}_4)^{2+}] \quad (16)$$

Thus, a plot of k_{corr} vs. [Cr([15]aneN₄)²⁺] is linear with an intercept of zero. Such a plot is shown for several radicals in Figure 2. The observed rate constants and the values calculated for k_{corr} are listed in Tables A15-A27. The second order rate constants are listed for all of the radicals studied in Table 2.

Another radical source that may be used in these experiments is the series RCo([14]aneN₄)²⁺. Several of these were used to measure k_{col} as a check on the purity and reliability of the organocobaloximes which allow a wider variety of R groups. These values are also listed in Table 2 with k_{obs} and k_{corr} listed in Tables A28-A31.

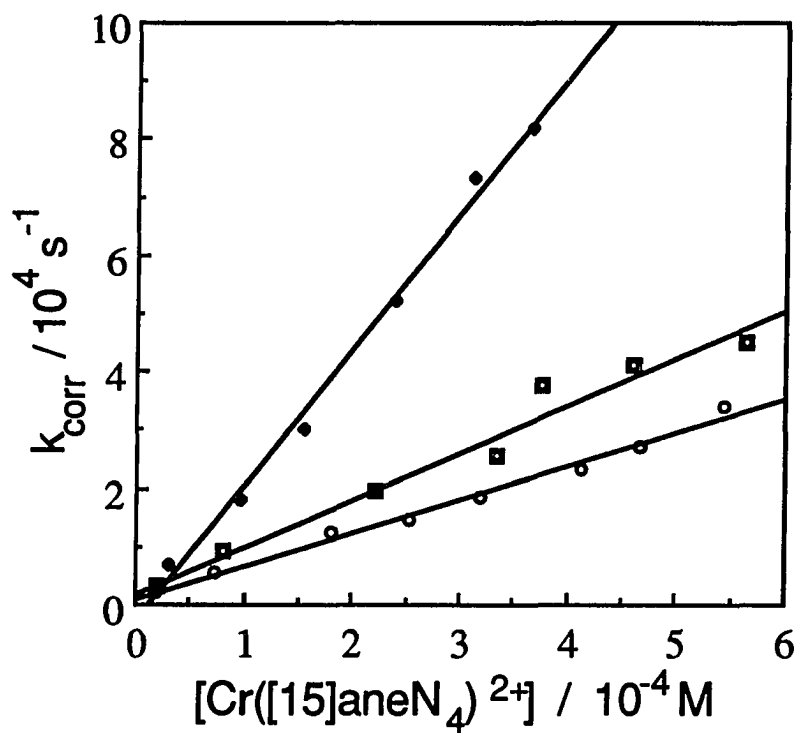


Figure 2. The observed pseudo-first-order rate constants, corrected for radical self-reactions and the reaction of $R\cdot$ with MV^{2+} , vary linearly with $[(H_2O)_2CrL^{2+}]$ for the reactions of $C_6H_5CH_2\cdot$ (diamonds), $1-C_4H_9\cdot$ (squares) and $\cdot CH(CH_3)C_2H_5$ (circles)

Table 2. Summary of the rate constants ($\text{L mol}^{-1} \text{s}^{-1}$) for the reactions of carbon-centered radicals with $\text{MV}^{+\bullet}$ and $\text{Cr}([\text{15]aneN}_4)^{2+}$ ^a

Radical	$k_{\text{MV}} / 10^9$	$k_{\text{CoI}} / 10^7$
CH ₃	1.5(±0.4)	16(±1) 19(±2) ^b
CH ₂ CH ₃	1.0(±0.1)	10(±1) 9.5(±0.2) ^b
CH ₂ C ₂ H ₅	1.0(±0.1)	8.5(±0.4)
CH(CH ₃) ₂	1.2(±0.1)	6.1(±0.3)
CH ₂ C ₃ H ₇	1.2(±0.1)	8.2(±0.5)
CH(CH ₃)C ₂ H ₅	1.1(±0.1)	3.9(±0.4)
CH ₂ CH(CH ₃) ₂	0.92(±0.09)	7.3(±0.2)
c-C ₅ H ₉	0.91(±0.09)	7.1(±0.4)
CH ₂ C(CH ₃) ₃	0.76(±0.08)	6.3(±0.2)
CH ₂ Ph	1.2(±0.1)	19(±1)
CH ₂ OCH ₃	1.1(±0.1)	16(±1) 14(±1) ^b
CH ₂ Cl	1.1(±0.2)	9.3(±0.7)
CH ₂ Br	1.5(±0.1)	13(±1) 16(±1) ^b

^aConditions: 25±1 °C, [R•] = 1-4 μM, [MV⁺•] = (0.1-0.8) × 10⁻⁴ M.

^bUsing RCo([\text{14]aneN}_4)^{2+} as the radical source.

DISCUSSION

Homolysis reactions

The modified Fenton reaction between $\text{Cr}(\text{H}_2\text{O})_6^{2+}$ and H_2O_2 in the presence of a suitable aliphatic substrate RH has proved to be a successful method for the preparation of $(\text{H}_2\text{O})_5\text{CrR}^{2+}$ complexes.^{1,5,34} The same method was used here to prepare macrocyclic analogues with $\text{R} = \text{CH}_2\text{OH}$, $\text{CH}(\text{CH}_3)\text{OH}$ and CH_2OCH_3 , but it failed for $\text{R} = \text{C}(\text{CH}_3)_2\text{OH}$. We suggest this is due to the homolysis of $(\text{CH}_3)_2\text{C}(\text{OH})\text{Cr}([\text{15}] \text{aneN}_4)\text{H}_2\text{O}^{2+}$ being too rapid, which is not unreasonable in view of the fact that the pentaqua analogue decomposes with $k_{\text{hom}} = 0.13 \text{ s}^{-1}$ ($\tau_{1/2} = 5.5 \text{ s}$) at $25 \text{ }^\circ\text{C}$.¹

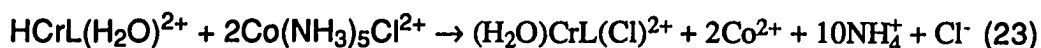
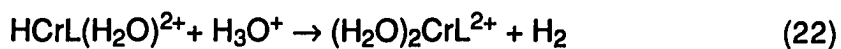
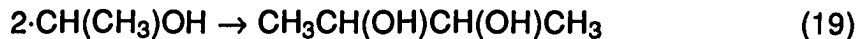
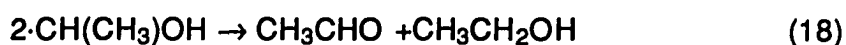
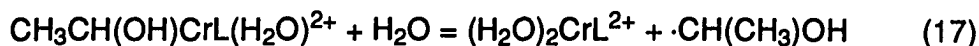
That the complex $\text{RCrL}(\text{H}_2\text{O})^{2+}$ with $\text{R} = \text{CH}_2\text{OH}$ does not decompose by homolysis is not unexpected, since the aqua complex reacts only slowly. That it and the complex with $\text{R} = \text{CH}_2\text{OCH}_3$ do not decompose by acidolysis to yield $(\text{H}_2\text{O})_2\text{CrL}^{3+}$ and CH_3OH or $(\text{CH}_3)_2\text{O}$, respectively, contrasts with the behavior of the $(\text{H}_2\text{O})_5\text{CrR}^{2+}$ analogues, which do so readily ($\text{R} = \text{CH}_2\text{OH}$) or slowly ($\text{R} = \text{CH}_2\text{OCH}_3$).^{1,35} This behavior is precented, however, in that the 1-propyl and 2-propyl macrocyclic complexes are completely stable toward acidolysis under conditions where their pentaqua counterparts readily react.³⁶ This contrast in reactivity is particularly striking, because the N_4 macrocycle, a good electron donating ligand, might be expected to increase the rate of electrophilic attack by virtue of its inductive effect. This may be further indication that electrophilic attack by water arises from the internal attack of cis-coordinated water in the $(\text{H}_2\text{O})_5\text{CrR}^{2+}$ series of complexes, which

cannot happen in the macrocycle. Earlier studies of the edta and nitrilotriacetate complexes^{11,37} gave rates that were similar, for the H₂O pathway, to those found in the pentaqua series. These authors¹¹ also found that CH₃CH(OH)CrL(H₂O)²⁺ does not undergo acidolysis with H₂O or H₃O⁺. They argued, however, that the similarity of rates for (H₂O)₅, edta, and nta complexes signaled the same mechanism for the H₂O path - attack of an external, noncoordinated water molecule. Evidently the basis for this is that the edta complex, which lacks a cis coordinated water, reacts similarly to the others. We suggest that the really striking feature is the failure of the [15]aneN₄ complexes to react at all. Perhaps the edta complex can, by hydrogen bonding, utilize a water molecule in the second coordination sphere.^{11,37}

The extreme slowness of electrophilic attack of H₃O⁺ on the macrocycles might therefore indicate the difficulty the small H₃O⁺ electrophile experiences in approaching the α -carbon atom by virtue of repulsion from the ligand. Larger electrophiles (Hg²⁺, Br₂, I₂) evidently do not show this effect, since these displacement reactions occur rapidly and readily.^{36,38}

On the basis of equations 12, 18 and 19 the expected yield of acetaldehyde in the absence of a radical scavenger is 0.2, given that $k_{18} = 1.1 \times 10^8$ ³⁹ and $k_{19} = 5.5 \times 10^8$ ⁴⁰ L mol⁻¹s⁻¹. To account for a yield of acetaldehyde that approaches 0.5, an additional reaction (equation 20 or 21) is proposed. Precedent for equation 20 can be found in the reaction between (H₂O)₅CrCH(CH₃)₂²⁺ and hydrogen peroxide⁴¹ and in the pulse radiolytic study of the homolysis of (H₂O)₅CrR²⁺ complexes.⁴² The latter

study suggested that rate constants for reactions of $R\cdot$ with CrR^{2+} can exceed $10^8 \text{ L mol}^{-1}\text{s}^{-1}$. If k_{20} has such a value, then the observed yield of CH_3CHO (0.5) might be explained. However, a very valid objection can be raised to equation 20 in this case. Upon its occurrence, a second organochromium is lost. If that were the dominant path, the k_{obs} would be $2k_{hom}$. That is, the experimental rate constant would be expected to drift by up to a factor of two as the reaction conditions and concentrations varied, which was not found experimentally.



We therefore consider equation 21, a β -elimination reaction. This sort of chemistry is well precedented elsewhere in organometallic

chemistry. It would also account for the extra acetaldehyde, if it occurs concurrently with homolysis. As such, it would not lead to the kinetic problems raised by equation 20. The pentaqua analog of the hydrido complex shown as a product is known independently^{43,44} to evolve hydrogen under these conditions (equation 22). Indeed, H₂ was observed as a product of decomposition of CH₃CH(OH)CrL(H₂O)²⁺.

In the presence of a scavenger such as Co(NH₃)₅Cl²⁺ additional reactions occur, such as those shown in equations 13-14 and 23. The yield of acetaldehyde now rises to 0.82, indicating Cr-C bond homolysis is also occurring. This is still lower than the expected value of 1, indicating that acidolysis of CH₃CH(OH)CrL(H₂O)²⁺ may be occurring to a minor extent, or simply that some acetaldehyde is lost despite cooling the solution in ice.

The predicted yield of Co²⁺ is 2.0 based on equations 13 and 14 if homolysis predominates. However, in 0.16 N HClO₄ the yield was only 0.56 ($[\text{Co}^{2+}]_{\infty} / [\text{RCrL}(\text{H}_2\text{O})^{2+}]_0$). This indicates that, at most, 28% of the organochromium complex decomposes by homolysis. Also, the Co²⁺ yield was found to be higher at lower acid concentration and to depend on Co(NH₃)₅Cl²⁺ concentration. This is understood in terms of equations 22 and 23. As cobalt concentration is increased, more hydrido complex reacts as in equation 22 and yields of Co²⁺ increase. At low [H⁺] and high cobalt concentration of 10.1 mM a yield of $[\text{Co}^{2+}]_{\infty} / [\text{RCrL}(\text{H}_2\text{O})^{2+}]_0 = 1.76$ was obtained. This is again slightly less than the expected yield of 2.0 and may be due to equation 22 or to a small contribution by acidolysis.

To summarize, the product studies indicate that a significant portion of the decomposition of $\text{CH}_3\text{CH}(\text{OH})\text{CrL}(\text{H}_2\text{O})^{2+}$ is β -elimination. The remainder may be homolysis, however, a small ($\leq 18\%$) contribution by acidolysis cannot be ruled out. This is similar to the case of isobutylcobalamin in which β -elimination and Co-C bond homolysis are competitive processes.⁴⁵

Colligation reactions

The rate constants k_{MV} , referring to equation 5, were previously determined for many of these same radicals.⁶ The values found here all agree within the experimental error; indeed, they were redetermined only because the subtraction inherent in the evaluation of k_{CoI} (see equation 8) requires accurate values under precisely the same conditions. There are two factors that combine to make MV^{+} an ideal probe for the reactions of alkyl radicals -- the high molar absorptivity of MV^{+} and the high values of k_{MV} which allow the use of low concentrations of MV^{+} and the monitoring of an appreciable absorbance change.

The values of k_{CoI} , referring to the reactions of $\text{R}\cdot$ with $(\text{H}_2\text{O})_2\text{CrL}^{2+}$, lie in a relatively narrow range, from $3.9 \times 10^7 \text{ L mol}^{-1}\text{s}^{-1}$ for $\text{R}\cdot = 1\text{-methylpropyl}$ to $1.9 \times 10^8 \text{ L mol}^{-1}\text{s}^{-1}$ for benzyl. If one searches for a steric effect, reflected in the values of k_{CoI} , say in a series like $\cdot\text{CH}_3$, $\cdot\text{C}_2\text{H}_5$, $\cdot\text{CH}(\text{CH}_3)_2$, it is largely absent. In the case of $\text{Cr}(\text{H}_2\text{O})_6^{2+}$, much the same result was found,^{5,6} with values of k_{CoI} all near $2 \times 10^8 \text{ L mol}^{-1}\text{s}^{-1}$. The small reduction in rates in going from $\text{Cr}(\text{H}_2\text{O})_6^{2+}$ to $(\text{H}_2\text{O})_2\text{CrL}^{2+}$ may perhaps be attributed to a statistical effect (6 vs. 2 replaceable water molecules), or to the macrocycle partially blocking the approach of $\text{R}\cdot$. If this reaction, in which chromium(II) is

oxidized, were really of an electron transfer character, one might have expected a faster reaction of the macrocyclic complex since it is the better reducing agent (E° -0.58 V vs. -0.41 V for $\text{Cr}(\text{H}_2\text{O})_6^{2+}$).

The important point is that the analogous reactions of the $\text{Ni}([\text{14}]aneN_4)^{2+}$ complexes do show a significant rate reduction along the series $\bullet\text{CH}_3 > \bullet\text{C}_2\text{H}_5 > \bullet\text{CH}(\text{CH}_3)_2$. The present results show that this cannot be attributed to an effect of the macrocycle. As suggested before,⁸ it is the steric effect of the radicals on the nickel reaction in which the coordination number changes, and the fact that the organonickel complexes readily homolyze since they have such weak metal-carbon bonds, that cause the large reactivity ratios. Also, a kinetic "leveling effect" may come into play for the six-coordinate cobalt(II) and chromium(II) complexes that is absent for four-coordinate nickel because colligation occurs with ligand interchange for them. Solvent exchange is itself not limiting (note $k_{ex} = 7 \times 10^9 \text{ s}^{-1}$ for $\text{Cr}(\text{H}_2\text{O})_6^{2+}$);⁴⁶ rather, we suggest a competition between radical and solvent for the coordination site.

Equilibrium

The opposing reactions of colligation and homolysis, as in equation 2, constitute a chemical equilibrium. The formation constant $K_f = k_{col} / k_{hom}$. Values in the $\text{RCrL}(\text{H}_2\text{O})_6^{2+}$ series are available for two R groups as summarized in Table 3 from this work and others.^{4,11}

The similarity of the two equilibrium constants merely reflects the few compounds whose homolysis rates fall in a measurable region. Complexes with R groups such as CH_3 , C_2H_5 , CH_2OH , and so on are much less prone to homolyze and therefore have much larger values of K_f . These very

substantial differences in K_f are, therefore, due to the variation in k_{hom} , since the k_{col} values do not change with R. That is, variations in the strengths of the chromium-carbon bonds are contained entirely in the dissociation rates, and not in those for bond formation. This is sensible, which is what makes the trend for nickel so remarkable in that rates in both directions show substantial and opposing effects.⁸

Table 3. Values of formation constants $K_f = k_{col} / k_{hom}$ for $RCrL(H_2O)_2^{2+}$ complexes

R	$k_{col} / 10^7 L \text{ mol}^{-1} \text{ s}^{-1}$	$k_{hom} / 10^{-4} \text{ s}^{-1}$	$\log(K_f / L \text{ mol}^{-1})$
$\bullet\text{CH}(\text{CH}_3)_2$	8.5	5.0	11.23
$\bullet\text{CH}_2(\text{C}_6\text{H}_5)$	19	1.24	12.19

The rates of equilibration in equation 12 is controlled by the composite constant $k_{col}[(H_2O)_2CrL^{2+}] + k_{hom}$. Under all conditions the first term is much larger than the second, and equilibrium is established very rapidly since k_{col} values are so large. Of course when a scavenger is added, the reaction, now controlled by k_{hom} , occurs very slowly.

The equilibrium constants for several organometals are given in Table 4. The organonickel complexes are much less stable than the organochromium complexes. This is certainly no surprising, because nickel(III) is more strongly oxidizing than chromium(III). The small values of

K_f for nickel may contribute to the fact that both of its components, k_{col} and k_{hom} , vary with R.

Table 4. Values of $\log K_f$ for organochromium and organonickel complexes

R	$(H_2O)_2CrL^{2+}$	$Cr(H_2O)_6^{2+}$	RRRR- [Ni([14]aneN ₄) ²⁺]
•CH(CH ₃) ₂	11.23	11.87	3.49
•CH ₂ C ₆ H ₅	12.19	10.52	-
•CH(CH ₃)OH	-	10.96	-
•CH ₂ OCH ₃	-	>13.8	6.82

REFERENCES

1. Kirker, G.W.; Bakac, A.; Espenson, J.H. *J. Am. Chem. Soc.* **1982**, *104*, 1249.
2. Mulac, W.A.; Cohen, H.; Meyerstein, D. *Inorg. Chem.* **1982**, *21*, 4016.
3. Espenson, J.H.; Connolly, P.; Meyerstein, D.; Cohen, H. *Inorg. Chem.* **1983**, *22*, 1009.
4. Shi, S.; Espenson, J.H.; Bakac, A. *Inorg. Chem.* **1990**, *29*, 4318.
5. Cohen, H.; Meyerstein, D. *Inorg. Chem.* **1974**, *13*, 2434.
6. Bakac, A.; Espenson, J.H. *Inorg. Chem.* **1989**, *28*, 3901.
7. Bakac, A.; Espenson, J.H. *Inorg. Chem.* **1989**, *28*, 4319.
8. (a) Kelley, D.G.; Espenson, J.H.; Bakac, A. *Inorg. Chem.* submitted; (b) Kelley, D.G.; Espenson, J.H.; Bakac, A. *J. Chem. Soc. Chem. Commun.* **1991**, 546.
9. Samuels, G.J.; Espenson, J.H. *Inorg. Chem.* **1979**, *18*, 2587.
10. Kochi, J.K.; Powers, J.W. *J. Am. Chem. Soc.* **1970**, *92*, 137.
11. Rotman, A.; Cohen, H.; Meyerstein, D. *Inorg. Chem.* **1985**, *24*, 4158.
12. Stevens, G.C.; Clark, R.M.; Hart, E.J. *J. Phys. Chem.* **1972**, *76*, 3863.
13. Fenton, H.J.H. *J. Chem. Soc.* **1894**, *65*, 899.
14. Czapski, G.; Samuni, A.; Meisel, D. *J. Phys. Chem.* **1971**, *75*, 3271.
15. (a) Czapski, G.; Levanon, H. *Isr. J. Chem.* **1969**, *7*, 375; (b) Samuni, A.; Czapski, G. *Isr. J. Chem.* **1970**, *8*, 563.
16. Barb, W.G.; Baxendale, J.H.; George, P.; Hargrave, K.R. *Trans. Faraday Soc.* **1951**, *47*, 462.
17. Samuni, A.; Meisel, D.; Czapski, G. *J. Chem. Soc. Dalton Trans.* **1972**, 1273.
18. Bakac, A.; Espenson, J.H. *Inorg. Chem.* **1983**, *22*, 779.

19. Diehl, H.; Clark, H.; Willard, H.H. *Inorg. Synth.* **1939**, *1*, 186.
20. Schlessinger, G.G. *Inorg. Synth.* **1967**, *9*, 160.
21. Lee, S.; Espenson, J.H.; Bakac, A. *Inorg. Chem.* **1990**, *29*, 3442.
22. Kelley, D.G.; Espenson, J.H.; Bakac, A. *Inorg. Chem.* **1990**, *29*, 4996.
23. Yamazaki, N. Hohokabe, Y. *Bull. Chem. Soc. Japan* **1971**, *44*, 63.
24. Bakac, A.; Espenson, J.H. *Inorg. Chem.* **1987**, *26*, 4353.
25. Holah, D.G.; Fackler, J.P. Jr. *Inorg. Synth.* **1969**, *10*, 26.
26. Haupt, G.W. *J. Res. Natl. Bur. Stand.* **1952**, *12*, 414.
27. Kitsen, R.E. *Anal. Chem.* **1950**, *22*, 664.
28. Watanabe, T.; Honda, K. *J. Phys. Chem.* **1982**, *86*, 2617.
29. Barshop, B.A.; Wrenn, C.F.; Frieden, C. *Anal. Biochem.* **1983**, *130*, 134.
We are grateful to Professor Frieden for a copy of this program.
30. Cohen, H.; Meyerstein, D. *J. Chem. Soc. Dalton, Trans.* **1977**, 1056.
31. Candlin, J.P.; Halpern, J. *Inorg. Chem.* **1965**, *4*, 766.
32. Burns, D.T.; Townshend, A.; Carter, A.H. *Inorg. Reaction Chem.* **1981**, *2*, 191.
33. Connolly, P.; Espenson, J.H. *Inorg. Chem.* **1986**, *25*, 2684.
34. Schmidt, W.; Swinehart, J.H.; Taube, H. *J. Am. Chem. Soc.* **1971**, *93*, 1117.
35. Espenson, J.H. *Adv. Inorg. Bioinorg. Mech.* **1982**, *1*, 1.
36. Shi, S.; Espenson, J.H.; Bakac, A. *J. Am. Chem. Soc.* **1990**, *112*, 1841.
37. Ogino, H.; Shimura, M.; Tanaka, N. *Inorg. Chem.* **1982**, *21*, 126.
38. Samuels, G.J.; Espenson, J.H. *Inorg. Chem.* **1980**, *19*, 233.
39. Taub, I.A.; Dorfman, L.F. *J. Am. Chem. Soc.* **1962**, *84*, 4053.
40. Dorfman, L.F.; Taub, I.A. *J. Am. Chem. Soc.* **1963**, *85*, 2370.

41. Bakac, A.; Blau, R.J.; Espenson, J.H. *Inorg. Chem.* **1983**, *22*, 3789.
42. Mulac, W.A. Cohen, H.; Meyerstein, D. *Inorg. Chem.* **1982**, *21*, 4016.
43. Cohen, H.; Meyerstein, D. *J. Chem. Soc. Dalton, Trans.* **1974**, 2559.
44. Ryan, D.A.; Espenson, J.H. *Inorg. Chem.* **1981**, *20*, 4401.
45. Schrauzer, G.N.; Grate, J.H. *J. Am. Chem. Soc.* **1981**, *103*, 541.
46. Connick, R.W. *Symposium on Relaxation Techniques*; Buffalo, N.Y. June 1965.

APPENDIX

Table A1. Kinetic data for the homolysis of $[(15)\text{aneN}_4]\text{CrCH}(\text{CH}_3)\text{OH}^{2+}$ ^a

$[\text{Co}(\text{NH}_3)_5\text{Cl}^{2+}] / 10^{-3} \text{ M}$	$k_{\text{obs}} / 10^{-4}$
16.0	1.80
14.0	1.75
10.0	1.70
6.0	1.82

^aConditions: 25 °C in 0.1 M HClO₄, [RCr] ~ 3 mM and $\mu = 1.0 \text{ M}$ (NaClO₄).

Table A2. Reaction of CH₃ radical with MV^{•+} ^a

$[\text{MV}^{\bullet+}]_0 / 10^{-6} \text{ M}$	$[\text{MV}^{\bullet+}]_{\infty} / 10^{-6} \text{ M}$	$k_{\text{obs}} / 10^4 \text{ s}^{-1}$	$k_{\text{corr}} / 10^4 \text{ s}^{-1}$
11.84	9.23	1.71	1.21
9.76	7.46	1.53	1.12
14.96	12.32	2.46	1.98
12.68	9.64	2.23	1.62
10.17	7.64	1.73	1.24
17.08	13.99	2.73	2.19
14.90	11.65	2.48	1.87
13.08	10.02	2.26	1.66
10.75	8.31	2.09	1.55

^aConditions: 25 °C, $[\text{CH}_3\text{Co}(\text{dmgH})_2] = 3.6 \times 10^{-5} \text{ M}$.

Table A3. Reaction of CH₂CH₃ radical with MV^{•+} a

[MV ^{•+}] ₀ /10 ⁻⁶ M	[MV ^{•+}] _∞ /10 ⁻⁶ M	k _{obs} /10 ⁴ s ⁻¹	k _{corr} /10 ⁴ s ⁻¹
64.94	61.02	7.01	6.57
56.75	52.87	5.60	5.20
82.59	78.78	7.82	7.45
74.23	70.25	8.59	8.12
50.34	46.71	5.20	4.81
43.78	40.10	4.65	4.24
35.11	32.51	3.39	3.31
30.09	26.97	3.28	2.92
24.35	21.45	2.68	2.34
38.43	34.02	4.21	3.70
32.87	28.91	3.83	3.34
27.40	24.01	3.12	2.71

^aConditions: 25 °C, [CH₃CH₂Co(dmgh)₂] = 1.0 x 10⁻⁴ M.

Table A4. Reaction of 1-C₃H₇ radical with MV^{•+} a

[MV ^{•+}] ₀ /10 ⁻⁶ M	[MV ^{•+}] _∞ /10 ⁻⁶ M	k _{obs} /10 ⁴ s ⁻¹	k _{corr} /10 ⁴ s ⁻¹
73.63	70.25	7.55	7.25
66.51	63.36	7.41	7.11
62.68	59.55	6.44	6.17
58.73	55.68	5.90	5.64
55.72	52.80	5.76	5.50
53.17	50.56	5.67	5.43
50.60	48.13	5.29	5.07
48.55	46.09	4.72	4.52
46.28	43.95	5.22	5.00
44.01	41.69	4.43	4.23
40.79	38.77	3.86	3.70
38.19	36.05	4.26	4.06
35.81	34.02	3.92	3.75
34.06	32.21	3.38	3.22

^aConditions: 25 °C, [1-C₃H₇Co(dmgh)₂] = 9.1 x 10⁻⁵.

Table A5. Reaction of $\text{CH}(\text{CH}_3)_2$ radical with MV^{++} a

$[\text{MV}^{++}]_0/10^{-6} \text{ M}$	$[\text{MV}^{++}]_\infty/10^{-6} \text{ M}$	$k_{\text{obs}}/10^4 \text{ s}^{-1}$	$k_{\text{corr}}/10^4 \text{ s}^{-1}$
19.53	16.19	2.25	1.80
15.36	11.94	2.27	1.66
11.78	9.02	2.05	1.47
9.67	7.17	1.80	1.23
24.79	20.47	3.01	2.40
21.25	17.39	2.83	2.23
18.62	15.15	2.68	2.09
16.06	12.90	2.25	1.73
30.74	26.17	3.65	3.03
26.61	22.49	2.94	2.42
22.84	19.31	2.90	2.38
19.96	16.82	2.65	2.17
31.58	27.50	3.98	3.40
26.72	22.68	3.62	2.99
21.83	18.28	3.26	2.65
17.67	14.55	2.61	2.07

aConditions: 25 °C, $[\text{CH}(\text{CH}_3)_2\text{Co}(\text{dmgH})_2] = 3.7 \times 10^{-5} \text{ M}$.

Table A6. Reaction of 1- C_4H_9 radical with MV^{++} a

$[\text{MV}^{++}]_0/10^{-6} \text{ M}$	$[\text{MV}^{++}]_\infty/10^{-6} \text{ M}$	$k_{\text{obs}}/10^4 \text{ s}^{-1}$	$k_{\text{corr}}/10^4 \text{ s}^{-1}$
28.63	25.08	3.52	3.05
25.29	21.94	3.52	3.02
22.42	19.39	3.13	2.68
19.72	17.11	2.81	2.41
52.51	47.99	4.99	4.54
48.32	43.82	4.59	4.14
43.81	39.56	4.07	3.66
39.98	36.14	4.01	3.61
30.05	26.60	3.88	3.41
26.93	23.74	3.58	3.13
24.08	21.09	2.96	2.57
21.72	19.15	3.01	2.63
33.41	29.60	3.88	3.41
28.10	24.06	3.55	3.00
22.45	18.82	2.50	2.06
18.04	15.05	2.27	1.86

aConditions: 25 °C, $[1\text{-C}_4\text{H}_9\text{Co}(\text{dmgH})_2] = 7.8 \times 10^{-5} \text{ M}$.

Table A7. Reaction of $C(CH_3)C_2H_5$ radical with $MV^{+•}$ ^a

$[MV^{+•}]_0/10^{-6}$ M	$[MV^{+•}]_{\infty}/10^{-6}$ M	$k_{obs}/10^4$ s ⁻¹	$k_{corr}/10^4$ s ⁻¹
51.98	47.72	6.28	5.74
47.13	43.29	5.30	4.85
42.34	39.00	4.92	4.52
38.62	35.42	4.41	4.03
33.73	30.72	4.04	3.66
29.69	26.88	3.42	3.08
26.20	23.93	3.08	2.80
23.57	21.43	3.37	3.05
45.81	42.30	4.83	4.45
41.56	37.98	4.78	4.35
37.27	34.06	4.14	3.77
32.14	29.41	3.40	3.10
28.27	25.73	3.12	2.83
24.05	21.88	2.40	2.17
20.92	18.79	2.54	2.27

^aConditions: 25 °C, $[C(CH_3)_2(C_2H_5)Co(dmgh)_2] = 5.2 \times 10^{-5}$ M.

Table A8. Reaction of $CH_2CH(CH_3)_2$ radical with $MV^{+•}$ ^a

$[MV^{+•}]_0/10^{-6}$ M	$[MV^{+•}]_{\infty}/10^{-6}$ M	$k_{obs}/10^4$ s ⁻¹	$k_{corr}/10^4$ s ⁻¹
64.73	59.37	6.23	5.69
57.29	52.05	5.53	5.00
50.83	46.11	5.14	4.64
45.47	41.20	4.49	4.05
40.29	36.84	4.30	3.92
34.42	30.65	3.77	3.33
29.34	25.58	3.09	2.67
58.10	53.73	5.40	4.98
63.34	58.26	6.06	5.55
53.12	48.65	4.80	4.38
48.70	44.24	4.73	4.28
43.51	39.87	3.96	3.61
38.81	35.33	3.66	3.32
35.00	31.84	3.43	3.11
31.78	28.91	3.09	2.80

^aConditions: 25 °C, $[CH_2CH(CH_3)_2Co(dmgh)_2] = 7.8 \times 10^{-5}$ M.

Table A9. Reaction of *c*-C₅H₉ radical with MV^{•+} ^a

$[MV^{•+}]_0/10^{-6} \text{ M}$	$[MV^{•+}]_{\infty}/10^{-6} \text{ M}$	$k_{\text{obs}}/10^4 \text{ s}^{-1}$	$k_{\text{corr}}/10^4 \text{ s}^{-1}$
71.35	67.29	6.62	6.23
66.57	62.98	5.71	5.39
62.86	59.54	5.71	5.40
58.98	55.83	5.92	5.60
55.82	52.74	4.87	4.59
52.48	49.67	4.37	4.13
49.92	47.29	4.67	4.42
47.51	45.02	4.83	4.57
42.53	40.46	3.88	3.69
44.85	42.52	4.19	3.97
40.17	38.26	4.09	3.89
53.85	49.56	4.84	4.44
46.71	42.86	4.91	4.49
40.98	37.17	4.10	3.70
35.48	32.03	3.72	3.34
30.02	26.91	2.86	2.55

^aConditions: 25 °C, $[c\text{-C}_5\text{H}_9\text{Co}(\text{dmgH})_2] = 3.8 \times 10^{-5} \text{ M}$.

Table A10. Reaction of $\text{CH}_2\text{C}(\text{CH}_3)_3$ radical with $\text{MV}^{+\bullet}$ ^a

$[\text{MV}^{+\bullet}]_0/10^{-6} \text{ M}$	$[\text{MV}^{+\bullet}]_\infty/10^{-6} \text{ M}$	$k_{\text{obs}}/10^4 \text{ s}^{-1}$	$k_{\text{corr}}/10^4 \text{ s}^{-1}$
45.83	38.51	4.33	3.37
39.69	32.93	3.72	2.83
34.26	28.28	3.46	2.61
29.20	23.77	2.97	2.19
84.37	78.05	6.97	6.27
79.46	73.19	6.01	5.38
75.44	69.98	6.05	5.47
71.27	66.33	5.50	4.99
67.08	62.47	5.52	5.02
63.45	58.91	5.24	4.74
59.82	55.67	4.93	4.48
56.06	51.83	4.27	3.84
52.43	48.73	4.15	3.76
49.41	45.68	3.78	3.40
46.95	43.80	3.85	3.51
44.33	41.09	3.51	3.17
42.26	35.81	3.78	2.98
36.27	30.36	3.27	2.53
31.53	27.64	2.96	2.46
28.11	24.01	2.53	2.02

^aConditions: 25 °C, $[\text{CH}_2\text{C}(\text{CH}_3)_3\text{Co}(\text{dmgH})_2] = 9.4 \times 10^{-5} \text{ M}$.

Table A11. Reaction of C₆H₅CH₂ radical with MV⁺⁺ ^a

[MV ⁺⁺] ₀ /10 ⁻⁶ M	[MV ⁺⁺] _∞ /10 ⁻⁶ M	k _{obs} /10 ⁴ s ⁻¹	k _{corr} /10 ⁴ s ⁻¹
43.00	40.26	5.03	4.74
39.21	36.36	4.91	4.59
36.05	33.38	4.42	4.13
32.36	29.73	4.12	3.82
28.21	25.61	3.86	3.54
24.58	22.07	3.32	3.01
21.41	19.08	2.91	2.62
61.25	58.54	7.35	7.06
55.92	53.40	6.45	6.19
52.55	50.29	6.11	5.88
48.87	47.13	6.19	6.00
45.78	43.57	5.70	5.46
42.29	39.96	5.07	4.82
39.34	36.93	5.06	4.78
36.18	33.76	4.29	4.03
53.44	50.66	6.11	5.83
49.08	45.84	5.60	5.27
46.14	43.24	5.42	5.12
43.17	40.15	5.04	4.73
39.63	36.96	4.47	4.20
36.00	33.16	4.03	3.73
32.23	29.65	3.87	3.59
29.19	26.69	3.43	3.17

^aConditions: 25 °C, [C₆H₅CH₂Co(dmgh)₂] = 4.2 x 10⁻⁵ M.

Table A12. Reaction of CH_3OCH_2 radical with $\text{MV}^{+\bullet}$ ^a

$[\text{MV}^{+\bullet}]_0/10^{-6} \text{ M}$	$[\text{MV}^{+\bullet}]_\infty/10^{-6} \text{ M}$	$k_{\text{obs}}/10^4 \text{ s}^{-1}$	$k_{\text{corr}}/10^4 \text{ s}^{-1}$
51.32	48.96	5.64	5.40
46.82	44.70	5.37	5.14
42.17	40.06	4.11	3.92
35.17	33.35	4.23	4.03
32.59	30.69	3.77	3.56
29.94	28.32	3.58	3.40
26.77	25.20	3.19	3.01
52.08	49.64	5.27	5.04
49.27	46.84	5.49	5.24
46.74	44.31	5.00	4.76
43.52	41.25	5.00	4.76
41.08	38.83	4.29	4.07
38.76	36.56	4.39	4.16
36.31	34.22	4.24	4.01

^aConditions: 25 °C, $[\text{CH}_3\text{OCH}_2\text{Co}(\text{dmgH})_2] = 3.6 \times 10^{-5} \text{ M}$.

Table A13. Reaction of ClCH₂ radical with MV⁺ a

$[MV^{+}]_0/10^{-6} \text{ M}$	$[MV^{+}]_{\infty}/10^{-6} \text{ M}$	$k_{\text{obs}}/10^4 \text{ s}^{-1}$	$k_{\text{corr}}/10^4 \text{ s}^{-1}$
43.36	41.39	5.42	5.20
39.17	37.03	4.41	4.19
35.44	33.51	3.76	3.58
41.77	39.57	5.09	4.85
44.30	42.32	4.58	4.40
35.84	33.41	3.97	3.73
33.14	30.70	3.88	3.62
27.76	25.64	3.30	3.07
24.55	22.19	2.69	2.45
20.64	18.33	2.48	2.22
47.64	45.57	6.06	5.83
40.02	37.42	4.41	4.15
36.04	33.78	4.03	3.80
29.76	27.47	3.55	3.30
25.28	23.32	2.88	2.68
21.34	19.26	2.28	2.08
58.10	55.80	6.31	6.09
49.57	46.89	5.67	5.40
42.55	40.00	4.45	4.21
36.11	33.84	4.54	4.28
30.48	28.01	3.50	3.24
26.65	24.32	3.33	3.07
22.19	20.03	2.55	2.32

^aConditions: 25 °C, [ClCH₂Co(dmgh)₂] = 3.7 x 10⁻⁵ M.

Table A14. Reaction of BrCH₂ radical with MV^{•+} ^a

$[MV^{•+}]_0/10^{-6} \text{ M}$	$[MV^{•+}]_{\infty}/10^{-6} \text{ M}$	$k_{\text{obs}}/10^4 \text{ s}^{-1}$	$k_{\text{corr}}/10^4 \text{ s}^{-1}$
41.52	38.66	6.72	6.40
49.28	46.11	8.18	7.82
58.11	54.95	9.03	8.69
70.94	68.17	11.4	11.1
25.96	23.05	4.01	3.69
20.59	17.71	3.47	3.12
14.87	12.63	2.47	2.20
43.30	39.72	5.69	5.36
31.26	28.23	5.15	4.80
25.54	22.81	3.95	3.65
20.76	18.39	3.53	3.25
68.87	66.06	10.4	10.1
52.00	49.17	8.62	8.30
45.65	42.91	8.05	7.72
28.31	25.93	4.67	4.40
23.01	20.54	3.45	3.19
63.69	60.56	10.9	10.5
47.72	45.25	6.88	6.64
37.42	35.10	5.04	4.83
52.48	49.88	5.61	5.42
58.22	55.61	9.72	9.42
45.64	42.89	7.89	7.56

^aConditions: 25 °C, $[\text{BrCH}_2\text{Co}(\text{dmgH})_2] = 3.3 \times 10^{-5} \text{ M}$.

Table A15. Reaction of CH₃ radical with Cr([15]aneN₄)²⁺ ^a

[Cr(II)] / 10 ⁻⁴ M	[MV ^{•+}] ₀ / 10 ⁻⁶ M	Δ[MV ^{•+}] / 10 ⁻⁶ M	k _{obs} / 10 ⁴ s ⁻¹	k _{corr} / 10 ⁴ s ⁻¹
0.50	44.80	2.72	6.04	0.51
0.50	40.02	2.91	5.78	0.79
0.50	35.49	2.73	5.05	0.62
1.00	60.54	2.91	8.88	1.43
1.00	56.06	3.12	9.33	2.34
1.00	54.50	2.98	9.32	2.52
1.00	49.89	2.86	6.68	0.54
1.00	46.23	2.66	6.27	0.57
1.50	39.50	1.44	8.50	3.58
1.50	42.07	1.56	7.80	2.60
2.00	42.14	2.13	8.16	2.88
2.00	39.20	1.82	8.53	3.60
2.00	37.14	1.71	7.83	3.17
2.50	42.00	1.35	10.1	4.83
2.50	39.50	1.15	9.43	4.53
2.50	37.47	0.90	8.89	4.27
3.00	39.94	1.63	11.0	5.88
3.00	37.03	1.37	9.56	4.90

^aConditions: 25 °C, [CH₃Co(dmgh)₂] = (1.0-1.3) x 10⁻⁴ M.

Table A16. Reaction of CH₃CH₂ radical with Cr([15]aneN₄)²⁺ a

[Cr(II)] / 10 ⁻⁴ M	[MV ⁺] ₀ / 10 ⁻⁶ M	Δ[MV ⁺] / 10 ⁻⁶ M	k _{obs} / 10 ⁴ s ⁻¹	k _{corr} / 10 ⁴ s ⁻¹
7.93	27.07	1.81	12.96	9.45
7.93	31.36	2.21	14.15	10.1
7.93	40.02	1.78	16.15	11.5
6.87	42.33	2.66	12.21	7.32
6.87	36.87	2.52	13.86	9.32
6.87	31.53	2.04	13.40	9.45
6.87	27.01	1.80	11.80	8.38
5.84	38.46	2.39	12.47	7.94
5.84	39.74	2.73	12.32	7.61
5.84	27.31	1.79	10.77	7.40
5.84	45.33	2.60	12.19	7.07
4.67	38.17	2.85	10.25	5.78
4.67	33.78	2.54	9.97	5.94
4.67	70.39	3.38	13.66	6.12
4.67	57.24	3.07	10.84	4.67
4.67	46.03	2.80	10.21	5.11
4.67	35.89	2.38	9.78	5.64
3.79	66.40	3.99	10.06	3.00
3.79	49.17	3.60	9.33	3.88
3.79	41.13	3.16	7.91	3.32
3.78	58.41	3.69	11.26	4.87
2.82	36.85	3.31	6.67	2.52
2.82	32.12	2.80	6.45	2.79
2.82	27.67	2.40	6.14	2.94
2.82	60.26	3.59	10.06	3.60
2.82	52.30	3.33	8.25	2.64
2.82	45.02	3.29	8.58	3.59
1.79	85.87	4.54	9.87	0.97
1.79	69.30	4.35	8.43	1.17
1.79	75.84	2.72	9.78	1.97
1.79	70.82	3.01	8.72	1.41
0.76	65.55	3.63	8.02	1.19
0.76	61.19	3.51	6.68	0.34
0.76	44.54	3.14	5.28	0.60
0.76	40.80	2.03	4.76	0.54
0.76	39.40	2.76	4.89	0.73
0.76	36.95	2.63	4.39	0.50

^aConditions: 25 °C, [CH₃CH₂Co(dmgh)₂] = (1.0-2.0) x 10⁻⁴ M.

Table A17. Reaction of 1-C₃H₇ radical with Cr([15]aneN₄)²⁺ ^a

[Cr(II)] / 10 ⁻⁴ M	[MV ^{•+}] ₀ / 10 ⁻⁶ M	Δ[MV ^{•+}] / 10 ⁻⁶ M	k _{obs} / 10 ⁴ s ⁻¹	k _{corr} / 10 ⁴ s ⁻¹
1.57	53.31	4.47	6.95	1.14
1.57	50.95	4.46	6.72	1.15
1.57	49.29	4.10	6.40	1.04
1.57	45.27	4.03	6.69	1.67
2.17	53.86	4.29	8.36	2.41
2.17	56.75	4.52	8.38	2.14
2.97	60.42	4.22	8.73	2.16
2.97	58.92	4.27	8.80	2.36
2.97	55.93	3.88	8.58	2.47
3.79	59.91	3.69	10.98	4.37
3.79	55.45	3.41	9.72	3.63
3.79	58.45	3.51	11.37	4.90
4.48	58.79	3.88	10.65	4.14
4.48	55.46	4.14	9.73	3.54
4.48	52.78	3.41	9.09	3.29
4.48	50.04	3.60	8.59	3.04
5.08	57.76	3.37	11.33	4.94
5.08	54.26	3.29	11.96	5.86
5.08	50.30	3.13	10.78	5.13
5.08	47.31	3.08	10.49	5.13

^aConditions: 25 °C, [1-C₃H₇Co(dmgh)₂] = (0.9-2.3) x 10⁻⁴ M.

Table A18. Reaction of $\text{CH}(\text{CH}_3)_2$ radical with $\text{Cr}([\text{15}] \text{aneN}_4)^{2+}$ a

$[\text{Cr}(\text{II})]$ / 10^{-4} M	$[\text{MV}^{+\cdot}]_0$ / 10^{-6} M	$\Delta[\text{MV}^{+\cdot}]$ / 10^{-6} M	k_{obs} / 10^4 s $^{-1}$	k_{corr} / 10^4 s $^{-1}$
0.95	39.22	6.25	6.32	1.16
0.95	24.89	4.83	4.63	1.15
0.95	31.23	5.66	4.75	0.62
0.95	20.40	3.97	4.40	1.43
0.95	25.62	4.45	4.68	1.18
0.95	31.67	5.43	4.91	0.74
2.20	36.90	4.60	6.37	1.60
2.20	40.82	5.13	6.56	1.33
2.20	47.98	5.53	7.30	1.25
2.20	52.15	6.15	7.39	0.86
2.20	45.85	4.85	6.78	1.05
2.20	50.51	5.16	6.77	0.54
2.20	56.20	5.53	7.80	0.86
3.46	47.98	4.96	8.61	2.48
3.46	41.86	4.79	7.49	2.10
3.46	37.06	4.27	7.03	2.21
3.46	55.06	5.17	9.29	2.37
3.46	49.09	4.90	8.48	2.26
3.46	42.71	4.38	7.17	1.77
3.46	37.57	4.14	6.94	2.09
4.87	24.10	2.86	6.91	3.51
4.87	32.32	3.71	7.66	3.30
4.87	36.78	4.29	8.70	3.73
4.87	23.50	2.78	7.20	3.84
4.87	26.95	3.21	7.76	3.95
4.87	30.69	3.51	8.05	3.83
4.87	35.06	3.95	7.71	3.05
5.95	35.71	3.92	7.92	3.19
5.95	30.35	3.38	8.68	4.45
5.95	51.60	4.35	9.47	2.97
5.95	41.82	3.90	9.98	4.48
5.95	22.80	2.96	7.77	4.35
5.95	31.68	3.23	8.18	3.91

Table A18 Continued

[Cr(II)] / 10 ⁻⁴ M	[MV ⁺⁺] ₀ / 10 ⁻⁶ M	Δ[MV ⁺⁺] / 10 ⁻⁶ M	k _{obs} / 10 ⁴ s ⁻¹	k _{corr} / 10 ⁴ s ⁻¹
7.28	30.09	3.32	9.67	5.38
7.28	36.39	3.66	8.68	3.85
7.28	44.00	4.37	10.11	4.31
7.28	52.37	4.93	10.80	4.05
7.28	32.92	3.47	8.82	4.33
7.28	39.09	3.98	9.29	4.10
7.28	45.64	4.48	9.46	3.55
7.28	52.90	5.08	11.67	4.77
8.32	41.48	4.42	9.64	4.12
8.32	33.00	3.63	8.97	4.43
8.32	27.59	3.33	9.65	5.56
8.32	21.39	2.79	7.14	3.95
8.32	50.15	4.47	11.09	4.60
8.32	42.35	4.10	10.36	4.74
8.32	35.51	3.49	9.46	4.67
8.32	28.64	3.06	8.81	4.79
9.54	29.42	2.72	12.11	7.82
9.54	24.08	2.21	9.59	6.11
9.54	20.53	1.77	9.43	6.41
9.54	17.38	1.54	9.73	7.02
9.54	36.37	3.34	11.34	6.35
9.54	30.32	3.00	10.53	6.22
9.54	25.81	2.55	9.91	6.16
9.54	21.44	2.10	9.42	6.21

^aConditions: 25 °C, [CH(CH₃)₂Co(dmgh)₂] = (1.2-1.6) x 10⁻⁴ M.

Table A19. Reaction of 1-C₄H₉ radical with Cr([15]aneN₄)²⁺ ^a

[Cr(II)] / 10 ⁻⁴ M	[MV ⁺⁺] ₀ / 10 ⁻⁶ M	Δ[MV ⁺⁺] / 10 ⁻⁶ M	k _{obs} / 10 ⁴ s ⁻¹	k _{corr} / 10 ⁴ s ⁻¹
0.22	26.21	2.84	3.69	0.43
0.22	29.59	3.03	3.81	0.17
0.81	67.25	3.37	8.58	0.53
0.81	74.63	4.17	10.25	1.26
2.23	38.68	2.59	6.87	2.09
2.23	44.69	3.04	7.38	1.88
2.23	44.79	3.85	7.40	1.82
3.35	52.92	2.78	9.27	2.81
3.35	57.85	2.97	9.39	2.37
3.35	63.52	3.12	10.20	2.51
3.78	57.12	2.19	10.51	3.60
3.78	60.93	2.62	10.07	2.72
3.78	65.41	2.89	12.63	4.66
3.78	68.82	2.68	12.36	4.05
4.61	53.30	2.79	9.57	3.06
4.61	40.65	2.42	9.19	4.09
5.65	43.84	2.19	10.87	5.39
5.65	47.96	2.22	9.97	4.08
5.65	51.40	2.37	10.31	4.02

^aConditions: 25 °C, [1-C₄H₉Co(dmgH)₂] = (0.45-0.89) x 10⁻⁴ M.

Table A2-20. Reaction of $C(CH_3)C_2H_5$ radical with $Cr([15]aneN_4)^{2+}$ ^a

$[Cr(II)]$ / 10^{-4} M	$[MV^{+}]_0$ / 10^{-6} M	$\Delta[MV^{+}]$ / 10^{-6} M	k_{obs} / 10^4 s ⁻¹	k_{corr} / 10^4 s ⁻¹
0.19	21.41	3.21	3.03	0.44
0.19	25.25	3.51	2.98	0.03
0.19	30.11	3.99	3.94	0.39
0.19	35.12	4.66	4.12	0.04
0.73	54.67	4.12	6.71	0.54
1.81	26.28	3.38	4.77	1.51
1.81	27.89	3.50	4.61	1.22
1.81	30.26	3.78	4.86	1.20
1.81	32.53	3.96	4.89	1.00
2.53	33.50	3.46	5.50	1.51
2.53	36.73	3.76	6.04	1.67
2.53	38.32	4.02	5.92	1.39
2.53	40.18	4.04	6.02	1.31
3.19	48.57	4.43	6.78	1.17
3.19	47.69	4.17	7.76	2.18
3.19	45.27	3.87	7.20	1.92
3.19	41.98	3.80	7.07	2.12
4.13	32.38	3.02	6.19	2.30
4.13	34.85	3.18	6.65	2.47
4.13	37.81	3.27	6.94	2.45
4.13	40.53	3.48	6.76	2.01
4.67	50.60	3.62	8.19	2.36
4.67	57.93	4.35	8.98	2.31
4.67	60.55	4.47	9.72	2.73
5.44	39.81	3.64	8.69	3.82
5.44	43.27	3.96	8.43	3.22
5.44	47.26	4.03	9.02	3.39
5.44	51.23	4.62	9.34	3.24

^aConditions: 25 °C, $[C(CH_3)C_2H_5Co(dmgH)_2] = (0.5-1.0) \times 10^{-4}$ M.

Table A21. Reaction of $\text{CH}_2\text{CH}(\text{CH}_3)_2$ radical with $\text{Cr}([\text{15}] \text{aneN}_4)^{2+}$ ^a

$[\text{Cr}(\text{II})]$ / 10^{-4} M	$[\text{MV}^{+\cdot}]_0$ / 10^{-6} M	$\Delta[\text{MV}^{+\cdot}]$ / 10^{-6} M	k_{obs} / 10^4 s ⁻¹	k_{corr} / 10^4 s ⁻¹
1.29	55.50	3.96	5.87	0.45
1.29	59.71	4.16	6.55	0.71
1.29	64.50	4.27	6.87	0.59
1.58	45.66	2.88	5.05	0.68
1.58	50.09	4.34	5.36	0.52
1.58	55.02	4.75	5.84	0.53
1.58	60.32	4.81	6.17	0.38
2.34	75.56	4.47	8.92	1.68
2.34	79.96	4.65	9.62	1.95
2.48	46.19	3.91	5.95	1.29
2.48	41.84	3.60	5.53	1.29
2.48	39.20	3.53	5.26	1.26
2.97	52.82	3.94	7.36	2.18
3.36	37.08	2.93	6.78	2.88
3.36	40.50	3.11	6.40	2.25
3.36	44.09	3.29	7.24	2.71
3.36	48.34	3.75	7.62	2.66
3.79	84.85	4.45	11.03	2.74
3.79	79.69	4.27	11.48	3.62
3.79	74.90	4.01	9.81	2.48
3.88	55.28	3.20	7.58	2.23
3.88	59.51	3.70	8.45	2.66
3.88	63.77	3.93	8.88	2.69
3.88	66.10	3.94	9.44	3.02
4.62	56.52	3.60	9.21	3.64
4.62	61.28	3.91	9.22	3.22
4.65	50.94	3.69	8.91	3.64
5.51	43.88	3.08	9.34	4.69
5.51	48.98	3.04	9.32	4.28
5.61	49.90	3.70	8.97	3.95
5.61	40.57	3.08	8.20	4.05

^aConditions: 25 °C, $[\text{CH}_2\text{CH}(\text{CH}_3)_2\text{Co}(\text{dmgH})_2] = (3.9\text{-}7.8) \times 10^{-5}$ M.

Table A22. Reaction of c-C₅H₉ radical with Cr([15]aneN₄)²⁺ ^a

[Cr(II)] / 10 ⁻⁴ M	[MV ^{•+}] ₀ / 10 ⁻⁶ M	Δ[MV ^{•+}] / 10 ⁻⁶ M	k _{obs} / 10 ⁴ s ⁻¹	k _{corr} / 10 ⁴ s ⁻¹
0.12	47.40	3.46	4.66	0.13
0.64	72.10	3.68	7.21	0.43
1.63	66.39	3.88	7.11	0.80
1.63	50.82	3.12	5.84	0.97
1.63	60.96	3.64	8.08	2.17
1.63	56.01	3.38	7.11	1.70
2.47	47.39	3.67	6.74	2.01
2.47	43.75	3.71	6.03	1.64
2.47	36.77	3.07	4.89	1.23
3.43	39.37	2.78	7.02	3.01
3.43	42.46	2.98	7.40	3.09
3.43	46.17	3.23	8.31	3.61
3.43	49.02	3.43	7.02	2.17
4.03	40.65	2.91	7.83	3.64
4.03	43.07	3.26	7.22	2.84
4.03	46.17	3.23	8.31	3.61
4.03	50.52	3.73	7.73	2.67
5.46	43.72	2.71	8.49	4.05
5.46	47.45	2.57	9.92	5.13
5.46	53.60	3.16	9.44	4.09

^aConditions: 25 °C, [c-C₅H₉Co(dmgH)₂] = (5.3-9.1) × 10⁻⁵ M.

Table A23. Reaction of $\text{CH}_2\text{C}(\text{CH}_3)_3$ radical with $\text{Cr}([\text{15}] \text{aneN}_4)^{2+}$ ^a

$[\text{Cr}(\text{II})]$ / 10^{-4} M	$[\text{MV}^{+\cdot}]_0$ / 10^{-6} M	$\Delta[\text{MV}^{+\cdot}]$ / 10^{-6} M	k_{obs} / 10^4 s ⁻¹	k_{corr} / 10^4 s ⁻¹
0.91	44.68	3.19	4.41	0.69
0.91	47.59	3.62	4.42	0.47
0.91	51.43	3.69	4.90	0.64
0.91	56.08	4.11	5.29	0.64
1.61	45.76	3.02	5.02	1.19
1.61	48.66	3.25	4.96	0.92
1.61	51.43	3.41	4.94	0.70
1.61	57.68	3.82	6.01	1.22
2.45	44.16	3.15	5.33	1.56
3.88	31.39	2.36	5.09	2.26
4.75	43.24	3.07	7.17	3.30
4.75	37.54	2.59	6.23	2.88
4.75	32.25	2.40	6.45	3.45
4.75	27.28	1.89	5.43	2.91
5.87	41.06	3.23	8.18	4.29
5.87	37.52	2.90	7.60	4.05
5.87	33.94	2.79	7.39	4.08
5.87	30.73	2.35	7.31	4.29

^aConditions: 25 °C, $[\text{CH}_2\text{C}(\text{CH}_3)_3\text{Co}(\text{dmgH})_2] = (3.3\text{-}7.5) \times 10^{-5}$ M.

Table A24. Reaction of $C_6H_5CH_2$ radical with $Cr([15]aneN_4)^{2+}$ ^a

$[Cr(II)]$ / 10^{-4} M	$[MV^{+}]_0$ / 10^{-6} M	$\Delta[MV^{+}]$ / 10^{-6} M	k_{obs} / 10^4 s ⁻¹	k_{corr} / 10^4 s ⁻¹
0.31	42.10	2.08	5.42	0.38
0.31	43.11	2.32	5.99	0.80
0.96	42.01	2.62	6.86	1.72
0.96	38.31	2.33	6.62	1.92
1.54	49.09	2.40	8.72	2.74
1.54	46.48	2.36	9.11	3.40
1.54	44.07	2.36	7.78	2.40
1.54	41.82	2.18	8.60	3.44
2.38	34.56	1.76	10.26	5.86
2.38	33.89	1.98	9.92	5.56
2.38	32.97	1.99	8.70	4.50
2.38	31.92	1.75	8.92	4.86
3.12	38.58	1.71	14.80	9.81
3.12	37.70	1.53	13.40	8.60
3.12	36.42	1.71	10.20	5.62
3.12	34.79	1.70	9.73	5.34
3.66	45.10	1.66	11.41	5.86
3.66	43.15	1.57	15.98	10.5

^aConditions: 25 °C, $[C_6H_5CH_2Co(dmgh)_2] = (0.6-1.3) \times 10^{-4}$ M.

Table A25. Reaction of CH_3OCH_2 radical with $\text{Cr}([\text{15}] \text{janeN}_4)^{2+}$ ^a

$[\text{Cr(II)}]$ / 10^{-4} M	$[\text{MV}^{+\cdot}]_0$ / 10^{-6} M	$\Delta[\text{MV}^{+\cdot}]$ / 10^{-6} M	k_{obs} / 10^4 s ⁻¹	k_{corr} / 10^4 s ⁻¹
0.13	42.04	3.09	4.79	0.15
0.13	37.97	3.08	4.45	0.23
0.13	34.40	2.75	4.24	0.41
0.64	73.67	3.48	8.98	0.95
0.64	68.60	3.44	8.37	0.87
1.49	55.00	3.10	8.92	2.77
1.49	49.57	3.17	8.28	2.68
1.49	46.21	2.83	8.62	3.36
1.49	42.12	2.70	7.61	2.81
2.21	57.73	2.85	9.50	3.08
2.21	54.21	2.57	9.90	3.84
2.21	50.48	2.60	9.21	3.54
2.21	47.33	2.46	9.98	4.59
2.97	51.21	2.95	10.21	4.37
2.97	47.14	2.72	9.81	4.41
3.79	52.96	2.54	11.41	5.40
3.79	49.42	2.27	12.32	6.66
3.79	46.46	2.47	12.21	6.79
3.79	42.96	2.30	10.93	5.93
4.65	55.63	2.16	14.78	8.45
4.65	67.53	2.12	15.91	8.39
5.38	59.85	2.18	15.85	9.07
5.38	62.86	1.95	14.27	7.29
5.38	56.37	1.95	15.44	9.06
5.38	52.92	1.49	15.84	9.88

^aConditions: 25 °C, $[\text{CH}_3\text{OCH}_2\text{Co}(\text{dmgH})_2] = (1.8\text{-}2.7) \times 10^{-5}$ M.

Table A26. Reaction of ClCH₂ radical with Cr([15]aneN₄)²⁺ ^a

[Cr(II)] / 10 ⁻⁴ M	[MV ⁺] ₀ / 10 ⁻⁶ M	Δ[MV ⁺] / 10 ⁻⁶ M	k _{obs} / 10 ⁴ s ⁻¹	k _{corr} / 10 ⁴ s ⁻¹
3.95	47.67	1.42	11.06	5.46
3.95	45.95	1.31	10.62	5.23
3.95	44.62	1.36	11.49	6.21
3.95	46.02	1.46	10.60	5.18
3.95	44.24	1.39	9.97	4.77
3.95	42.42	1.60	9.48	4.45
3.38	42.89	1.66	9.18	4.11
3.38	40.71	2.00	8.43	3.57
3.38	39.38	1.65	8.23	3.56
3.38	57.88	1.62	10.56	3.85
3.38	54.05	1.73	10.90	4.58
2.80	47.23	1.90	8.21	2.68
2.80	45.76	1.90	8.48	3.10
2.80	44.22	2.06	8.62	3.38
2.80	48.97	2.06	9.30	3.53
2.80	46.66	1.98	8.62	3.13
2.80	44.78	2.10	8.54	3.24
2.42	49.36	2.49	8.29	2.47
2.42	46.07	2.13	7.49	2.09
2.42	43.36	2.48	7.13	2.00
2.42	51.69	2.16	8.43	2.39
2.42	44.64	2.19	6.76	1.54
1.85	41.72	2.30	6.65	1.73
1.85	38.84	2.44	6.16	1.56
1.85	36.85	2.46	5.97	1.58
1.85	47.11	2.21	6.84	1.35
1.85	44.51	2.23	6.79	1.58
1.85	41.71	2.28	6.56	1.65
1.39	69.31	2.81	10.01	1.97
1.39	57.92	2.99	7.85	1.11
1.39	60.59	3.30	7.63	0.59
1.39	54.30	3.08	7.31	0.97
1.39	49.44	3.04	6.61	0.82
0.90	55.32	2.54	6.84	0.45
0.90	52.02	2.44	6.70	0.67
0.90	54.03	2.43	6.81	0.56

^aConditions: 25 °C, [ClCH₂Co(dmgh)₂] = (1.3-1.7) x 10⁻⁴ M.

Table A27. Reaction of BrCH₂ radical with Cr([15]aneN₄)²⁺ ^a

[Cr(II)] / 10 ⁻⁴ M	[MV ⁺] ₀ / 10 ⁻⁶ M	Δ[MV ⁺] / 10 ⁻⁶ M	k _{obs} / 10 ⁴ s ⁻¹	k _{corr} / 10 ⁴ s ⁻¹
3.50	34.09	0.69	12.55	6.33
3.50	31.93	0.76	11.14	5.31
3.50	34.37	0.93	11.18	4.91
3.00	31.09	1.03	11.19	5.48
3.00	27.82	1.39	8.55	3.42
3.00	44.83	1.52	11.74	3.58
3.00	32.46	1.63	9.76	3.78
2.50	41.15	1.81	11.37	3.84
2.50	32.18	1.84	9.71	3.77
2.50	26.56	1.73	7.88	2.96
2.50	20.85	1.69	5.94	2.06
2.50	16.20	1.51	5.77	2.68
2.00	26.31	1.58	7.48	2.63
1.50	34.81	2.11	8.20	1.84
1.50	26.41	2.08	6.95	2.07
1.50	20.95	1.89	6.12	2.20
1.50	38.77	2.25	9.83	2.73
1.50	29.18	1.97	7.97	2.59
1.50	22.76	1.93	5.98	1.76
1.00	30.91	2.06	6.73	1.09
1.00	36.98	2.33	8.13	1.39
0.50	42.13	2.68	8.18	0.54

^aConditions: 25 °C, [BrCH₂Co(dmgh)₂] = (1.3-2.6) x 10⁻⁴ M.

Table A28. Reaction of CH₃ radical with Cr([15]aneN₄)²⁺ using RCo([14]aneN₄)²⁺ ^a

[Cr(II)] / 10 ⁻⁴ M	[MV ⁺⁺] ₀ / 10 ⁻⁶ M	Δ[MV ⁺⁺] / 10 ⁻⁶ M	k _{obs} / 10 ⁴ s ⁻¹	k _{corr} / 10 ⁴ s ⁻¹
0.40	30.74	3.40	4.61	0.68
0.40	28.66	2.70	4.33	0.70
0.80	27.45	2.36	4.67	1.17
0.80	25.00	2.41	4.13	0.93
1.20	31.29	1.89	6.41	2.44
1.20	30.75	1.76	6.32	2.43
1.20	29.59	2.00	6.00	2.22
1.20	28.67	2.00	6.04	2.36
1.60	30.50	1.74	7.96	4.01
1.60	29.78	1.70	7.64	3.79
1.60	28.94	1.66	7.35	3.62
1.60	27.91	1.62	7.51	3.88
2.00	27.01	1.16	8.75	5.26
2.00	30.19	1.22	9.83	5.94
2.00	29.80	1.19	9.86	6.02
2.40	32.85	1.83	10.59	6.25
2.40	31.13	1.84	9.97	5.84
2.40	28.84	1.75	10.28	6.39
2.80	19.43	1.16	9.20	6.47
2.80	18.67	1.15	9.41	6.74
2.80	17.83	0.99	9.20	6.68
3.20	25.29	1.27	12.01	8.54
3.20	28.53	1.40	10.49	6.71

^aConditions: 25 °C, [CH₃Co([14]aneN₄)²⁺] = 2.0 × 10⁻⁵ M.

Table A29. Reaction of CH_3CH_2 radical with $\text{Cr}([\text{15}]\text{aneN}_4)^{2+}$ using $\text{RCo}([\text{14}]\text{aneN}_4)^{2+}$ ^a

$[\text{Cr}(\text{II})]$ / 10^{-4} M	$[\text{MV}^{+\cdot}]_0$ / 10^{-6} M	$\Delta[\text{MV}^{+\cdot}]$ / 10^{-6} M	k_{obs} / 10^4 s^{-1}	k_{corr} / 10^4 s^{-1}
0.40	10.73	1.73	1.63	0.36
0.90	53.24	4.10	6.52	0.88
0.90	50.00	3.75	6.08	0.79
0.90	47.96	4.02	6.16	1.03
1.80	41.54	3.54	6.65	2.08
1.80	40.75	3.83	6.41	1.89
1.80	40.61	3.74	5.81	1.38
2.60	69.13	2.30	8.59	1.50
2.60	71.38	2.64	9.07	1.72
2.60	72.25	3.16	8.74	1.28
3.30	52.12	2.67	8.78	3.24
3.30	53.21	2.57	8.03	2.44
3.30	53.73	2.40	9.09	3.42
4.00	67.32	2.18	11.64	4.63
4.00	69.70	2.53	10.65	3.41
4.00	68.44	2.40	10.38	3.29
5.00	44.95	1.86	10.03	5.20
5.00	44.02	1.75	9.06	4.38

^aConditions: 25 °C, $[\text{CH}_3\text{CH}_2\text{Co}([\text{14}]\text{aneN}_4)^{2+}] = (3.3\text{-}5.0) \times 10^{-5}$ M.

Table A30. Reaction of CH_3OCH_2 radical with $\text{Cr}([\text{15}] \text{aneN}_4)^{2+}$ using $\text{RCo}([\text{14}] \text{aneN}_4)^{2+}$ ^a

$[\text{Cr}(\text{II})]$ / 10^{-4} M	$[\text{MV}^{+\cdot}]_0$ / 10^{-6} M	$\Delta[\text{MV}^{+\cdot}]$ / 10^{-6} M	k_{obs} / 10^4 s^{-1}	k_{corr} / 10^4 s^{-1}
0.74	60.74	2.88	7.59	0.96
1.63	74.59	3.44	10.12	1.95
2.54	45.80	2.41	8.82	3.64
2.54	46.29	2.33	9.03	3.81
2.54	46.22	2.43	9.39	4.14
3.09	64.54	2.64	10.79	3.66
3.09	63.51	2.53	10.90	3.88
3.09	60.63	2.59	12.51	5.71
3.73	57.41	1.99	12.67	6.27
3.73	58.58	2.38	12.24	5.68
3.73	58.16	2.02	10.80	4.38
3.73	56.39	2.41	10.65	4.36
4.48	50.88	1.90	11.39	5.69
4.48	60.96	1.74	13.29	6.56
4.48	57.80	1.86	14.17	7.70
4.48	54.55	1.86	14.28	8.13
5.38	44.72	1.26	12.15	7.15
5.38	43.12	1.35	13.50	8.60
5.38	40.54	1.50	12.99	8.31
5.38	38.40	1.46	12.47	8.02

^aConditions: 25 °C, $[\text{CH}_3\text{OCH}_2\text{Co}([\text{14}] \text{aneN}_4)^{2+}] = 6.7 \times 10^{-5}$ M.

Table A31. Reaction of CH₂Br radical with Cr([15]aneN₄)²⁺ using RCo([14]aneN₄)²⁺ ^a

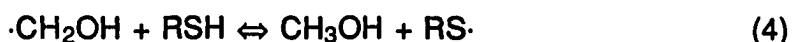
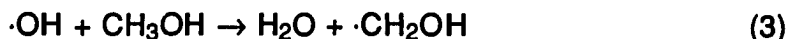
[Cr(II)] / 10 ⁻⁴ M	[MV ^{•+}] ₀ / 10 ⁻⁶ M	Δ[MV ^{•+}] / 10 ⁻⁶ M	k _{obs} / 10 ⁴ s ⁻¹	k _{corr} / 10 ⁴ s ⁻¹
0.40	41.57	2.52	8.12	0.62
0.40	38.52	2.39	6.99	0.06
0.40	35.87	2.29	7.86	1.35
0.70	61.79	2.28	12.21	1.10
0.70	59.77	2.12	12.53	1.77
0.70	57.83	1.97	11.30	0.91
1.00	41.99	2.09	9.27	1.68
1.00	40.11	0.93	7.92	0.72
1.00	38.61	1.89	9.80	2.78
1.00	36.35	1.88	7.91	1.34
1.30	35.72	1.79	8.84	2.35
1.30	37.85	2.00	7.83	1.00
1.30	40.48	2.01	9.51	2.17
1.60	43.15	1.93	10.02	2.21
1.60	41.91	1.81	11.99	4.35
1.60	45.83	1.80	10.55	2.27
1.60	45.08	2.08	10.94	2.77
1.90	48.01	1.90	11.57	2.89
1.90	44.96	1.80	10.93	2.79
2.10	35.11	1.65	8.59	2.22
2.10	32.26	1.83	10.31	4.36
2.10	30.27	1.59	9.83	4.26
2.10	28.17	1.50	7.44	2.30
2.40	34.71	1.68	9.14	2.82
2.40	32.33	1.83	12.08	6.06
2.40	29.98	1.75	8.88	3.37
2.40	27.69	1.69	8.64	3.53

^aConditions: 25 °C, [BrCH₂Co([14]aneN₄)²⁺] = 3.3 × 10⁻⁵ M.

**PART III REACTIONS OF THIYL RADICALS WITH
TRANSITION METAL COMPLEXES**

INTRODUCTION

Thiyl radicals are intermediates in the oxidation of thiols to disulfides. These sulfur-centered radicals have been shown to be produced in biological systems in reactions of oxidative enzymes with thiols.¹⁻⁴ Thiyl radicals have most often been generated for chemical studies using the technique of pulse radiolysis. This is accomplished by reactions of $\text{H}\cdot$ or $\cdot\text{OH}$ with thiols (eq. 1 and 2). With alcohols present hydroxyalkyl radicals are generated (eq 3), which abstract a hydrogen atom from a thiol in the so-called repair reaction⁵⁻⁸ (eq 4). This reaction is utilized in biological systems to protect against radiation damage and against naturally occurring radicals. Studies of the repair reaction involving a variety of carbon-centered radicals with thiols such as cysteine, glutathione, cysteamine and mercapto-ethanol have been carried out pulse radiolytically. These studies have included radicals derived from alcohols, glucose, acetone, nucleic acid components (uracil, thymine, dihydrothymine and thymidine) as well as polymers such as ethylene glycol and polyethylene oxide.⁵⁻⁸ The forward reaction typically has rate constants, k_4 , on the order of 10^7 - 10^9 $\text{L mol}^{-1}\text{s}^{-1}$. The sulfur-hydrogen bond dissociation Enthalpy in alkane thiols is 88 kcal mol^{-1} and is independent of the length and configuration of the alkyl chain.⁹ Thus, alkane thiyl radicals are able to abstract hydrogen in the reverse of the repair reaction. This reverse reaction generally occurs much more slowly with $k_{-4} = 10^3$ - 10^7 , depending on how strongly activated the C-H bond is,^{10,11} and is believed not to be important here.



Direct (UV) photolysis of disulfides may lead to cleavage of the S-S or a C-S bond (eq 5 and 6). For simple (methyl, ethyl) disulfides reaction 6 was found to be unimportant.¹² In the photolysis of mixtures of neat methyl and ethyldisulfides, the sole detectable product was ethylmethyl disulfide formed with extremely high quantum yield ($\phi = 330$) attributed to a chain propagating step (eq 7).¹³ With more highly substituted disulfides, such as di-tert-butyl and penicillamine disulfides, reaction 6 becomes much more important. From gas phase studies the S-S bond energy in disulfides was found to be 68.1 kcal mol⁻¹ and was independent of the nature of R. The C-S bond energy in the case of EtSSR (R = H, alkyl) was found to be 57.6 kcal mol⁻¹.⁹ Photons of 250-290 nm have enough energy to break these C-S bonds, so other factors must affect the yields. The cleavage of the C-S bond is apparently not very important unless particularly stable alkyl radicals are products.¹⁴





Thiyl radicals have been identified by spin trapping studies employing DMPO and TMPO.^{4,15-17} The lack of nuclear spin in the main sulfur isotope, ³²S, prevents any information from ESR on structural aspects. Thiyl radicals are not easily detectable spectroscopically, having molar absorptivities of only several hundred at 300 nm.¹⁸ For this reason many studies involving RS· have been carried out in strongly alkaline media (pH > 8), where the thiol is deprotonated and the disulfide radical anion is formed (eq 8).^{19,20} This species is highly colored¹⁸ with a molar absorptivity of ~9000 L mol⁻¹cm⁻¹ around 420 nm. The reverse of reaction 8 is also a convenient method of producing thiyl radicals. One electron reduction of disulfides generates the disulfide radical anion, which rapidly decays, especially in the absence of excess thiolate.

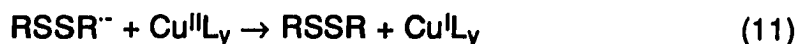


Simple aliphatic thiyl radicals react with molecular oxygen (eq 9) in what may actually be a reversible process, with rate constants on the order of 10⁸ L mol⁻¹s⁻¹.²¹



Reactions of arenethiyl radicals with olefins have been studied and have been shown to be reversible. The reaction is an addition to the double bond and occurs with rate constants on the order of 10^6 - 10^7 L mol⁻¹s⁻¹ for systems such as styrene that give stabilized carbon-centered radicals.²² This reaction has been used in the case of 1,1-diphenyl ethylene to yield the highly colored substituted diphenyl methyl radical. This was then used as a kinetic probe in isooctane.²³

The thiyl radical oxidizes compounds such as ferrocyclochrome c,²⁴ NADH,²⁵ ascorbate, phenothiazines²⁶ and organometallic substrates such as boranes, phosphines and phosphites.²³ The potential for the RS•/RS⁻ couple has been estimated as 0.77 V vs NHE.²⁷ Recently, two studies of RS• oxidizing complexes of Cu(I) have been carried out.^{28,29} The thiyl radicals oxidize the Cu(I)L₂ complex (L = cysteine) with a diffusion controlled rate constant, $k = 1.8 \times 10^9$ L mol⁻¹s⁻¹. These studies were complicated by the equilibrium with Cu₂L₃ (eq 10), by acid-base equilibria and by back reactions such as reaction 11.



The presence of sulfur in the active site of many enzymes and its role in electron transfer reactions makes such studies of interest. Transition metal-thiolate complexes may serve as models in understanding the metal-thiol interactions in systems like non-heme iron-sulfur proteins.³⁰

In this study a simple method for generating sulfur-centered radicals and studying their reactions was developed using visible laser flash photolysis. This method involved well-established reactions to generate the radicals and allowed the study of their reactions in acidic and neutral aqueous solution. This was done by taking advantage of the repair reaction and by using two kinetic probes: ABTS²⁻ (2,2'-azino-bis(3-ethylbenz-thiazoline-6-sulfonate) ion) and TMPD (N,N,N',N'-tetramethyl-1,4-phenylenediamine). Thiyl radicals were also generated by direct photolysis of diethyl disulfide at 266 nm. Studies of thiyl radicals with a variety of transition metal complexes are described here. Hexaaqua metal ions of chromium(II), iron(II) and vanadium(II) were studied, along with a series of cobalt(II) macrocyclic complexes. Product studies were carried out to elucidate the mechanisms involved.

EXPERIMENTAL

Materials

All water used in this study was in-house distilled, deionized water passed through a Millipore-Q purification system. All chemicals were used as received unless noted below. Solutions were degassed by purging with water-saturated argon (99.99 % pure, Air Products Corp.). Solutions were transferred anaerobically using syringe and septa techniques. Ethane thiol (Johnson Matthey Electronics) was purified by passing it through neutral activated alumina having a Brockman activity of 1 and 80-200 mesh (Fisher). This removed the less soluble disulfide impurity. The complexes $\text{RCo}([\text{14}] \text{aneN}_4)^{2+}$ ($\text{R} = \text{CH}_3, \text{C}_2\text{H}_5$) were prepared according to literature procedures.³¹ Stock solutions of these radical precursors were protected from light. Stock solutions of N,N,N',N'-tetramethyl-1,4-phenylenediamine (Aldrich) were prepared by addition of the solid to degassed water and were protected from light. A solution of phosphate buffer (0.10 M) was prepared by mixing solutions of KH_2PO_4 and K_2HPO_4 until the pH was 7.0 as determined by a Jenco pH meter.

Solutions of $\text{Cr}(\text{H}_2\text{O})_6^{2+}$ in aqueous perchloric acid were prepared by reduction of solutions of $\text{Cr}(\text{ClO}_4)_3$ over zinc amalgam. Solutions of VO^{2+} in aqueous perchloric acid were prepared from $\text{VOSO}_4 \cdot x\text{H}_2\text{O}$, which was adsorbed onto Dowex 50W-X4 cation exchange resin. Sulfate ions were rinsed from the column with dilute HClO_4 and VO^{2+} was eluted with 2 M HClO_4 . The concentration of VO^{2+} was determined spectrophotometrically ($\epsilon_{760} = 17.5 \text{ L mol}^{-1}\text{cm}^{-1}$) and the acid content was determined by difference. Solutions of $\text{V}(\text{H}_2\text{O})_6^{2+}$ were prepared by reduction of VO^{2+} over

zinc amalgam and used immediately. Solutions of $\text{Fe}(\text{ClO}_4)_2 \cdot 6\text{H}_2\text{O}$ were prepared in dilute aqueous perchloric acid, degassed, and placed over zinc amalgam. The concentration was determined spectrophotometrically by addition of an aliquot to excess 1,10-phenanthroline (Fisher), forming $\text{Fe}(\text{phen})_3^{2+}$ which has $\epsilon_{510} = 1.11 \times 10^4 \text{ L mol}^{-1}\text{cm}^{-1}$.³² Solutions of $\text{Ru}(\text{NH}_3)_6(\text{ClO}_4)_2$ were prepared by dissolution in dilute perchloric acid. These were flushed with argon and placed over zinc amalgam. Concentrations were determined spectrophotometrically at 275 nm ($\epsilon = 620 \text{ L mol}^{-1}\text{cm}^{-1}$). Titanium(III) solutions were prepared and treated as described in Part I of this dissertation.

The complexes $[\text{Co}(\text{C-meso-Me}_6[14]\text{aneN}_4)(\text{H}_2\text{O})_2](\text{ClO}_4)_2$ and meso- $[\text{Co}(\text{Me}_6[14]4,11\text{-dieneN}_4)(\text{H}_2\text{O})_2](\text{ClO}_4)_2$ were prepared as described in the literature.³³ Solutions of $\text{trans-Co}([14]\text{aneN}_4)(\text{H}_2\text{O})_2^{2+}$ were prepared by mixing anaerobic degassed solutions of $\text{Co}(\text{ClO}_4)_2$ and cyclam (Aldrich). This was stirred until complex formation was complete (ca. 10 min.), acidified to 0.05 M HClO_4 and transferred without contact with air to zinc amalgam.³⁴ The complex was stored in ice and used within 1.5 hours. Concentrations were determined spectrophotometrically at 460 nm ($\epsilon = 21.5 \text{ L mol}^{-1}\text{cm}^{-1}$).^{35,36} The complex was added to cells buffered at pH 7.0 just before the flash photolysis experiment to minimize isomerization to the cis isomer.^{37,38} Solutions of B_{12r} were prepared by zinc amalgam reduction of B_{12a} in neutral solution and used immediately.

Thiolatochromium(III) complexes of the formula $(\text{H}_2\text{O})_5\text{CrSR}^{2+}$ were prepared and purified using several different methods. An acidic aqueous solution of $\text{Cr}(\text{H}_2\text{O})_6^{2+}$ and excess disulfide was photolyzed at 254 nm using

a Rayonet photochemical reactor with medium pressure mercury lamps. The reaction mixture was ion-exchanged on a cooled, degassed column of Sephadex C25 cation-exchange resin. However, despite repeated washings, the sample, eluted with 0.5 M NaClO₄ in 0.01 M HClO₄, still contained disulfide. A second method was similar to the laser experiments, using similar concentrations of RCo([14]aneN₄)²⁺, RSH and Cr²⁺, but on a much larger scale (~ 15 times larger). Upon cation exchange the pure yellow complex was eluted with 0.5 M NaClO₄ in 0.01 M HClO₄. This method allowed small amounts of CrSR²⁺ to be obtained pure. The last method employed was the reaction^{39,40} of Cr(H₂O)₆²⁺ with (CH₃)₂CHSCo(dmgH)₂ which was prepared according to the literature procedure for the MeS- and PhS-derivatives.⁴¹ The complex was again purified by cation-exchange chromatography and eluted with 0.8 M HClO₄. This last method allowed preparations to be carried out on a much larger scale.

Analyses

Chromium analyses were carried out on the thiolatochromium(III) complexes by oxidation to chromate ($\epsilon_{372} = 4830 \text{ L mol}^{-1}\text{cm}^{-1}$) in basic peroxide.⁴² Ethane thiol was detected using a Hewlett Packard 5790 Å gas chromatograph with a Porapak Q column at 170 °C.

The sulfur to chromium ratio was determined using inductively coupled plasma mass spectrometry (ICP/MS). First the complex, (H₂O)₅CrSC₂H₅²⁺, was prepared by photolyzing a solution containing CH₃Co([14]aneN₄)²⁺, C₂H₅SH and Cr²⁺ with visible light, as described above. The product mixture was ion-exchanged on Sephadex C-25 as above, but eluted with 0.10 M LiBr/2 mM HBr. Sodium must be avoided because of the space

charge effect and chlorine must be avoided because its mass to charge ratio is similar to that of sulfur. The instrument, as described previously,⁴³ was a Sciex Elan Model 250 (Perkin-Elmer, Thornhill, Ontario). Sample was introduced to the plasma by means of a Cetac U-5000 ultrasonic nebulizer. The ICP torch was of Ames Laboratory design described previously.⁴⁴ Sulfur was monitored at m/z of 34 and chromium at both mass to charge ratios of 52 and 53. A blank solution containing 0.10 M LiBr/2 mM HBr was injected to determine the background readings. Also, a standard was prepared containing 1.1×10^{-4} M CrBr₃ and 5.5×10^{-5} M diethyl disulfide in 0.10 M LiBr/2 mM HBr.

Laser experiments

Reactions of carbon- and sulfur-centered radicals were measured using a visible dye laser flash photolysis system like that described in Part I of this dissertation. The excitation dye (Exciton) used was LD 490 (1×10^{-4} M in methanol containing 1 % Ammonyx LO). The increases in absorbance due to formation of ABTS^{•-} or TMPD^{•+} were monitored at 650 nm ($\epsilon = 1.20 \times 10^4$ L mol⁻¹cm⁻¹)⁴¹ for ABTS^{•-} and at 565 nm ($\epsilon = 1.25 \times 10^4$ L mol⁻¹cm⁻¹)⁴⁵ for TMPD^{•+}.

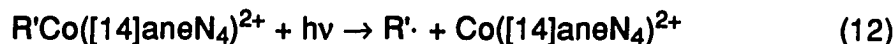
The Nd:YAG laser system used here was an LKS.50 Laser Photolysis Spectrometer from Applied Photophysics Limited. The laser itself was an SL800 system from Spectron Laser Systems. The fundamental wavelength output from the Nd:YAG laser (Q-switched) was frequency quadrupled by propagation through nonlinear harmonic generating crystals yielding 266 nm light. The laser beam was set up perpendicular to the monitoring beam, a pulsed xenon lamp. The monitoring beam passed through the cell and

through a grating monochromator to a five stage photomultiplier tube. The signal was recorded on a PM3323 Philips digital oscilloscope interfaced to an Archimedes 420/1 computer. The software used to control the laser system and to fit the kinetic data was developed by Applied Photophysics Limited. Using this system, diethyl disulfide was photolyzed directly at 266 nm in the presence of $\text{Cr}(\text{H}_2\text{O})_6^{2+}$. The formation of $(\text{H}_2\text{O})_5\text{CrSR}^{2+}$ was monitored directly at 280 nm without the use of a kinetic probe. The data were fitted to a first-order equation, $\text{Abs}_t = \text{Abs}_\infty + (\text{Abs}_0 - \text{Abs}_\infty)\exp(-kt)$.

RESULTS

Generation of radicals

One method used in this study involved producing a burst of carbon-centered radicals ($\sim 1 \times 10^{-6}$ M) by visible (490 nm) laser flash photolysis of aqueous solutions containing $R'Co([14]aneN_4)(H_2O)^{2+}$ (typically 1×10^{-4} M) as in eq 12.³⁴ With a water-soluble thiol present, such as ethanethiol, cysteine or glutathione, the repair reaction was employed to generate thiyl radicals (eq 13). Because thiyl radicals are not highly colored,¹⁸ two kinetic probes were used. Thiyl radicals were allowed to react with $ABTS^{2-}$ in a known reaction (eq 14)^{47,48} to yield the highly colored radical anion, $ABTS^{\cdot-}$. Another probe used was TMPD, which is easily oxidized to the radical cation $TMPD^{\cdot+}$, which is also highly colored. Thiyl radicals were observed to oxidize TMPD in neutral solution, but not in acidic solution, as the protonated amine is much less easily oxidized.



Kinetics

The repair reaction was studied using this method for methyl and ethyl radicals. With $[ABTS^{2-}] \gg [RSH]$ (10^{-2} and 10^{-4} M, typically) reaction 13 is rate limiting. Under these conditions the observed rate constant is given by eq 16. The first term in eq 16 is due to carbon-centered radical dimerization⁴⁹ and is small (generally $< 5\%$ of k_{obs}). The second term, $k_{13}[RSH]$, is due to the repair reaction (eq 13). As described in Part II of this dissertation eq 16 may be approximated by first order kinetics with the first term being approximately $2k_d[R\cdot]$. Thus, the first order rate constant is directly proportional to $[RSH]$ and is independent of $[ABTS^{2-}]$. A plot of k_{obs} vs. $[RSH]$ is expected to be linear with a slope corresponding to the second order repair reaction rate constant, k_r , and a small intercept due to radical dimerization. Such a plot is given in Figure 1 for the reaction of $\cdot CH_3$ with cysteine at pH 7.0. The repair reaction was also studied for $\cdot CH_3$ with ethane thiol and glutathione and for $\cdot C_2H_5$ with ethane thiol. The second order rate constants are given in Table 1 and the corresponding plots of k_{obs} vs. $[RSH]$ are given in the Appendix in Figures A1-A4. Also given in Table 1 are several repair reaction rate constants from pulse radiolysis studies carried out previously.^{5,6,8}

$$k_{obs} = 2k_{14}[R\cdot]^2 + k_{13}[RSH] \quad (16)$$

When $[ABTS^{2-}] \ll [RSH]$, reaction 13 is rapid and rates of reaction of $RS\cdot$ with $ABTS^{2-}$ can be determined. With 0.10 M thiol present reaction 13 is complete within 1 μs and reaction 15 (carbon-centered radical dimerization)

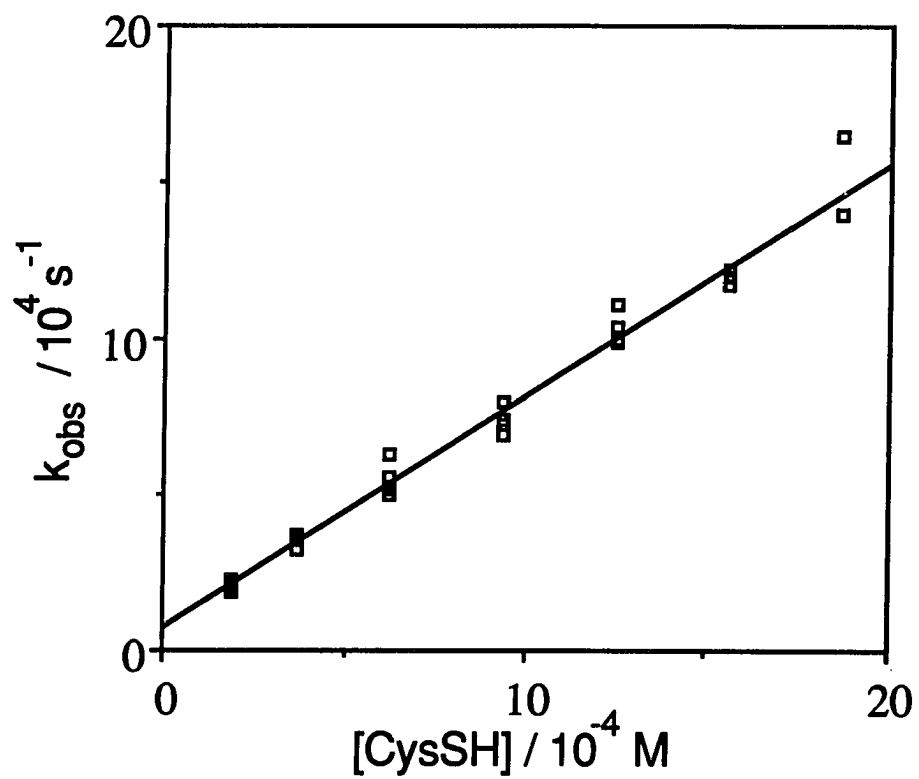


Figure 1. Reaction of $\cdot\text{CH}_3$ with cysteine at pH 7.0 using ABTS^{2-} as a kinetic probe

Table I. Rate constants (25 °C) for hydrogen abstraction by methyl and ethyl radicals from thiols (CysSH = cysteine, GSH = glutathione)^a

R•	RSH	pH	k ₁₃ / 10 ⁷ L mol ⁻¹ s ⁻¹
CH ₃ •	CH ₃ SH	11	7.4 ^b
	C ₂ H ₅ SH	1.0	4.0 ± 0.2
		7.0	4.7 ± 0.2
	CysSH	7.0	7.4 ± 0.2
	GSH	7.0	7.1 ± 0.2
CH ₃ CH ₂ •	C ₂ H ₅ SH	7.0	2.8 ± 0.1
•CH ₂ OH	CysSH	7.0	4.2 ^c
	HOCH ₂ CH ₂ SH	10	13 ^b
	NH ₂ CH ₂ CH ₂ SH	7.6	6.8 ^d

^a Errors given are standard deviations in the dataset as calculated by a nonlinear least-squares fitting program. ^b Reference 8. ^cReference 5. ^dReference 6.

is unimportant. With relatively low (10⁻⁴ M) concentrations of ABTS²⁻ present, reaction 17 must also be considered as a small, yet significant contribution to the observed rate constant (eq 18). Thus, a plot of k_{obs} vs. [ABTS²⁻] should be linear with an intercept corresponding to the thiyl radical dimerization and a slope of the second order rate constant for oxidation of ABTS²⁻. Figure 2 shows such a plot for the reaction of ethane thiyl radicals with ABTS²⁻ at pH 1.0. The second order rate constant for this reaction as well as for the oxidation by cysteinyl radical are listed in Table 2 along with two values for cysteinyl radical from previous studies.⁴⁷⁻⁴⁹ TMPD was also

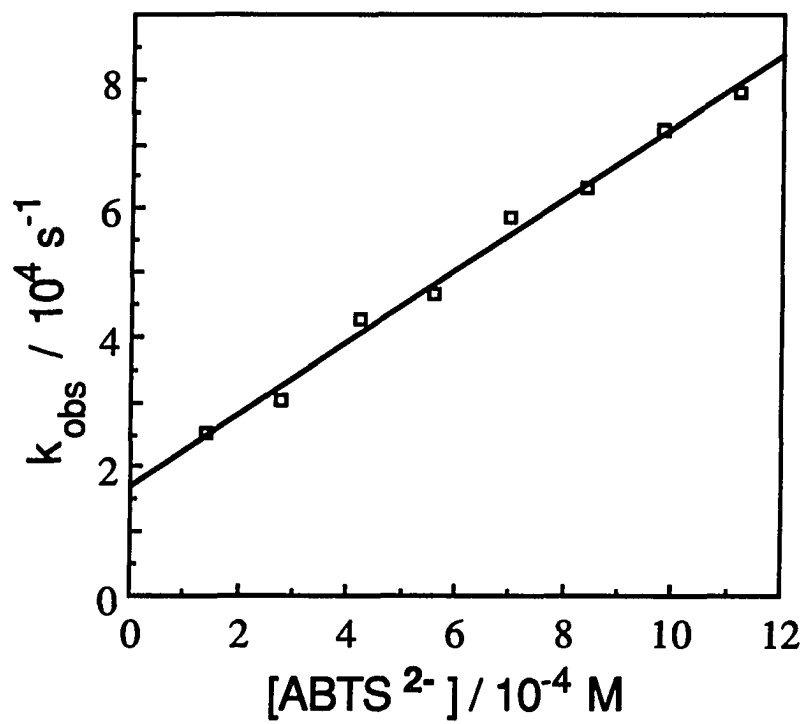


Figure 2. Oxidation of ABTS^{2-} by $\text{C}_2\text{H}_5\text{S}^\bullet$ at pH 4.0

Table 2. Rate constants (25 °C) for reactions of thiyl radicals with kinetic probes^a

Probe	RS•	pH	k / 10 ⁷ L mol ⁻¹ s ⁻¹
ABTS ²⁻	C ₂ H ₅ S•	1.0	5.6 ± 0.2
	CysS•	4.0	78 ± 2
		3.75	100 ^b
		7.1	50 ^c
TMPD	C ₂ H ₅ S•	7.0	260 ± 10

^a Errors given are standard deviations in the dataset as calculated by a nonlinear least-squares fitting program. ^b Reference 45. ^cReference 46.

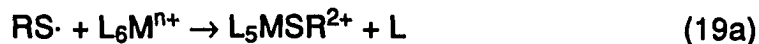
oxidized by C₂H₅S•, forming TMPD^{•+} at pH 7.0. The value of the second order rate constant for reaction of C₂H₅S• with TMPD is also listed in Table 2. Corresponding plots of k_{obs} vs. [ABTS²⁻] or [TMPD] are given in the Appendix in Figures A5 and A6.



$$k_{\text{obs}} = 2k_{\text{s}}[\text{RS}\cdot]^2 + k_{\text{A}}[\text{ABTS}^{2-}] \quad (18)$$

Knowledge of the rate constants for reactions of thiyl radicals with kinetic probes allows the study of their reactions with various metal complexes, using the competition method. Typical conditions used were as follows: 1 x 10⁻⁴ M CH₃Co([14]aneN₄)²⁺, which would generate ~1 x 10⁶ M •CH₃ in the laser flash (eq12); 0.10 M C₂H₅SH, to efficiently capture methyl radicals,

generating $C_2H_5S\cdot$ (eq 13); $\sim 6 \times 10^{-4}$ M ABTS $^{2-}$ or $\sim 2 \times 10^5$ M TMPD as a kinetic probe; and appropriate amount of reduced metal complex (eq 19) to make a measurable contribution to the observed pseudo-first order rate constant (eq 20). A trace is shown in Figure 3 with 1.2×10^{-4} M Cr(H $_2$ O) $_6^{2+}$ present. Because of the data acquisition sequencing, the plot shows several points before the flash and immediately following there is a rapid increase in absorbance at 650 nm. (Note also the slower decay in absorbance second stage that is explained below.) A corrected first-order rate constant, k_{corr} , is calculated according to equation 21. Thus, a plot of k_{corr} vs. $[L_6M^{n+}]$ is expected to be a straight line with a slope of k_m and a zero intercept. Such a plot is shown in Figure 4 for the reaction of $C_2H_5S\cdot$ with Cr(H $_2$ O) $_6^{2+}$. Each point on the line is the average of 3-4 shots on one cell. The rate constants for reactions of $C_2H_5S\cdot$ with a variety of metal complexes are given in Table 3. The corresponding plots of k_{corr} vs. $[L_6M^{n+}]$ are given in the Appendix in Figures A7-A12. The macrocyclic cobalt(II) complexes precipitate out in the presence of the required amount of ABTS $^{2-}$, so TMPD was used as the probe in those cases.



$$k_{obs} = 2k_s[RS\cdot]^2 + k_A[ABTS^{2-}] + k_m[L_6M^{n+}] \quad (20)$$

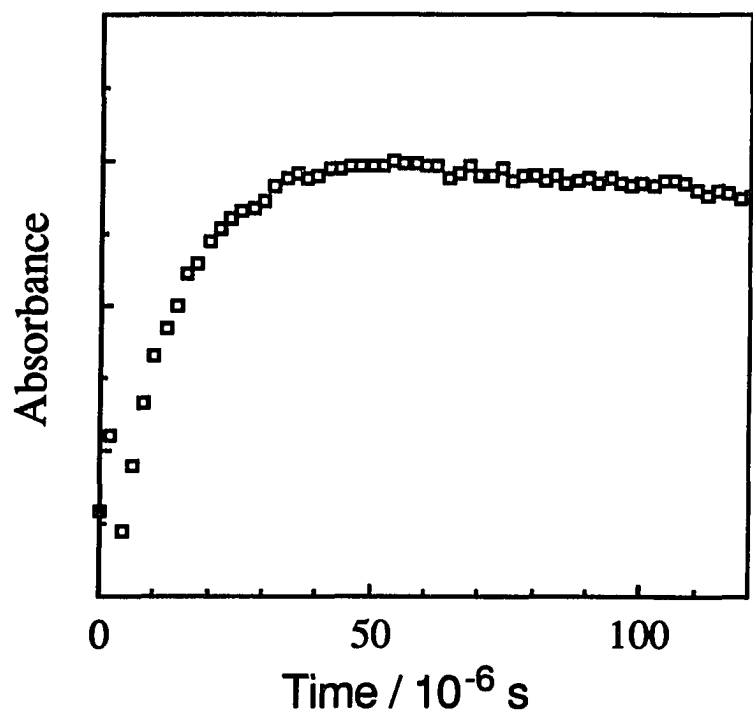


Figure 3. Kinetic trace monitored at 650 nm due to formation of ABTS^{•-} in the presence of 1.2×10^{-4} M Cr²⁺ at pH 1.0.

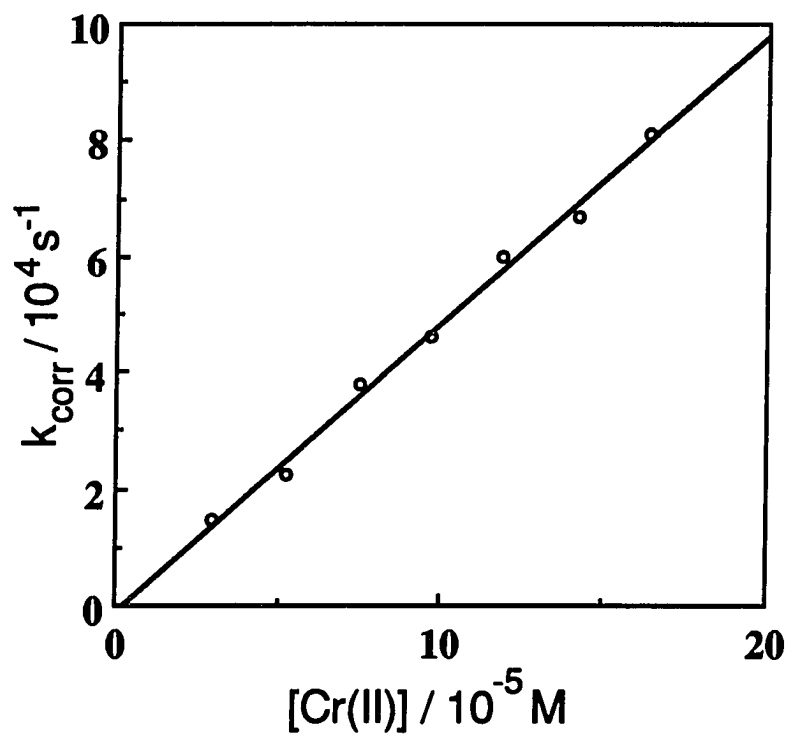


Figure 4. Reaction of $\text{C}_2\text{H}_5\text{S}\cdot$ with Cr(II) at pH 1.0 using ABTS^{2-} as a kinetic probe

Table 3. Rate constants (25 °C) for reactions of C₂H₅S• with transition metal complexes.^a

Metal Complex	$k_m / \text{L mol}^{-1}\text{s}^{-1}$	pH
Cr(H ₂ O) ₆ ²⁺	$(4.9 \pm 0.2) \times 10^8$	1.0
V(H ₂ O) ₆ ²⁺	$(6.5 \pm 0.3) \times 10^8$	1.0
Fe(H ₂ O) ₆ ²⁺	$(1.2 \pm 0.1) \times 10^6$	1.0
Co([14]aneN ₄) ²⁺	$\sim 4.5 \times 10^8$	7.0
Co([Me ₆ [14]aneN ₄]) ²⁺	$(3.3 \pm 0.3) \times 10^8$	7.0
Co(Me ₆ [14]dieneN ₄) ²⁺	$(3.1 \pm 0.3) \times 10^8$	7.0
Vitamin B _{12r}	$(1.0 \pm 0.1) \times 10^9$	7.0

^aErrors given are standard deviations in the dataset as calculated by a nonlinear least-squares fitting program.

$$k_{\text{corr}} = k_{\text{obs}} - (2k_s[\text{RS}\cdot]^2 + k_A[\text{ABTS}^{2-}]) = k_m[\text{L}_6\text{M}^{n+}] \quad (21)$$

Formation of ethanethiolatochromium(III) was observed directly at 280 nm. Using a Nd:YAG laser, diethyl disulfide was directly photolyzed at 266 nm in the presence of Cr(H₂O)₆²⁺. This laser system allowed much higher concentrations of Cr(H₂O)₆²⁺ to be used, as it is capable of measuring much higher rates. Thus, the radical dimerization reaction was even less significant. At 280 nm a single exponential increase in absorbance was observed and was permanent for at least 400 μs. The k_{obs} value was directly proportional to [Cr(H₂O)₆²⁺] as given by eq 22. A plot of k_{obs} vs. [Cr(H₂O)₆²⁺] is given in Figure 5 and the slope of the line corresponds to $k_{\text{Cr}} = (4.9 \pm 0.2) \times 10^8 \text{ L mol}^{-1}\text{s}^{-1}$.

$$k_{\text{obs}} = 2k_s[\text{RS}\cdot]^2 + k_{\text{Cr}}[\text{Cr}^{2+}] \quad (22)$$

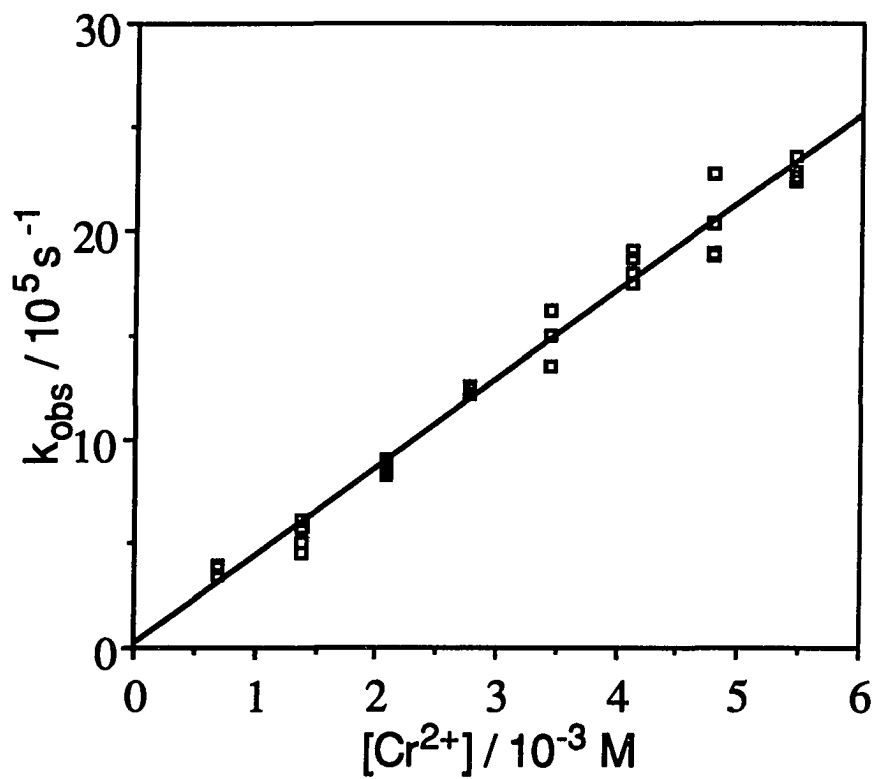


Figure 5. Reaction of $\text{C}_2\text{H}_5\text{S}\cdot$ with $\text{Cr}(\text{H}_2\text{O})_6^{2+}$ studied by photolyzing diethyl disulfide at 266 nm and monitoring thiolato-chromium formation at 280 nm

Product studies

Ethanethiolatochromium(III) was prepared by photolyzing a solution containing $\text{CH}_3\text{Co}([\text{14}] \text{aneN}_4)^{2+}$, $\text{C}_2\text{H}_5\text{SH}$ and Cr^{2+} with visible light on a scale ~ 15 times that of the laser experiments and was purified by cation-exchange chromatography. It was destroyed by addition of O_2 , Hg(II) or Br_2 . In the case of $(\text{H}_2\text{O})_5\text{CrSC}_2\text{H}_5^{2+}$ the complex has a half-life of ~ 30 min. in 0.10 M HClO_4 and exhibits $\lambda_{\text{max}} = 280 \text{ nm}$ ($\epsilon = 7400 \pm 100 \text{ L mol}^{-1}\text{cm}^{-1}$). The chromium to sulfur ratio was determined by ICP/MS to be 1.1:1; consistent with the formula $(\text{H}_2\text{O})_5\text{CrSC}_2\text{H}_5^{2+}$.

To check for reaction 19b, disulfide was photolyzed at 254 nm in the presence of the metal complex. With either $\text{V}(\text{H}_2\text{O})_6^{2+}$ or $\text{Fe}(\text{H}_2\text{O})_6^{2+}$ present, thiol was detected as a product using GC. However, no thiol was found when diethyl disulfide was photolyzed with $\text{Cr}(\text{H}_2\text{O})_6^{2+}$ present.

When reactions of thiyl radicals with $\text{Cr}(\text{H}_2\text{O})_6^{2+}$ or $\text{V}(\text{H}_2\text{O})_6^{2+}$ are studied using ABTS^{2-} as a kinetic probe, two stages of reaction are observed. Following the laser flash there is an increase in absorbance at 650 nm due to the formation of $\text{ABTS}^{\bullet-}$ (eq 15). But there is also a slower decrease in absorbance due to the reaction of $\text{Cr}(\text{H}_2\text{O})_6^{2+}$ or $\text{V}(\text{H}_2\text{O})_6^{2+}$ with $\text{ABTS}^{\bullet-}$ (eq 23). This reaction was studied by using relatively high concentrations of ABTS^{2-} , so that the first stage was very fast. A typical trace is shown for the reaction of V(II) with $\text{ABTS}^{\bullet-}$ in Figure 6. The second stage was studied by varying the concentration of metal ion. The second order rate constants for the reduction of $\text{ABTS}^{\bullet-}$ are $(1.1 \pm 0.1) \times 10^8$ and $(2.6 \pm 0.1) \times 10^8 \text{ L mol}^{-1}\text{s}^{-1}$ for $\text{Cr}(\text{H}_2\text{O})_6^{2+}$ and $\text{V}(\text{H}_2\text{O})_6^{2+}$ respectively.



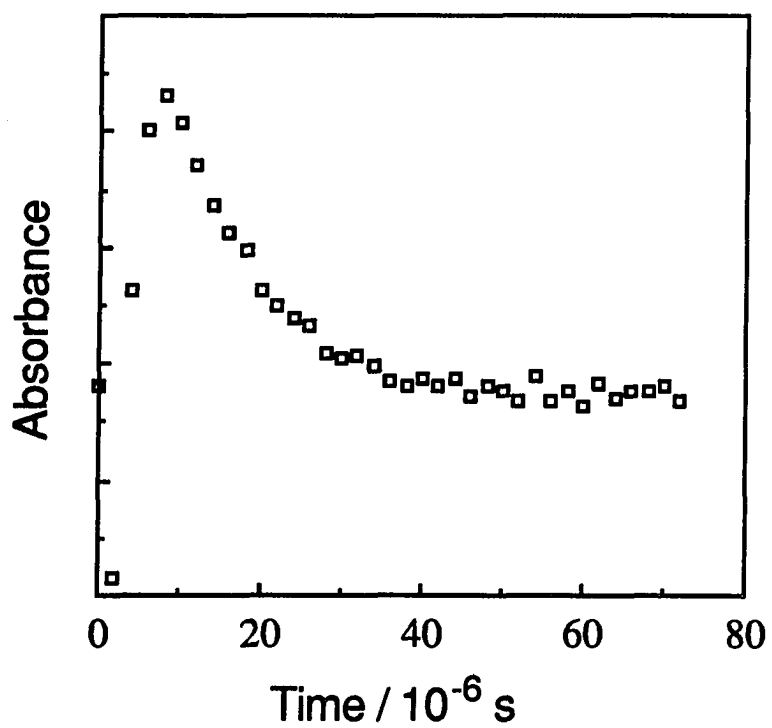


Figure 6. Kinetic trace monitored at 650 nm due to formation and loss of $\text{ABTS}^{\cdot-}$ in the presence of 6.2 mM ABTS^{2-} and 3×10^{-4} M V^{2+} at pH 1.0.

DISCUSSION

The complexes $\text{RCo}([\text{14}] \text{aneN}_4)^{2+}$ with $\text{R} = \text{Me}$ and Et are known to generate carbon-centered radicals when photolyzed with visible (490 nm) light and have been used in studies of alkyl radicals with metal complexes.⁵⁰ Here, it is not the carbon-centered radicals that are of primary interest and they have been used simply as a means for generating sulfur-centered radicals.

Probably the most important reaction involving thiyl radicals is the reversible¹¹ repair reaction (eq 4). A number of studies, mostly pulse radiolysis studies, have been carried out on this subject and usually involved α -hydroxyalkyl radicals. However, such equipment is not available to most researchers. The use of $\text{RCo}([\text{14}] \text{aneN}_4)^{2+}$ complexes allows a series of primary hydrocarbon radicals to be studied.³⁴ In this study methyl and ethyl radicals were studied with thiols such as ethane thiol, cysteine and glutathione. Glutathione is the most important thiol to use in repair reaction studies, because of its presence in cells in the body ($\text{GSH} \leq 0.01 \text{ M}$).⁵¹ Almost no steric effect is observed in the abstraction of a hydrogen atom from ethane thiol (see Table I). At pH 7.0 methyl radical reacts with ethane thiol with a second order rate constant of $(4.7 \pm 0.2) \times 10^7 \text{ L mol}^{-1}\text{s}^{-1}$ and ethyl radical reacts with a second order rate constant of $(2.8 \pm 0.1) \times 10^7 \text{ L mol}^{-1}\text{s}^{-1}$. This small difference is not unexpected as no steric effect was reported in going from primary to tertiary alkyl radicals for abstraction of hydrogen from thiophenol.⁵² Cysteine and glutathione were found to have virtually the same rate of repair with methyl radicals ($\sim 7 \times 10^7 \text{ L mol}^{-1}\text{s}^{-1}$). The repair reaction rate constant for $\text{CH}_3\cdot$ with $\text{C}_2\text{H}_5\text{SH}$ was also determined

at pH 1, since the reactions with simple hexaaqua metal ions were studied at pH 1. A few values of repair reaction rate constants from the literature are also listed in Table I. These values show that $k_r = 10^7$ - 10^8 L mol⁻¹s⁻¹ are typical.

The reverse of the repair reaction (eq 24) has been studied for alcohols and occurs with rate constants of 10^3 - 10^4 L mol⁻¹s⁻¹.^{11,53} For this reason cosolvents were avoided and all studies were carried out in strictly aqueous solution. Thiols were chosen based on their solubility, and most of the studies with metal complexes were carried out with ethane thiol as it has a solubility in water at 20 °C of 0.112 M, more than enough to efficiently capture virtually all •CH₃. Of course, cysteine and glutathione are also soluble.



The thiyl radicals are difficult to observe directly and studies have often been carried out in the presence of excess thiolate. Under these conditions the disulfide radical anion forms readily (eq 8). These absorb in the region 380-450 nm with extinction coefficients of $(6-7) \times 10^3$ L mol⁻¹cm⁻¹.¹⁸ However, the pK_a values for most thiols ≥ 8 . There is also the problem under these conditions of separating reactions of thiyl radicals from those of the disulfide radical anion. Thus, for the study of metal complexes in acidic and neutral aqueous solution, we turned to kinetic probes that would be stable in the region pH 1-7.

Cysteinyl radicals have been reported^{30,47,49} to oxidize ABTS^{2-} to ABTS^{\bullet} , a highly colored, persistent radical. As $\bullet\text{CH}_3$ does not oxidize ABTS^{2-} , the increases in absorbance at 650 nm upon addition of thiol were indicative of the formation of thiyl radicals. The oxidation of ABTS^{2-} was studied for cysteinyl radicals at pH 4 (see Table 2) and the second-order rate constant obtained was relatively close to the value of $1.0 \times 10^9 \text{ L mol}^{-1}\text{s}^{-1}$ reported at pH 3.75.⁴⁷ The reaction of $\text{C}_2\text{H}_5\text{S}^{\bullet}$ with ABTS^{2-} was studied under the same conditions as the reactions with metal complexes (pH 1, see below). This is a much slower reaction, probably because the protonated form, HABTS^- , is more difficult to oxidize than the unprotonated form ($\text{pK}_a = 2.2$).

As mentioned above, the cobalt(II) complexes used in this study precipitated out with ABTS^{2-} . Thus, another probe, TMPD, was also used. TMPD is easily oxidized, having $E^\circ = 0.27 \text{ V vs. NHE}$ at pH 7. The radical cation, $\text{TMPD}^{\bullet+}$, is stable for more than a week.⁵⁴ Ethane thiyl radicals were found to oxidize TMPD in a diffusion-controlled process (see Table 2). The mechanism of oxidation is most likely electron transfer as other radicals react at similar rates and a reaction involving hydrogen transfer should be slower. Other studies have shown that TMPD is oxidized by the radical $\bullet\text{CH}_2\text{CHO}$ ⁵⁴ with a rate constant of $2.1 \times 10^9 \text{ L mol}^{-1}\text{s}^{-1}$ and by substituted methylperoxyl radicals at rates that vary from 10^6 - $10^9 \text{ L mol}^{-1}\text{s}^{-1}$, increasing as the electron-withdrawing capacity of the substituent on the peroxy group increases.⁵⁵ The lack of reaction at pH 1 is due to protonation of the TMPD, which has a $\text{pK}_a = 5.3$.^{56,57} The discovery of this simple reaction may actually be a very significant portion of this work. TMPD may be used to easily detect thiyl

radicals and follow their reactions at physiological pH. The high rate of reaction means that very low concentrations of TMPD will efficiently capture any $RS\cdot$ formed.

We have examined reactions between $C_2H_5S\cdot$ and $M(H_2O)_6^{2+}$ ($M = Cr, V, Fe$) at pH 1 using $ABTS^{2-}$ as a kinetic probe. The reactions of thiyl radicals with Cr^{2+} occur about twice as fast as those of alkyl radicals.³⁴ The dimerization reactions of thiyl radicals^{58,59} also occur slightly faster than those of alkyl radicals.⁶⁰ The reaction with Cr^{2+} was expected to be an inner-sphere process (eq 19a) and to form stable thiolatochromium(III) as a product. Two similar compounds that are known to be stable for hours are $(H_2O)_5CrSC_6H_4NH_3^{3+}$ and $(H_2O)_5CrSC_6H_4N(CH_3)_3^{3+}$.⁶¹ Also known is the hydrogensulfidochromium(III) ion, $(H_2O)_5CrSH^{2+}$.⁶² Indeed, Cr^{2+} was observed to react with $C_2H_5S\cdot$ by an inner-sphere mechanism. When disulfide was photolyzed in the presence of Cr^{2+} , an increase in absorbance at wavelengths below 300 nm was observed, suggesting Cr-S bond formation. No free thiol was detected as a product as would be expected from an outer-sphere reaction (eq 19b). Ethanethiolatochromium was isolated by cation-exchange chromatography and exhibited an absorption band at 280 nm, characteristic of a Cr-S MLCT band.⁶¹⁻⁶⁴ This work has shown that generating thiyl radicals in the presence of Cr^{2+} is one method of preparing the thiolatochromium(III) complexes, since Cr^{2+} does not react directly with simple (methyl, ethyl) disulfides.

The $Fe(H_2O)_6^{2+}$ reaction with $C_2H_5S\cdot$ is inferred to also go by inner sphere mechanism since its rate constant ($1.2 \times 10^6 \text{ L mol}^{-1}\text{s}^{-1}$) is comparable to that for the reaction of Br_2^- with $Fe(H_2O)_6^{2+}$ ($3.6 \times 10^6 \text{ L}$

mol⁻¹s⁻¹), which is known to be an inner sphere process.⁶⁵ The substitution rate for Fe(H₂O)₆³⁺ is ca. 10⁻¹⁰ L mol⁻¹s⁻¹ and can be considered to be inert on the time scale of the oxidation by ethane thiy radicals. However, the initial product of the reaction, (H₂O)₅FeSC₂H₅²⁺, was not observed, probably due to low extinction coefficients.

Oxidation of V(H₂O)₆²⁺ by alkyl radicals in aqueous solution occurs with rate constants in the range (1-6) x 10⁵ L mol⁻¹s⁻¹ and shows little dependence on the steric bulk of the radical. The mechanism suggested for this reaction involves radical attack at a trigonal face of V(H₂O)₆²⁺. This allows for electron transfer to occur, yielding a transient seven coordinate intermediate, (H₂O)₆VR²⁺, which undergoes protonolysis to yield V(III) and alkane.^{66,67} Ethane thiy radical oxidizes V(H₂O)₆²⁺ with a second order rate constant of (6.5 ± 0.3) x 10⁸ L mol⁻¹s⁻¹. It seems likely that the mechanism again involves radical attack at a trigonal face of V(H₂O)₆²⁺ where a bond to sulfur can be formed as the electron is transferred. However, the thiy radical reacts much more rapidly than the alkyl radical despite the lower driving force for the reaction. The large sulfur-centered radical may be better able to provide orbital overlap than a carbon-centered radical, facilitating electron transfer. The proposed intermediate, (H₂O)₆VSR²⁺, was not observed directly, which I attribute to either its expected short lifetime or low extinction coefficients.

In the reactions of ethane thiy radicals with CoL²⁺ complexes where L = [14]aneN₄, Me₆[14]aneN₄ and Me₆[14]4,11-diene, the rate constants are all about the same, falling in the range (3.1-4.5) x 10⁸ L mol⁻¹s⁻¹. The faster reaction with B_{12r} is probably due to the larger driving force.⁶⁸ It may also be

significant that the cobalt of B_{12r} is penta-coordinate in neutral solution.⁶⁹ The complexes of $Co([14]aneN_4)^{2+}$, $Co(Me_6[14]aneN_4)^{2+}$ and $Co(Me_6[14]4,11-diene)^{2+}$ are most likely hexa-coordinate in solution.^{70,71} Again the thiyl radicals are observed to react faster than alkyl radicals.⁷⁰ The reactions of methyl and ethyl radicals with $Co([14]aneN_4)^{2+}$ and $Co(Me_6[14]aneN_4)^{2+}$ have rate constants of $(1-4) \times 10^7 \text{ L mol}^{-1}\text{s}^{-1}$. Rate constants for reactions of alkyl radicals with B_{12r} are typically $(4-6) \times 10^8$, while $C_2H_5S\cdot$ reacts with a rate constant of $(1.0 \pm 0.1) \times 10^9 \text{ L mol}^{-1}\text{s}^{-1}$.

The reactions of thiyl radicals with these cobalt(II) complexes are expected to yield thiolatocobalt(III) complexes. However the formation of these complexes was not observed directly, despite the expected LMCT band in the 250-300 nm region.⁷² This band should occur at lower energy (and thus, be more easily observable) than the thiolatochromium(III) LMCT band, since cobalt(III) is a better oxidant than Cr(III). It may be that these cobalt(III) complexes are simply less strongly absorbing. The lack of thiol formation when disulfide is photolyzed in the presence of $Co([14]aneN_4)^{2+}$ supports an inner-sphere reaction with the formation of a stable thiolatocobalt(III) product. Also, a number of mono- and bidentate thiolatocobalt(III) complexes are known to be stable, such as $Co(en)_2SR^{2+}$ ⁷³ and $RSCo(dmgh)_2$.³⁹

Many of the previous studies involving thiyl radicals were carried out pulse radiolytically. We have now developed a convenient method of generating and studying reactions of thiyl radicals using visible laser flash photolysis. Pulse radiolysis and flash photolysis have often been complementary in terms of the experiments that could be carried out. Pulse

radiolysis produces hydroxyl radicals, which behave as oxidants, as well as solvated electrons and hydrogen atoms, which are reductants. The capability to produce either reducing or oxidizing species (by using suitable concentrations of HCO_2^- and N_2O) is sometimes a great advantage. However, flash photolysis has the advantage that it allows a specific molecule to be targeted by choosing an appropriate excitation wavelength. The method described here may be applied to the study of the biologically significant cysteinyl and glutathionyl radicals without requiring the pulse radiolysis equipment. It is particularly suited to the study of thiyl radicals with metal complexes and should prove useful in many inorganic and bioinorganic studies.

REFERENCES

1. Foureman, G.L.; Eling, T.E. *Arch. Biochem. Biophys.* **1989**, *269*, 55.
2. Wariishi, H.; Valli, K.; Renganathan, V.; Gold, M.H. *J. Biol. Chem.* **1989**, *264*, 14185.
3. Stock, B.H.; Schreiber, J.; Guenat, C.; Mason, R.P.; Bend, J.R.; Eling, T.E. *J. Biol. Chem.* **1986**, *261*, 15915.
4. Ross, D.; Norbeck, K.; Moldéus, P. *J. Biol. Chem.* **1985**, *260*, 15028.
5. Adams, G.E.; McNaughton, G.S.; Michael, B.D. *Trans. Faraday Soc.* **1968**, *64*, 902.
6. Nucifora, G.; Smaller, B.; Remko, R.; Avery, E.C. *Radiat. Res.* **1972**, *49*, 96.
7. Adams, G.E.; Armstrong, R.C.; Charlesby, A.; Michael, B.D.; Willson, R.L. *Trans. Faraday Soc.* **1969**, *65*, 732.
8. Karmann, W.; Granzow, A.; Meissner, G.; Henglein, A. *Int. J. Radiat. Phys. Chem.* **1969**, *1*, 395.
9. Griller, D.; Simoes, J.A.M.; Wagner, D.D.M. "Sulfur-centered Reactive Intermediates in Chemistry and Biology," C. Chatilialoglu and K.-D. Asmus (eds.) Plenum Press, New York, 1990, p.37.
10. Schöneich, C.; Asmus, K.-D.; Dillinger, V.; von Bruchhausen, F. *Biochem. Biophys. Res. Commun.* **1989**, *161*, 113.
11. Schöneich, C.; Bonifacic, M.; Asmus, K.-D. *Free Rad. Res. Commun.* **1989**, *6*, 393.
12. Morine, G.H.; Kuntz, R.R. *Photochem. Photobiol.* **1981**, *33*, 1.
13. (a) Sayamol, K.; Knight, A.R. *Can. J. Chem.* **1968**, *46*, 999; (b) Gupta, D.; Knight, A.R. *Can. J. Chem.* **1980**, *58*, 1350.
14. Byers, G.W.; Gruen, H.; Giles, H.G.; Scholt, H.N.; Kampmeier, J.A. *J. Am. Chem. Soc.* **1972**, *94*, 1016.
15. Davies, M.J.; Forni, L.G.; Shuter, S.L. *Chem. -Biol. Interactions* **1985**, *61*, 177.

16. Buettner, G.R. *FEBS Lett.* **1985**, *177*, 295.
17. Harman, L.S.; Mottley, C.; Mason, R.P. *J. Biol. Chem.* **1984**, *259*, 5606.
18. (a) Hoffman, M.Z.; Hayon, E. *J. Am. Chem. Soc.* **1972**, *94*, 7950; (b) Quintilliani, M.; Badiello, R.; Tamba, M.; Esfandi, A.; Gorin, G. *Int. J. Radiat. Biol.* **1977**, *32*, 195.
19. Purdie, J.W.; Gillis, H.A.; Klassen, N.V. *Can. J. Chem.* **1973**, *51*, 3132.
20. Karmann, W.; Granzow, A.; Meissner, G.; Henglein, A. *Int. J. Radiat. Phys. Chem.* **1969**, *1*, 395.
21. Asmus, K.-D. *Radioprot. Radiocarc.* **1983**, 23.
22. Ito, O.; Matsuda, M. *Chemical Kinetics of Small Organic Radicals* Z.B. Aifassi, ed., Vol. III, p. 133.
23. McPhee, D.J.; Campredon, M.; Lesage, M.; Griller, D.J. *Am. Chem. Soc.* **1989**, *111*, 7563.
24. Forni, L.G.; Willson, R.L. *Biochem. J.* **1986**, *240*, 905.
25. Forni, L.G.; Willson, R.L. *Biochem J.* **1986**, *240*, 897.
26. Forni, L.G.; Mönig, J.; Mora-Arellano, V.O.; Willson, R.L. *J. Chem. Soc. Perkin Trans. II* **1983**, 961.
27. Surdhar, P.S.; Armstrong, D.A. *J. Phys. Chem.* **1987**, *91*, 6532.
28. Leu, A.-D.; Armstrong, D.A. *J. Phys. Chem.* **1986**, *90*, 1449.
29. Mezyk, S.P.; Armstrong, D.A. *Can. J. Chem.* **1989**, *67*, 736.
30. Malkin, R.; Rabinowitz, J.C. *Ann. Rev. Biochem.* **1967**, *36*, 113.
31. Bakac, A.; Espenson, J.H. *Inorg. Chem.* **1987**, *26*, 4353. [14]aneN₄ = 1,4,8,11-tetraazacyclotetradecane (cyclam).
32. Carlyle, D.W.; Espenson, J.H. *Inorg. Chem.* **1967**, *6*, 1370.
33. Rillema, D.P.; Endicott, J.F.; Papaconstantinou, E. *Inorg. Chem.* **1971**, *10*, 1739.
34. Bakac, A.; Espenson, J.H. *Inorg. Chem.* **1989**, *28*, 3901.

35. Heckman, R.A.; Espenson, J.H. *Inorg. Chem.* **1979**, *18*, 38.
36. Balasubramanian, P.N.; Pillai, G.C.; Carlson, R.R.; Linn, D.E., Jr.; Gould, E.S. *Inorg. Chem.* **1988**, *27*, 780.
37. Poon, C.K.; Tobe, M.L. *J. Chem. Soc. (A)* **1968**, 1549.
38. Tsintavis, C.; Li, H.-L.; Chambers, J.Q. *Inorg. Chim. Acta* **1990**, *171*, 1.
39. Lane, R.H.; Sedor, F.A.; Gilroy, M.J.; Eisenhardt, P.F.; Bennett, J.P., Jr.; Ewall, R.X.; Bennett, L.E. *Inorg. Chem.* **1977**, *16*, 93.
40. Lane, R.H.; Sedor, F.A.; Gilroy, M.J.; Bennett, L.E. *Inorg. Chem.* **1977**, *16*, 102.
41. Schrauzer, G.N.; Windgassen, R.J. *J. Am. Chem. Soc.* **1967**, *89*, 3607.
42. Haupt, G.W. *J. Res. Natl. Bur. Stand.* **1952**, *12*, 414.
43. Smith, F.G.; Houk, R.S. *J. Am. Soc. Mass Spectrom.* **1990**, *1*, 284.
44. Scott, R.H.; Fassel, V.A.; Knisely, R.N.; Dixon, D.E. *Anal. Chem.* **1974**, *46*, 75.
45. Hünig, S.; Balli, H.; Conrad, H.; Schott, A. *Leibigs Ann. Chem.* **1964**, *676*, 36.
46. Fujita, S.; Steeken, S. *J. Am. Chem. Soc.* **1981**, *103*, 2540.
47. Lal, M.; Mahal, H.S. *Can. J. Chem.* **1990**, *68*, 1376.
48. Wolfenden, B.S.; Willson, R.L. *J. Chem. Soc. Perkin Trans. II* **1982**, 805.
49. Stevens, G.C.; Clarke, R.M.; Hart, E.J. *J. Phys. Chem.* **1990**, *29*, 4996.
50. Bakac, A.; Espenson, J.H. *Inorg. Chem.* **1989**, *28*, 3901.
51. Wahlländer, A.; Soboll, S.; Sies, H. *FEBS Lett.* **1979**, *97*, 138.
52. Franz, J.A.; Bushaw, B.A.; Alnajjar, M.S. *J. Am. Chem. Soc.* **1989**, *111*, 268.
53. Schöneich, C.; Asmus, K.-D. *Radiat. Environ. Biophys.* **1990**, *29*, 263.
54. Steenken, S.; Neta, P. *J. Phys. Chem.* **1982**, *86*, 3661.

55. Neta, P.; Huie, R.E.; Mosseri, S.; Shastri, L.V.; Mittal, J.P.; Maruthamuthu, P.; Steenken, S. *J. Phys. Chem.* **1989**, *93*, 4099.
56. Rao, R.S.; Hayon, E. *J. Phys. Chem.* **1975**, *79*, 1063.
57. Huie, R.E. *J. Phys. Chem.* **1985**, *89*, 1783.
58. Adams, G.E.; Armstrong, R.C.; Charlesby, A.; Michael, B.D.; Willson, R.L. *Trans. Faraday Soc.* **1969**, *65*, 732.
59. Purdie, J.W.; Gillis, H.A.; Klassen, N.V. *Can. J. Chem.* **1973**, *51*, 3132.
60. Stevens, G.C.; Clark, R.M.; Hart, E.J. *J. Phys. Chem.* **1972**, *76*, 3863.
61. Asher, L.E.; Deutsch, E. *Inorg. Chem.* **1972**, *11*, 2927.
62. Ardon, M.; Taube, H. *J. Am. Chem. Soc.* **1967**, *89*, 3661.
63. Asher, L.E.; Deutsch, E. *Inorg. Chem.* **1973**, *12*, 1774.
64. Adzamli, I.K.; Deutsch, E. *Inorg. Chem.* **1980**, *19*, 1336.
65. Thornton, A.T.; Laurence, G.S. *J. Chem. Soc. Dalton Trans.* **1973**, 804.
66. Espenson, J.H.; Bakac, A.; Kim, J.-H., submitted for publication.
67. Dobson, J.C.; Sano, M.; Taube, H. *Inorg. Chem.* **1991**, *30*, 456.
68. Lexa, D.; Saveant, J.-M. *Acc. Chem. Res.* **1983**, *16*, 235.
69. Schrauzer, G.N.; Lee, L.-P. *J. Am. Chem. Soc.* **1968**, *90*, 6541.
70. Bakac, A.; Espenson, J.H. *Inorg. Chem.* **1989**, *28*, 4319.
71. Endicott, J.F.; Lillie, J.; Kuszaj, J.M.; Ramaswamy, B.S.; Schmonsees, W.G.; Glick M.G.; Rillema, D.P. *J. Am. Chem. Soc.* **1977**, *99*, 429.
72. Adzamli, I.K.; Deutsch, E. *Inorg. Chem.* **1980**, *19*, 1367.
73. Lane, R.H.; Sedor, F.A.; Gilroy, M.J.; Eisenhardt, P.F.; Bennett, J.P., Jr.; Ewall, R.X.; Bennett, L.E. *Inorg. Chem.* **1977**, *16*, 93.

APPENDIX

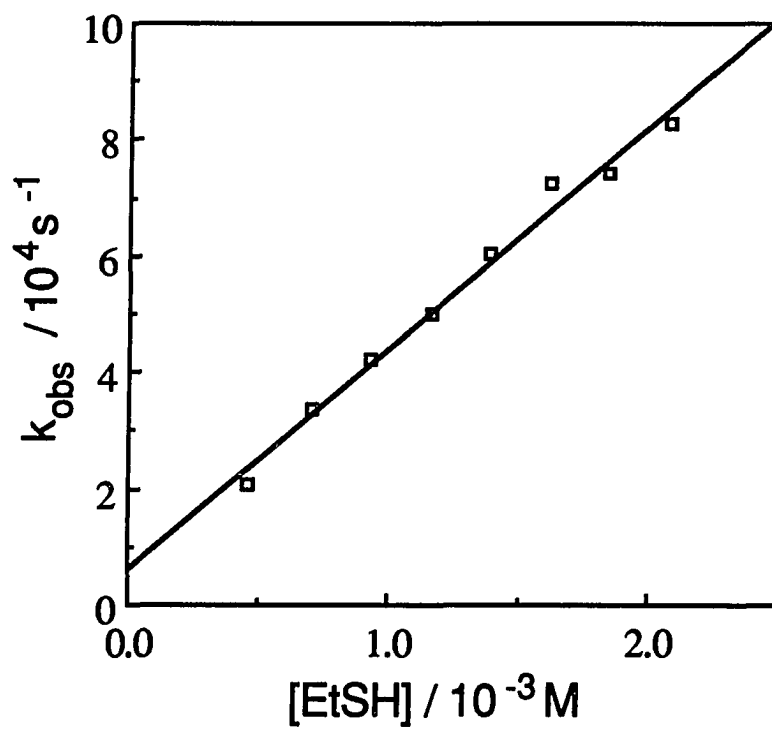


Figure A1. Reaction of $\cdot\text{CH}_3$ with $\text{C}_2\text{H}_5\text{SH}$ at pH 1.0 using ABTS^{2-} as a kinetic probe

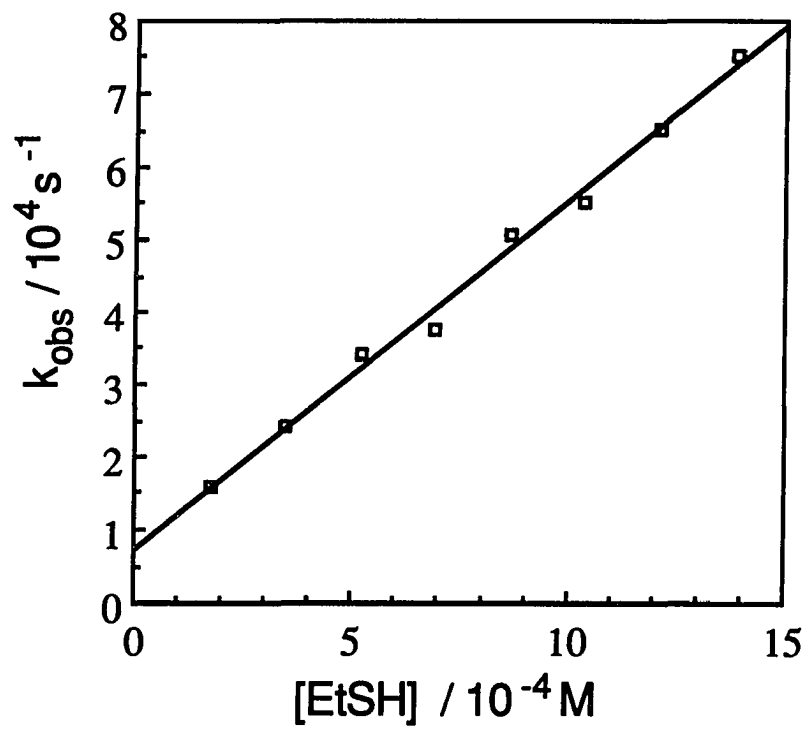


Figure A2. Reaction of $\cdot\text{CH}_3$ with $\text{C}_2\text{H}_5\text{SH}$ at pH 7.0 using ABTS^{2-} as a kinetic probe

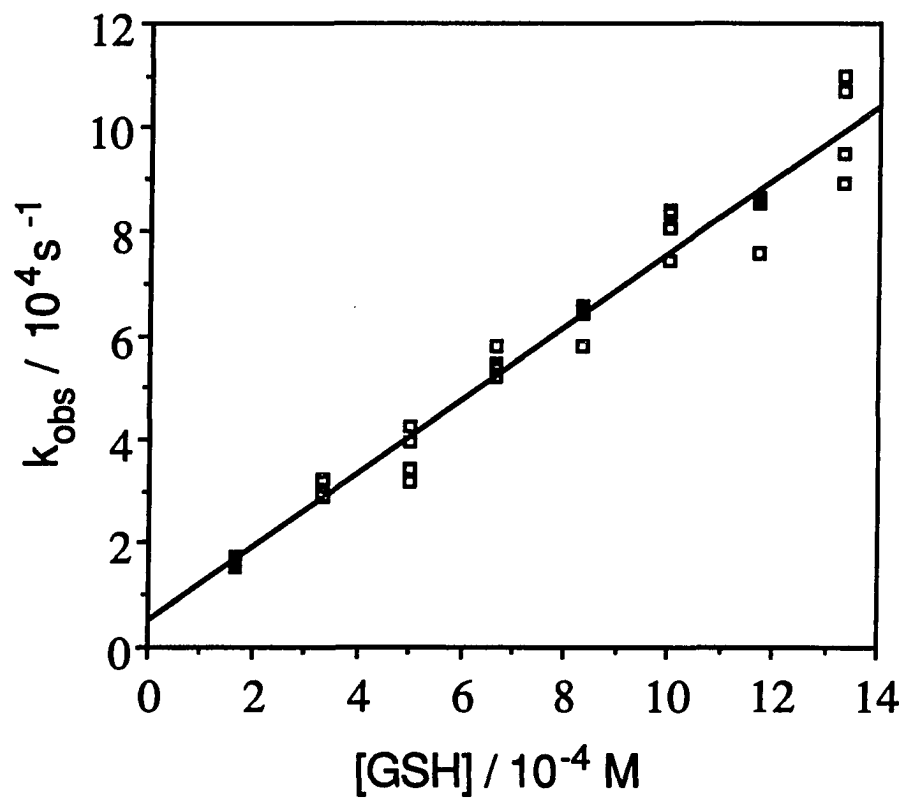


Figure A3. Reaction of $\cdot\text{CH}_3$ with glutathione at pH 7.0 using ABTS^{2-} as a kinetic probe

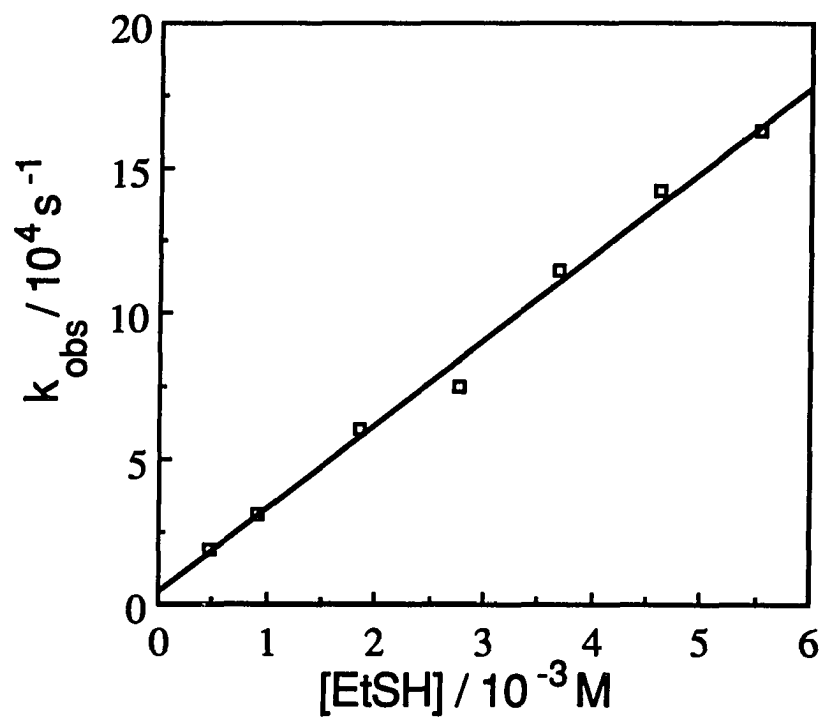


Figure A4. Reaction of $\cdot\text{CH}_2\text{CH}_3$ with $\text{C}_2\text{H}_5\text{SH}$ at pH 7.0 using ABTS^{2-} as a kinetic probe

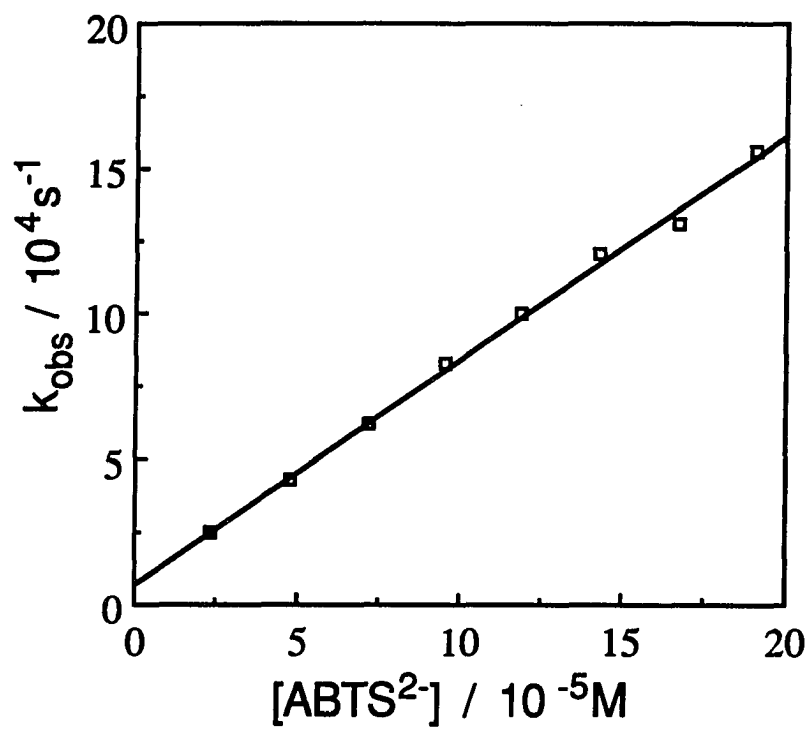


Figure A5. Reaction of CysS• with ABTS²⁻ at pH 4.0

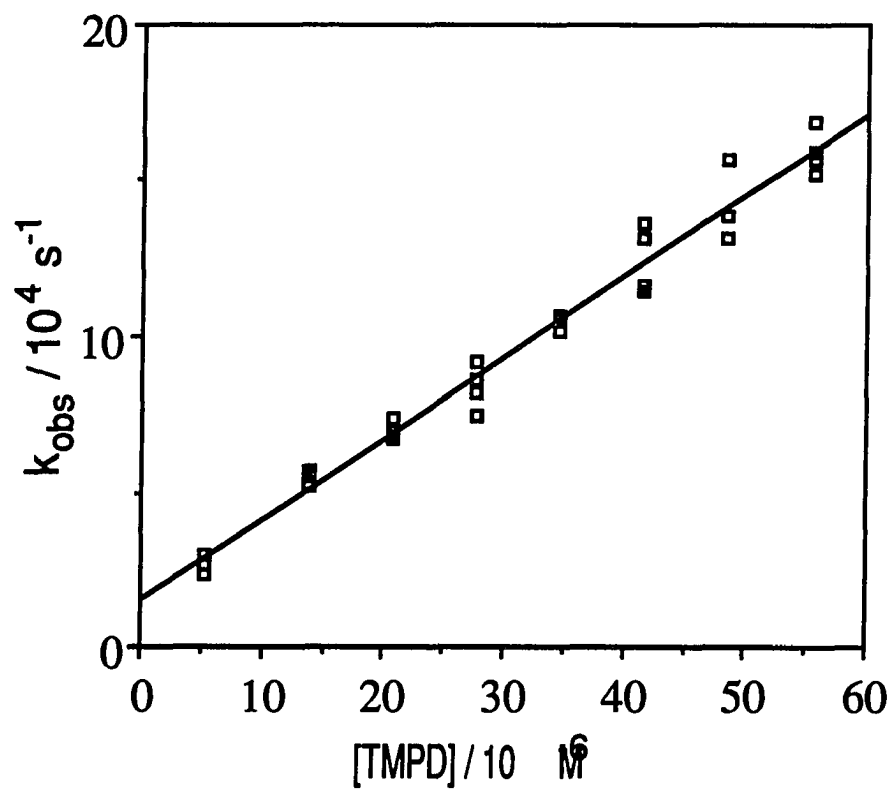


Figure A6. Reaction of $\text{C}_2\text{H}_5\text{S}^\bullet$ with TMPD at pH 7.0

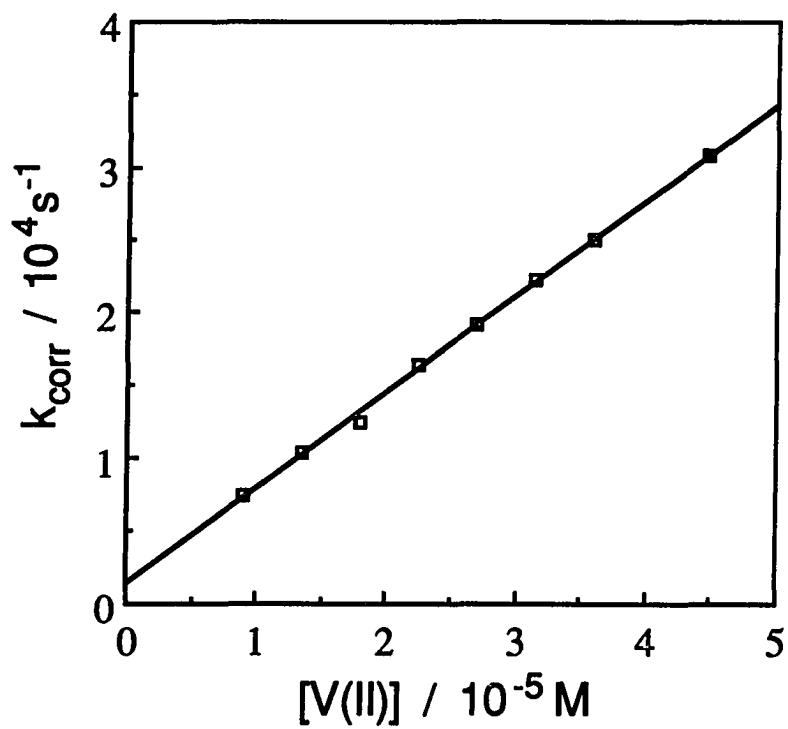


Figure A7. Reaction of $\text{C}_2\text{H}_5\text{S}\cdot$ with $\text{V}(\text{H}_2\text{O})_6^{2+}$ at pH 1.0 using ABTS^{2-} as a kinetic probe

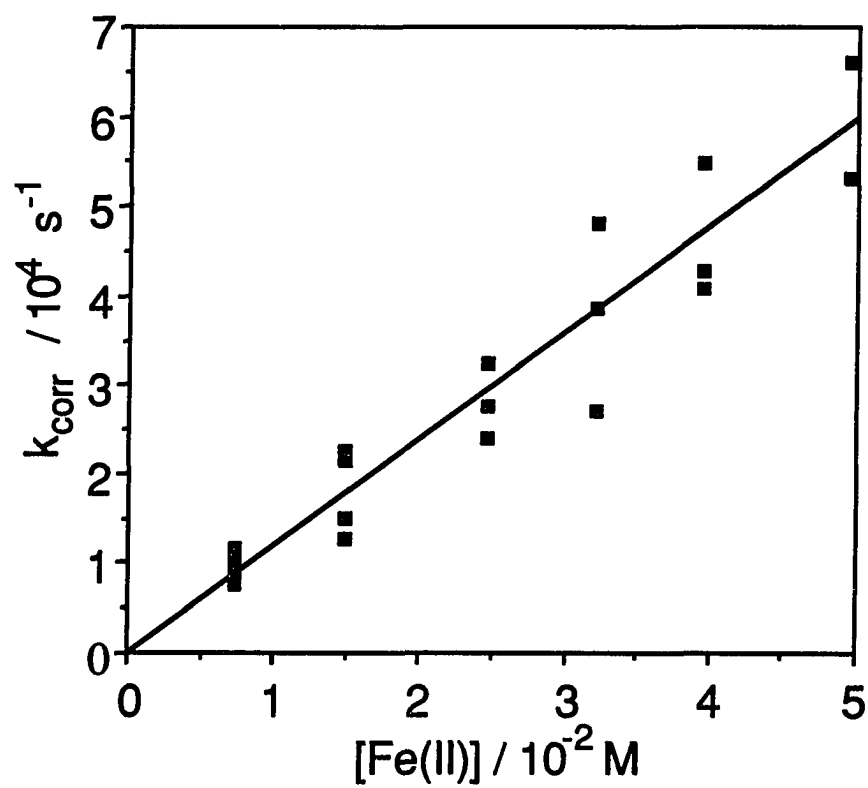


Figure A8. Reaction of $\text{C}_2\text{H}_5\text{S}\cdot$ with $\text{Fe}(\text{H}_2\text{O})_6^{2+}$ at pH 1.0 using ABTS^{2-} as a kinetic probe

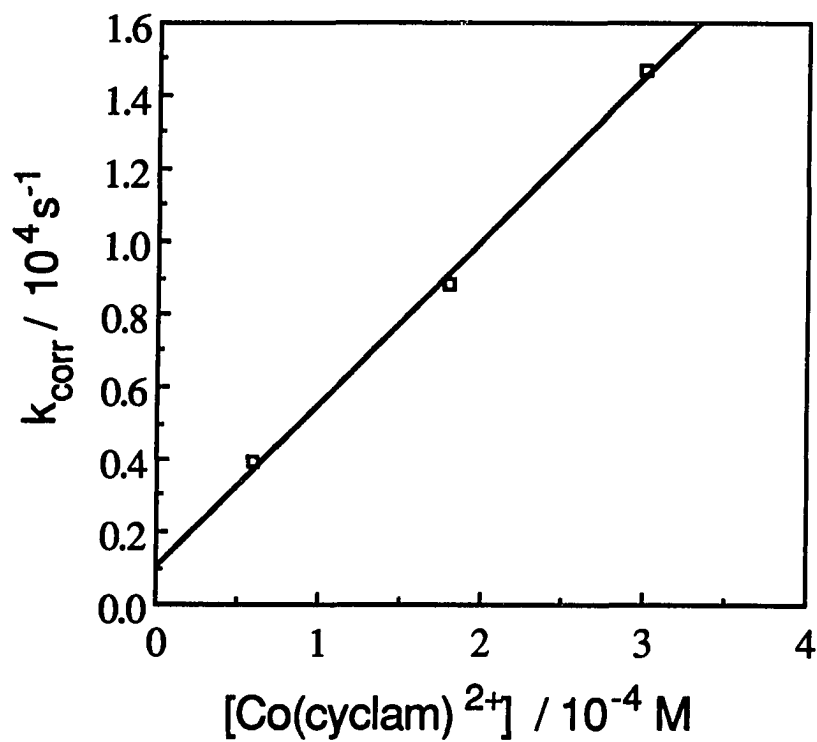


Figure A9. Reaction of $\text{C}_2\text{H}_5\text{S}\cdot$ with $\text{Co}(\text{cyclam})^{2+}$ at pH 7.0 using TMPD as a kinetic probe

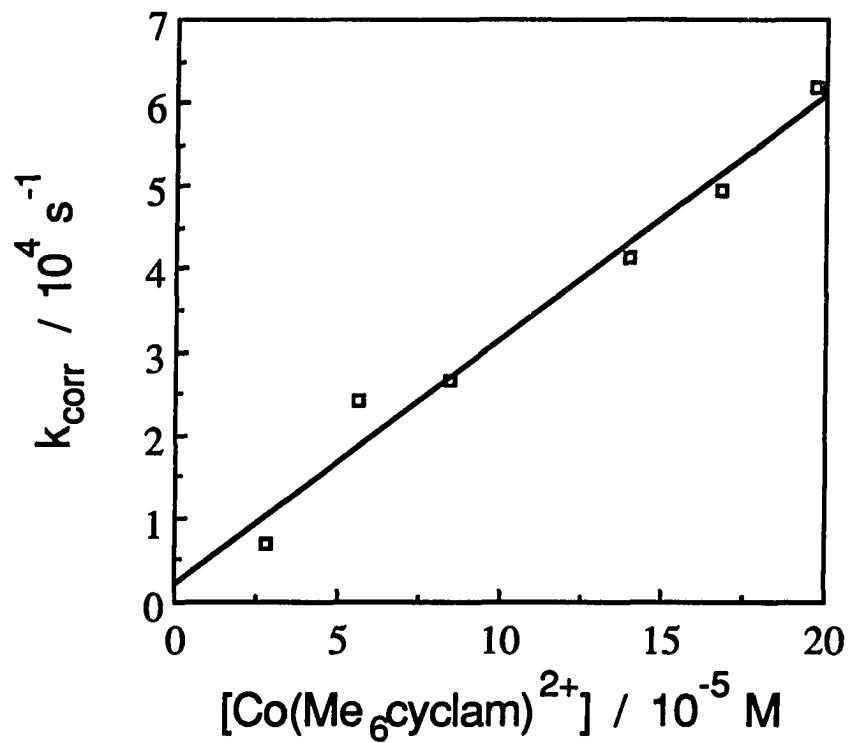


Figure A10. Reaction of $\text{C}_2\text{H}_5^\bullet$ with $\text{Co}(\text{Me}_6\text{cyclam})^{2+}$ at pH 7.0 using TMPD as a kinetic probe

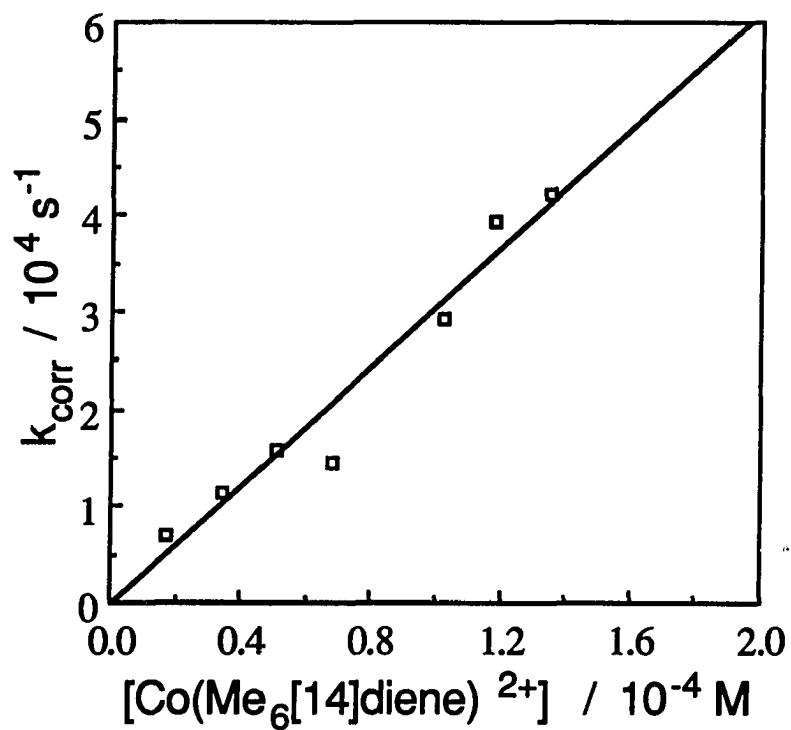


Figure A11. Reaction of $\text{C}_2\text{H}_5^\bullet$ with $\text{Co}(\text{Me}_6\text{dieneN}_4)^{2+}$ at pH 7.0 using TMPD as a kinetic probe

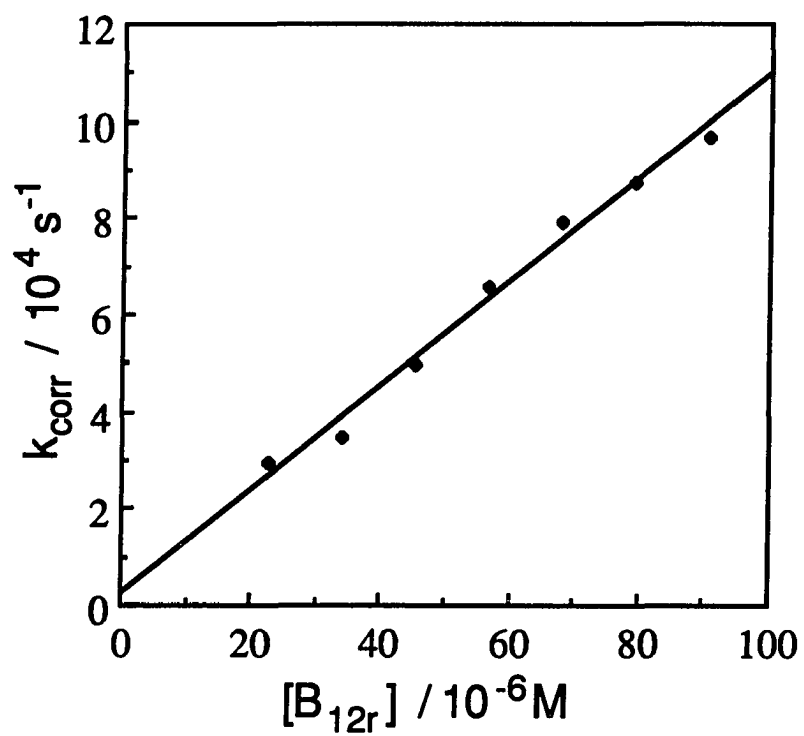


Figure A12. Reaction of $C_2H_5\cdot$ with Vitamin B_{12r} at pH 7.0 using TMPD as a kinetic probe

GENERAL SUMMARY

The kinetics of the quenching of the 2E excited state of chromium polypyridine complexes by Ti(III) were studied by laser flash photolysis. The dependence of the rate on hydrogen ion concentration indicates that both $Ti(H_2O)_6^{3+}$ and $(H_2O)_5Ti(OH)^{2+}$ quench. The formation of a stable Cr(II) product was observed spectrophotometrically, indicating back electron transfer occurs too slowly to measure. This is explained by the instability of TiO^+ , the immediate product of back electron transfer.

Alkyl radicals, generated from the photolysis of organocobalt complexes, were allowed to react with $(H_2O)_2Cr([15]aneN_4)^{2+}$ ($[15]aneN_4 = 1,4,8,12$ -tetraazacyclopentadecane). The reaction rates were evaluated by laser flash photolysis, using the known reaction between R^\bullet and the methyl viologen radical cation as a kinetic probe.

Thiyl radicals were generated by reaction of carbon-centered radicals with thiols. This reaction, known as the repair reaction, was studied for alkyl radicals with ethane thiol, cysteine and glutathione. Reactions of thiyl radicals with various transition-metal complexes were investigated using $ABTS^{2-}$ and TMPD as kinetic probes.

ACKNOWLEDGEMENTS

I would like to thank Professor James H. Espenson and Dr. Andreja Bakac for their guidance during my graduate career. I am also grateful to the members of the research group for helpful discussions and for their friendship. The ICP/MS work was performed by Dr. Sam Houk and Mr. Sam Shum.

I would like to thank my family for their support and encouragement. Finally, I would like to acknowledge The Reverend Steven P. Sabin for his patience and friendship.

This work was performed at Ames Laboratory under contract no. W-7405-eng-82 with the U.S. Department of Energy. The United States government has assigned the DOE Report number IS-T 1600 to this dissertation.